

Data Applications for Advanced Distribution Networks Operation

PROEFSCHRIFT

ter verkrijging van de graad van doctor aan de
Technische Universiteit Eindhoven, op gezag van de
rector magnificus, prof.dr.ir. C.J. van Duijn, voor een
commissie aangewezen door het College voor
Promoties in het openbaar te verdedigen
op woensdag 28 augustus 2013 om 16.00 uur

door

Petr Kad'ůrek

geboren te Půřlepy, Tsjechië

Dit proefschrift is goedgekeurd door de promotiecommissie:

voorzitter: prof.dr.ir. A.C.P.M. Backx
1^e promotor: prof.ir. W.L. Kling
2^e promotor: prof.dr.ir. J.F.G. Cobben
leden: prof.dr.ir. J. Driesen (Katholieke Universiteit Leuven)
prof.dr.ir. J.A. La Poutré (Universiteit Utrecht)
prof.dr.ir. J.G. Slootweg
Univ.-Prof.Dr.-Ing. J.M.A. Myrzik (Technische Universität Dortmund)
adviseur: S. Suryanarayanan, Ph.D. (Colorado State University)

To my parents ...

Rodičům ...

This work is part of the IOP EMVT ("Innovatiegerichte Onderzoeksprogramma's Elektromagnetische Vermogenstechniek") program, which is funded by Agentschap NL, an agency of the Dutch Ministry of Economic Affairs.

Printed by Ipskamp drukkers, Enschede.
Cover design by L-Seven Design, Arnhem.

A catalogue record is available from the Eindhoven University of Technology Library.

ISBN: 978-90-386-3418-0

Copyright © 2013 Petr Kadůrek, Eindhoven, the Netherlands
All rights reserved. No part of this publication may be reproduced or transmitted in any form or by any means, electronic, mechanical, including photocopy, recording, or any information storage and retrieval system, without the prior written permission of the copyright owner.

Summary

Economical reasons, security of supply as well as the ecological background are the key drivers for changes happening at different levels of our energy delivery systems. Both the supply and the demand side of it will have to be redesigned in the search for available energy sources without harming our environment. That this process is happening, is visible especially at numerous premises of electricity network users connected to the electricity network. Our electricity system therefore can not be left behind without adjusting itself to become more flexible and capable of meeting efficiently our future needs.

The electricity distribution network was designed for unidirectional power flows and is being operated in a relative reliable way for many decades. The insight into the operation of the distribution network is very limited and nearly no measurements are conducted in it. The distribution network as part of our electricity system will be exposed to many challenges, which will be realized at network users connections. More efficient use of energy in many applications can result in a higher use of electricity. The shift towards electro-mobility and the proliferation of distributed small-scale local generation are among the most important challenges for the future infrastructure.

Many aspects are points for discussion in the concept of our future electricity infrastructure. The perspective of the distribution system operator is an important one, since the network operator has the task to provide a reliable connection for the electricity network users in the uncertain environment and effectively invest in distribution assets.

The scope of the work presented in this dissertation focuses on the operation of the distribution network to assess it from the perspective of a distribution system operator. The research deals with the application of data and advanced distribution network technologies for distribution network operation.

In the first part of this dissertation is identified that the expected functionality of the future distribution network leads to guidelines for deployment of possible technological alternatives and assets, which can assist the network operator in achieving enhanced

network performance. The solutions with the largest impact on the distribution network performance enhancement are examined in this dissertation. The voltage level control and monitoring are indicated among the most important functionalities for the future operation of the distribution network. Suitable technological alternatives applicable within the regulatory framework of distribution network operators in the Netherlands are proposed and their implications on network performance are assessed in this dissertation. A voltage control strategy at the medium-to-low voltage substation is proposed to increase the hosting capacity of the distribution network for accommodation of distributed generators. This application can be to a certain extent an alternative to grid extensions. The increasing number of power electronic appliances in the system calls for more attention and for the evaluation of the quality of supply voltage. The distribution network operator shall conduct measurements to evaluate the distortion levels of supply voltage in the network. The measurements should provide sufficient insight to the network operator to take measures if needed in a cost-effective way. Therefore, the distortion propagation throughout the distribution network is studied in the second part of this work with the aim to evaluate the most suitable locations for power quality measurements to assess the distortion levels in the network.

Many developments can span beyond the intended scope of their proposed application. Therefore, new applications of data and advanced network assets are presented in the third part of this work. It is pointed out that advanced network assets can additionally provide new services to the electricity system without jeopardizing their initial purpose. Those applications can have a very profound impact on the system operation and can help to make it more efficient and rational. The application of data from the network is proposed to be used in different ways, for instance applications to reveal the location of illegal abstraction of electricity in the network or to assess the loading conditions on not measured distribution network assets are presented. The application of voltage level control in the distribution network to influence demand with the aim to support power system balancing is assessed in detail. It is demonstrated, that the proposed application can efficiently reduce power system imbalances without affecting its main operational purpose.

The research presented in this dissertation was performed by means of computer simulations and laboratory experiments. The focus is on distribution networks in the Netherlands, which are particular due to the high use of underground cables. An important element of this work was the possibility to validate proposed concepts in field tests in the real distribution network of Alliander in the Netherlands.

Contents

Summary	i
1 Introduction	1
1.1 General background	1
1.2 Power system structure	2
1.3 Research objective and scope	3
1.4 Research questions	4
1.5 Research approach	5
1.6 IOP EMVT research program	5
1.7 Dissertation outline	6
2 Electricity distribution	9
2.1 Introduction	9
2.2 Organization of electricity transmission and distribution	9
2.3 Future challenges	12
2.3.1 Proliferation of DG in distribution networks	12
2.3.2 Increasing load in the network	13
2.3.3 Limited insight in the distribution network	15
2.4 Initiatives to modernize power systems	16
2.4.1 Metering infrastructure	16
2.4.2 Distribution network automation	17
2.5 Conclusions	17
3 Functionality of distribution networks	19
3.1 Introduction	19
3.2 Analytic Hierarchy Process as a MCDA tool	20
3.2.1 AHP applications in power systems	20
3.2.2 AHP methodology	21

3.3	Functionality expectations of distribution networks	29
3.4	Alternatives selection	30
3.5	Conclusions	33
4	LV distribution networks	35
4.1	Introduction	35
4.2	Typical LV distribution network in the Netherlands	36
4.3	Electricity load profile characterization for residential LV network users	36
4.3.1	Load characterization based on field measurements	36
4.3.2	Generation of LV load profiles based on field measurements	38
4.4	Voltage deviations in distribution networks	41
4.5	Voltage level conditioning with OLTC	43
4.5.1	OLTC at MV/LV transformer	43
4.5.2	OLTC at MV/LV transformer - case studies on Dutch LV network	44
4.6	Power quality measurements and data	52
4.6.1	Flicker distortion in LV networks	52
4.6.2	Flicker propagation in LV networks	54
4.6.3	Harmonic distortion in LV networks	58
4.6.4	Propagation of harmonic distortion in LV networks	59
4.7	Conclusions	62
5	MV distribution networks	65
5.1	Introduction	65
5.2	MV networks in the Netherlands	66
5.2.1	Current MV network topology	67
5.2.2	New MV network topology	68
5.3	MV supply voltage conditioning	70
5.3.1	MV supply voltage characteristics	70
5.3.2	Voltage level conditioning with OLTC in MV networks	71
5.3.3	Implications of MV/LV OLTC control on MV network - case studies	72
5.4	Power quality measurements and data	76
5.4.1	PQ phenomena propagation in current 10 kV MV networks	76
5.4.2	PQ phenomena propagation in 20/10 kV MV network	83
5.5	Conclusions	86
6	Data applications	89
6.1	Introduction	89
6.2	Application of OLTC for demand side management	90
6.2.1	Field test with OLTC	90
6.2.2	The available voltage range to induce DR	93
6.2.3	The availability of induced DR	98
6.2.4	Supporting system balancing with OLTC	100
6.2.5	Impact on distribution network losses	107

6.2.6	Enabling technologies	108
6.3	Theft detection	110
6.3.1	Value of non-technical loss in the Netherlands	110
6.3.2	Detection methods used to reveal illegal electricity abstraction	113
6.3.3	Proposed application to reveal NTL	115
6.3.4	Influence of topology and measurement uncertainty	119
6.4	Evaluating heavy loading conditions in LV network	121
6.4.1	Predisposition of LV networks to heavy loading conditions	122
6.4.2	Case studies	124
6.4.3	Practical implications	130
6.5	Conclusions	132
7	Conclusions, contributions and recommendations	135
7.1	Conclusions	135
7.2	Dissertation contributions	136
7.3	Recommendations for future work	137
A	Transfer coefficients	139
A.1	Flicker propagation	139
A.2	Harmonic propagation	140
B	Demand Response with IDS	143
	Bibliography	147
	Nomenclature	163
	List of acronyms	163
	List of symbols	165
	List of indices	167
	List of publications	169
	Journal publications	169
	Conference publications	169
	Acknowledgements	173
	Curriculum Vitae	175

Introduction

1.1 General background

Over decades, the dependency of our society on electric energy has reached levels, where modern civilizations would struggle to function without ubiquitously available electricity. There are myriads of electric devices, which have penetrated our everyday life and which boosted our productivity. Without electricity, our society might come temporarily to a standstill. Our dependency on electricity is underpinned by the fact, that a large power outage or a disruption in electricity supply caused by a natural disaster or other cause, has a significant socio-economic impact for a whole country [1], [2].

Considerable price volatility on hydrocarbon markets was observed in the last decade, which rise the questions about the energy security [3]. Significant price increase could be observed in the Europe Brent oil, which average annual price has in the last decade more than quadrupled and the fuel prices are currently predicted to grow in the future [4]. The development of crude oil prices for Europe in last decades is depicted in figure 1.1. Together with diminishing explorable reserves of hydrocarbons within Europe, Member States could become increasingly dependent on imports of hydrocarbons from outside Europe. The concerns related to affordability, energy security and energy independence are among the main drivers for the support of renewable energy sources integration into our power system. Europe aims to get 20 % of its energy from renewable sources by the year 2020 [5]. To achieve this goal, European Renewable Energy Directive 2009/28/EC [6] established mandatory renewable energy targets for Member States as the share of the final energy generated from renewable sources by the year 2020. Simultaneously, the share of the electricity on the final energy consumption in European Union (EU) is forecasted to increase to $\approx 25\%$ in 2030, but at the same time, the carbon intensity of power generation is predicted to decrease significantly per MWh generated. The extended use of solar and

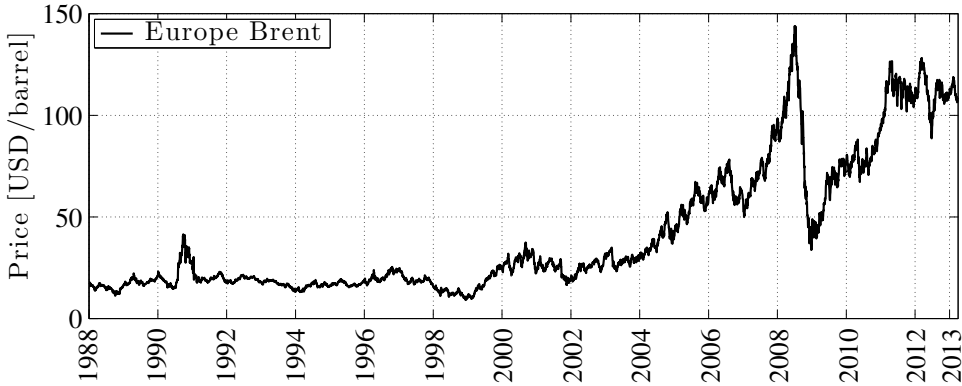


Figure 1.1: The development of the daily average crude oil prices in Europe [9].

wind technologies on power generation is expected to realize the reduction of carbon emissions on power generation in the future. In spite of a higher share of electricity being generated by renewable sources, fossil fuels will be still dominating the power generation in the near future [4].

On a global scale the electricity demand is expected to grow. A growth by more than one-third till the year 2035 is expected, where the majority of growth will take place in developing countries [7]. In Europe, average annual consumption growth in the period till the year 2020 of $\approx 1\%$, and after the growth of $\approx 0.8\%$ is foreseen by the ENTSO-E area (European Network of Transmission System Operators for Electricity) [8].

1.2 Power system structure

Our current power system is regarded as the most complicated and the largest man-made machine ever made [10]. The inventions by Thomas Edison and Nikola Tesla laid the foundations for building modern electric grids at the end of 19th century [11]. The invention of transformers enabled proliferation of the three-phase alternating current transmission, which is nowadays the base of the power system.

The power system facilitates generation, transmission, distribution and use of electricity and enables electricity markets. In past, the power used to be generated in conventional power plants in centralized manner and it was transmitted and distributed via the transmission and the distribution network to network users of electricity. The electricity distribution used to be passive without active control of production and consumption and mostly unidirectional power flows were present. Nowadays, generation takes place in different parts of the system, also at the distribution level and bidirectional power flows in the power system are increasingly happening as well

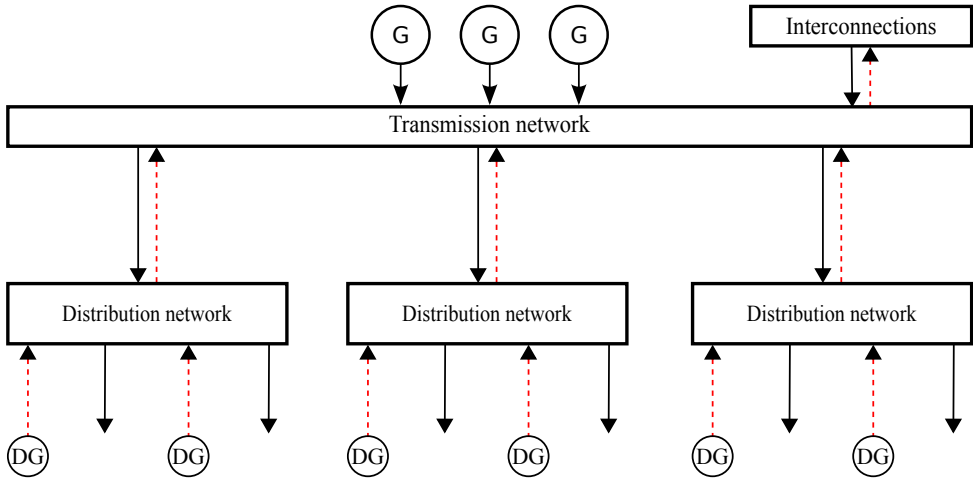


Figure 1.2: The schematic power system structure with indicated bidirectional power flow in distribution and between distribution and transmission network. The international interconnections with neighboring power systems are indicated.

as the continuous changing power exchange with neighboring countries. Those current trends in the power system structure are depicted in figure 1.2.

The supply side of our power system is changing also due to proliferation of small distributed energy resources (DER) [12] and distributed generators (DGs) in particular, which are being connected in large quantities to the distribution network at the voltage level of electricity network users. The electricity demand is envisioned to change and the increase in load can be significant when the shift to electro-mobility occurs. Since the distribution networks are not designed for bidirectional power flows, ensuring reliability of power delivery is and will be a very important task for the operators of our power system. The vision of the future power system, known as the "smart grid" or "intelligent grid", envisions omnipresent communication infrastructure interwoven with the electrical infrastructure to address the challenges in our future power system, which will accompany among others the integration of diversified and distributed generation into the power system [13].

1.3 Research objective and scope

The developments at the supply and the demand side of our power system will have implications on system operation at different levels. Those developments challenge network operators as they have to find adequate solutions for operation, management and planning of their networks. In the future power system, more knowledge about

the operation and performance of various parts of the power system will be required to enable more efficient use of current power system assets.

Numerous developments will take place in the distribution network. The distribution network nowadays is passive and little information is available about its operation and it is not able to handle efficiently envisioned challenges in the future. The lifetime of an electricity network is several decades, but the distribution network has to be flexible enough to accommodate our current and the future needs. In addition, the distribution network has a large number of branches and connected network users. With nearly no measurements in the network, the operator of the distribution network has a challenging task to provide the required service quality of electricity distribution to all network users at reasonable cost. Currently, the deployment of measurements at all nodes of the network will lead to excessive costs for the operators. Ergo, to assess the quality of electricity supply in the distribution network, observation at specified locations can be satisfactory to provide the required insight to the network operator.

Therefore, the main objective of this work is twofold:

- To assess measurements and the evaluation of measured data to assess the quality of electricity supply in the distribution network
- To propose new applications of advanced distribution network technologies (assets) to enable more efficient operation of distribution networks

Within the scope of this dissertation are assessed the technical challenges related to the supplied power quality assessment in distribution networks and the technical challenges related to the operation of distribution network with presence of emerging technologies such as distributed generation. The solutions to those challenges in terms of application of data and advanced network technologies, which are applicable to distribution system operators in the time span of about a decade are researched. Socio-economical aspects, regulation, policy and reliability issues of distribution networks are not within the scope of this dissertation.

The proposed applications and concepts shall be feasible within the current distribution network structure and they shall be also applicable for the future distribution network to enable the transition towards it.

1.4 Research questions

Based on the research objective and scope presented in 1.3, the main research questions can be formulated:

- What are the requirements for the future distribution network?
- How to achieve a higher performance of the distribution network in the future? Which network functions and what kind of advanced network technologies will enable the higher performance?

- What, where and how to measure in the distribution network to provide satisfactory information to its operator about the supplied voltage quality to electricity network users?
- What kind of functions and new applications can be enabled with future distribution network assets owned by DSO?

1.5 Research approach

Throughout this dissertation, the following research approach was persuaded:

- The requirements on current and the future distribution networks are identified. The set of functional criteria and the set of available technological alternatives is assessed based on the developments, which impact the operation of distribution networks. The investigation was done within a multi-criteria decision analysis framework, where the analytic hierarchy process technique is utilized to structure and analyze this decision making process. The functions and the technological alternatives to enable a higher performance of distribution networks are assessed
- A model of the current and possible future MV distribution networks in the Netherlands is developed to assess the performance and implications of the proposed technological alternatives applied on the network. The model is also used to assess the propagation of the power quality phenomena throughout the distribution network and to derive the most suitable locations for observation of distortion levels in the network
- The verification of the proposed applications was performed with laboratory experiments and with a field tests in the distribution network of Alliander in the Netherlands.

1.6 IOP EMVT research program

The research presented in this dissertation has been conducted within the framework of the "Innovatiegerichte Onderzoeksprogramma's Elektromagnetische Vermogenstechniek" (IOP EMVT) research program [14]. The program is supported by numerous industrial partners under the umbrella of Agentschap NL, an agency of the Ministry of Economic Affairs in the Netherlands.

Within the IOP EMVT framework, the IDEaNeD project was admitted. The IDEaNeD stands for Intelligent and Decentralized Management of Networks and Data and the project aims to investigate the possibilities of data applications for advanced distribution network monitoring and management to increase the network flexibility. The project contributes with its findings to shape the future sensing infrastructure used

for advanced data applications and for the operation of distribution networks. The output of the project should contribute in field of distribution network measurements, data applications and substations automation.

The industrial partners within the IDEaNeD project are: Alliander, DNV KEMA, Stedin, Phase to Phase, Joulz, Early Minute and Alfen.

The project leader of the IDEaNeD project is prof.dr.ir. J.A. La Poutré at the "Centrum voor Wiskunde & Informatica" (CWI). CWI is the national research institute for mathematics and computer science in the Netherlands, which concentrates on energy research as one of its societally-relevant themes.

1.7 Dissertation outline

The outline of the research and findings presented in this dissertation is as follows:

- **Chapter 1: Introduction** provides background information to this dissertation, the main research questions are stated and the research description is presented
- **Chapter 2: Electricity distribution** provides information about the distribution network, the future challenges on it and the current state of measurements and distribution network automation in the Netherlands
- **Chapter 3: Functionality of distribution networks** is assessed with the application of a multi-criteria decision making tool, where the requirements on the future distribution network with the focus on MV/LV are identified. Within this chapter a set of functional criteria used for evaluation of available technological alternatives to improve the performance of distribution networks is defined. The available technological alternatives are ranked and their applicability within the regulatory framework in the Netherlands is discussed
- **Chapter 4: LV distribution networks**, their operational and power quality aspects in the changing environment are discussed. The locations to oversee the levels of evaluated power quality phenomena in the distribution network are proposed. It is shown, that the voltage level control will be necessary to accommodate a high penetration of DG in the network and the application of advanced distribution network technology is proposed to address this problem
- **Chapter 5: MV distribution networks**, their current and possible future structure in the Netherlands is discussed. The propagation of the power quality phenomena in the MV network structure is evaluated to propose the measurement locations to evaluate the levels of distortions. The implications of different voltage level conditioning control strategies on MV networks are assessed and the most suitable control strategy is proposed

- **Chapter 6: Data applications** and the applications of advanced distribution network technologies are shown to unlock new network functions at the distribution level. First, the application of on-line voltage control to manage demand in the LV network is presented and thanks to some of its unique characteristics, it is proposed to support system balancing. Second, the application exploiting measurements from the smart metering infrastructure for electricity theft detection and localization in LV networks is proposed. Third, the application of data from smart metering infrastructure is proposed to assess the heavy loading conditions in the distribution networks
- **Chapter 7: Conclusions, contributions and recommendations** give the summary of the results achieved in this research and highlights the most important conclusions and contributions. Recommendations and ideas for the future research are described.

Electricity distribution

2.1 Introduction

The purpose of this chapter is to present the background of the electricity system with the focus on the distribution system in the Netherlands. The organization, current measurements at the distribution network are introduced together with the future challenges and visions to answer those challenges.

2.2 Organization of electricity transmission and distribution

Many companies in the electricity sector nowadays stem from former vertically integrated utilities. To boost competitiveness and to allow fair access to the infrastructure, legal separation of companies in the electricity sector was required. In the Netherlands ownership unbundling is mandatory since the year 2010 and is mainly associated with the separation of companies operating networks from vertically integrated holdings for energy supply [15].

The purpose of the electricity system is to deliver reliable, safe and economically affordable electricity to its network users [16]. The system should provide transport of electricity at minimum cost, with minimal ecological impact and enable electricity markets. To accomplish the connection between entities of the electricity system, the electrical network utilizes:

- Transmission system
- Distribution system

Transmission System is operated and maintained by the transmission system operator (TSO). It is used to transport electricity in the TSO service area, mostly from large power plants towards large load centers and to interconnect with other TSO

service areas. Since 2011 the TSO in the Netherlands (TenneT TSO) operates also electricity networks with voltage levels ≥ 110 kV [17].

Distribution System is operated by the distribution system operator (DSO). The DSO is defined as:

"Distribution system operator means a natural or legal person responsible for operating, ensuring the maintenance of and, if necessary, developing the distribution system in a given area and, where applicable, its interconnections with other systems and for ensuring the long-term ability of the system to meet reasonable demands for the distribution of electricity", from [18].

The DSOs operate as natural monopoly the distribution network in their service area. There are 8 DSOs in the Netherlands providing connection to $\approx 8\,089\,000$ electricity network users [19]. Three major DSOs in the Netherlands operate distribution networks with > 2 millions of network users, namely: Enexis, Liander (part of Alliander) and Stedin. In the Dutch distribution network, approximately 75 % of MV/LV substations supply LV residential network users (consumers) with relative small average peak power [20].

The schematics of the electricity system in the Netherlands with its interconnections, common voltage levels and the operational areas of DSOs and TSO is shown in figure 2.1. The DSOs in the Netherlands operate mainly MV networks, LV networks and partially also a HV network, as addressed in chapter 4 and in chapter 5.

The efficiency of a electricity system can be indicated by the total electricity loss. An efficient electricity system has usually a total loss, including electricity transmission and distribution loss, lower than 6 % [22]. The electricity system in the Netherlands is very efficient (mainly because of short distances and high load density) with the average total loss of 4.32 % in the period from 2000 till 2012. To provide comparison for the same period, the estimated average total loss for the European Union was 5.69 %, 4.73 % for Belgium, 4.77 % for Germany, 5.90 % for the United States of America and 5.99 % for Czech Republic [23].

Most of the distribution network has been designed many years ago and have been very reliably operated as passive networks with the "fix-and-forget" approach. The average lifetime of distribution network assets in the Netherlands is expected to be about 40 to 50 years, but distribution network assets with much longer time in service can be found.

Additional information concerning the distribution networks in the Netherlands can be found in [24]. Substantial work with the focus on the Dutch distribution networks was done and it is presented for instance in the area of design aspects in [25], [26], in the area of power quality in [27], [28] [29] and in the area of protection issues in [21]. The work presented in this dissertation is complementary to this.

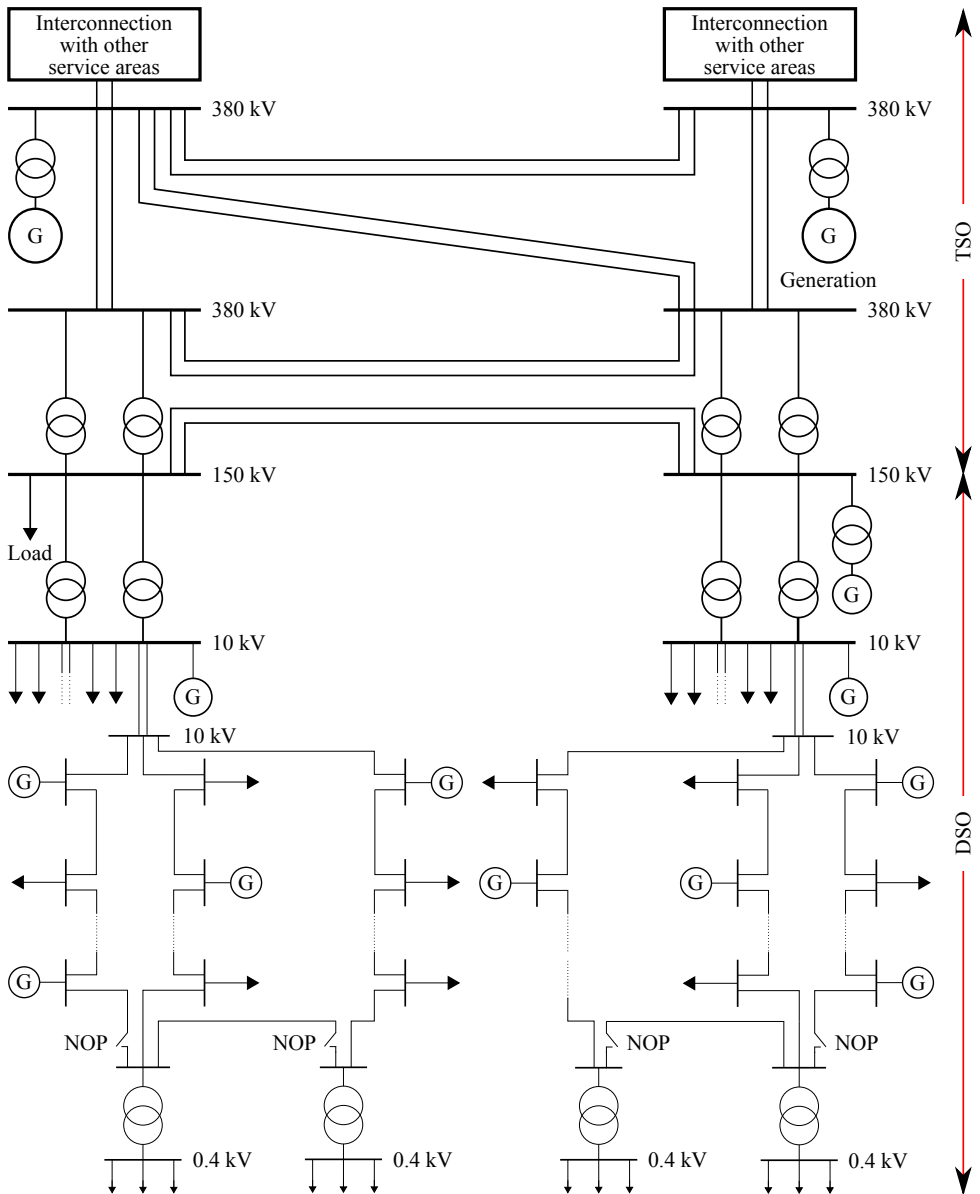


Figure 2.1: Schematic structure of the electricity system in the Netherlands with the most common voltage levels in transmission and distribution network operated by Dutch TSO and DSOs. The interconnections with other service areas (TSOs outside the Netherlands) are also indicated [21].

2.3 Future challenges

The distribution networks were designed to accommodate mainly network users loads. Bidirectional power flows in the distribution network were not expected in the past and the "fix-and-forget" approach could have been applied successfully in passively operated network. However, as the society develops, the electricity system and the distribution network shall advance as well to accommodate new demands which were not envisioned in the past.

The main challenges for the future distribution network operation are:

- Proliferation of DER and DG in particular, which is discussed in 2.3.1
- Specific load growth, which is discussed in 2.3.2

The uncertainty in distribution network operation used to be low. But the predictability of distribution network operation is expected to decrease when specific loads will be randomly connected to the network and when they will operate simultaneously with intermittent DGs in the network. The net energy demand observed at the network users point of connection (POC) can change and it can vary significantly over time. The possible developments of future demand profiles of Dutch electricity network users and their impact on distribution networks are presented in detail in [30].

2.3.1 Proliferation of DG in distribution networks

The Netherlands aims for 14 % of final energy consumption to be generated by renewable sources by the year 2020. The interim target of the final electricity consumption from renewable sources for the Netherlands was set to 4.7 %, where 4.3 % was achieved by the end of the year 2011 and the electricity generated from PV systems accounted only to 0.3 % of the total electricity generated by renewable sources [5], [31].

A DG is an electricity generator, which can be powered by renewable sources, connected either directly to the distribution network or via a network users installation. Many different forms of DGs exist and they differ in used energy source and scale. An overview is presented for instance in [21].

The proliferation of DGs and PV installations in particular takes place in many countries. Different DG systems are being connected to the LV and MV networks. The installed capacity of PV installations connected to distribution networks at LV voltage level has increased rapidly, it challenges the operation of distribution networks and it rises concerns about the management of their integration [32]. For instance in Germany, strong feed-in tariffs and falling prices of PV installations resulted in significant increase in PV systems installed. During some periods of the year 2012, PV installations contributed already to about ≈ 40 % of the peak power demand. In Germany, about ≈ 70 to 80 % of the installed peak PV capacity is connected to the LV distribution network [32], [33]. Expensive grid reinforcements are needed or are

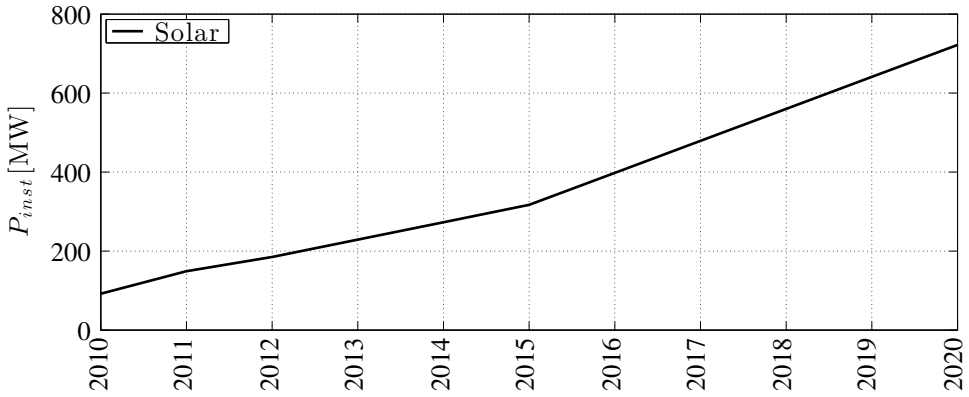


Figure 2.2: The predicted installed capacity of solar installations in the Netherlands by the year 2020, source [35].

expected to accommodate a high share of DGs in the distribution network [30]. The subsidiary scheme in the Netherlands has not stimulated such a progressive increase of PV installations, but a growing trend of installed PV capacity is predicted. The expected installed capacity of solar installations by the year 2020 for the Netherlands is depicted in figure 2.2. The growth of installed capacity continued also in the year 2011, where additional installed PV capacity of 40 MW was connected and 90 GWh in total were generated by PV installations in the year 2011 in the Netherlands [34].

In addition, the installed capacity of other renewable sources is also expected to increase in the Netherlands. The wind power (on-shore and off-shore) is expected to increase from $P_{inst} = 2\,221$ MW in the year 2010 to $P_{inst} = 11\,178$ MW in the year 2020 [35]. And very high shares of renewable energy are envisioned for periods after the year 2020 by the European Union [36].

The proliferation of DGs has implications on the power quality of supplied network users, especially in terms of increasing harmonic distortion [37] or voltage level deviations, as discussed in chapter 4 and in chapter 5, or addressed in [21], [27].

The rapid proliferation of DGs presents new demands on the distribution network, which was designed to accommodate only loads and unidirectional power flows. The secure and reliable operation of distribution network with a high penetration of DGs presents a challenge for DSOs, which have to search for technical and operational alternatives to manage the integration of DGs into their networks.

2.3.2 Increasing load in the network

The electricity demand in the Netherlands is expected to increase and large part of it will have to be accommodated by the distribution network. The increasing trend in total

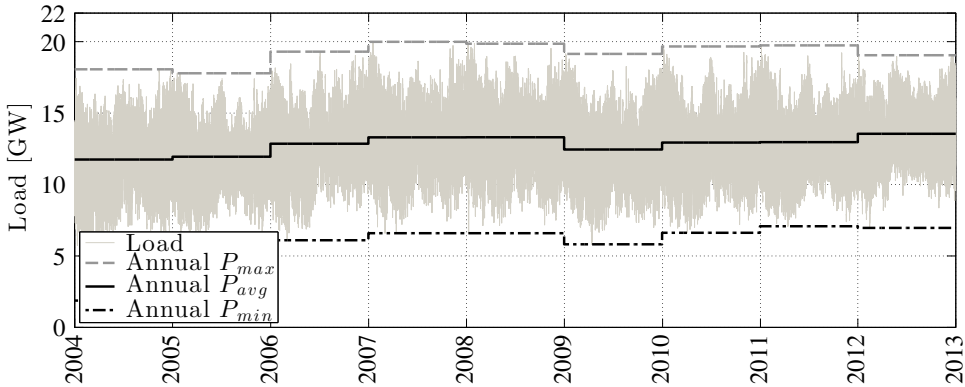


Figure 2.3: Electricity load in the Netherlands in the period from the beginning of the year 2004 till the end of the year 2012. The load annual maxima, average and minima are depicted (source: TenneT TSO).

electricity demand is linked to the economical activity and can be observed especially in the period before the year 2008, as depicted in figure 2.3. The slowly recovering economic activity is reflected on the country electricity demand in the later period.

A high annual load growth of 3 % till the year 2030 is assumed by the Dutch TSO for central and western areas of the Netherlands [38]. A strong load growth in distribution networks is also expected by DSOs, where growth of 2 % annually is anticipated in the period till the year 2025 [24]. A significant growth of peak load without load management is also predicted in coming decades [39].

Applications improving overall efficiency of energy use will result in increasing use of electricity, such as the application of heat pumps or the shift towards electromobility [24]. Electric vehicles (EVs) are envisioned to penetrate the transportation sector in the future. EVs will represent significant additional load, which can increase the loading of the distribution network beyond its capacity if charging is not managed. The annual additional load for an average EV can be as high as the annual electricity consumption of an average Dutch household [40]. Similar observation is made also for Belgium, where the magnitude of additional EV load is expected to be comparable to the magnitude of annual electricity consumption in a typical household [41].

The impact of EVs on distribution network can be severe and even a relatively low penetration of EVs in the system could lead to overloads of network components [42].

The envisioned EV penetration for the Netherlands nowadays predicts 1 million EVs by the year 2025 [43]. The charging demands of EVs are uncertain, but an average additional load of 0.84 GW could be expected for 10 % EV market penetration (corresponds to 1 million EVs) in the Netherlands [44].

It shall be recognized that the additional loads will be connected to the distribution network, which can be already heavily loaded and can have difficulties to accommodate them.

An increasing number of appliances powered via an electronic interface is expected to be connected to the distribution network in the future. Implications on supplied power quality in distribution networks can be expected [27], [45].

2.3.3 Limited insight in the distribution network

A DSO shall design and operate its networks to accommodate electricity demands of connected network users and to comply with the standard for supplied voltage quality EN 50160 [46] and the National grid code [47]. Operational measurements in the distribution network were not economically justified in the past, where the connected network users were passive and the sensing infrastructure together with the communication infrastructure were expensive for mass deployment. Only very limited measurements are conducted in the distribution network in the Netherlands:

- Maximum power/current measurements recorded at certain locations, where the maximum value from the last reading is read about once a year on average
- Measurements at specific locations following a complaint of a network users or when a suspected activity was detected in the network (e.g., illegal abstraction of electricity)
- Week measurements at randomly selected locations for overview of power quality performance

The power quality measurements in the Dutch network are conducted annually to provide indicative overview of the supplied voltage quality in HV, MV and LV networks. The measurements are conducted on weekly basis at random locations in the MV and LV network. The measurements in the HV network are from 20 fixed locations. The power quality overview for the year 2011 was based on 50 week measurements at different locations in the LV network and on the same amount of measurements in the MV network [48]. The measurements capture only a small share of the network, which has about 120 000 MV/LV substations in operation in the distribution network in the Netherlands.

It is concluded, that the observed average values for total harmonic distortion (THD) and flicker severity in Dutch MV and LV networks were far below the requirements of the EN 50160 standard [48]. The median value of THD in the year 2011 was $\approx 2.3\%$ for the LV network and $\approx 1.7\%$ for the MV network. The median values of the flicker severity levels for LV networks of ≈ 0.23 and for MV networks of ≈ 0.14 were observed in the same year. Nevertheless, levels of harmonic distortion not complying with the EN 50160 standard were observed at certain locations in LV network. It is estimated that about 74 % to 94 % of LV network users in the Netherlands (with the confidence level of 90 %) are supplied with voltage quality according to the EN 50160 standard [48].

2.4 Initiatives to modernize power systems

The existing distribution and transmission networks were designed to operate in the conditions envisioned at the time of their conception. In the Netherlands, the distribution networks serve its purpose well and they deliver electricity with a very high reliability [49]. However, efforts to decarbonize our electricity system will make the operation of the electricity system and distribution networks more challenging. The existing electricity system can be basically characterized by the following statement:

"The system is essentially a one-way pipeline where the source has no real-time information about the service parameters of the termination points.", from [13].

The operators of electricity system will have to respond to the envisioned challenges and rationally use the available infrastructure to accommodate the predicted demands, as discussed in 2.3. The electricity system is undergoing modernization which is commonly labeled as the "Smart Grid" or "Intelligent Grid" vision and used in plethora of concepts. Therefore, the expected functionality of the system and the applicability of technological solutions to respond to the challenges is uncertain. Although there are many aspects, visions and different perspectives resulting in different requirements on the future electricity system around the globe, they jointly envision that the future electricity network will be enhanced with a sensing and communication layer to enable more insight into the operation of the network and to facilitate control actions. The future electricity system is expected to support the objectives of sustainability, security of supply and competitiveness in Europe [13], [50], [51], [52].

The European Technology Platform SmartGrids characterizes our future electricity system as:

"A SmartGrid is an electricity network that can intelligently integrate the actions of all users connected to it - generators, consumers and those that do both - in order to efficiently deliver sustainable, economic and secure electricity supplies.", from [53].

Flexibility, cost-efficiency, reliability and disturbance resilience are the important aspects of the future electricity system [54]. Therefore, DSOs in the future will need to gain more visibility and control over their assets to perform automated actions and to provide adequate response to different system states.

2.4.1 Metering infrastructure

The metering infrastructure with advanced electricity meters, commonly labeled as "Smart Meters", is expected to provide enhanced functionality beyond the current metering infrastructure. The smart metering infrastructure will be an important part of the future system, which will facilitate some important functionalities and enable two-way communication [50]. The deployment of a cost-effective advanced metering

infrastructure is supported by the EU to promote mainly: efficient use of energy, to encourage active participation of electricity network users on energy markets, to support the accommodation and increasing use of distributed (renewable sources) on electricity generation (increase awareness of power injections), to provide network users with accurate and frequent billing and to promote participation on active demand-side management [55], [56].

The roll-out of the smart metering infrastructure in the Netherlands was delayed by the flawed legal framework and privacy concerns of electricity network users. The expected compulsory roll-out was based on the positive cost-benefit analysis, but it was blocked in the year 2009 [57], [58]. An updated cost-benefit analysis was performed later to reflect the current economic situation and expected functionality in the Netherlands [59]. In 2012 were put into force amendments on the Dutch Electricity Act and the Gas Act, which requires DSOs to offer smart meters to its network users (households and small businesses). Network users are empowered to limit the functionality of their smart meter and they have to authorize frequency of meter readings exceeding the minimum bi-monthly requirement [60].

The body representing the energy regulators in Europe provides a set of smart metering functionality requirements and guidelines to Member States in the EU [55], [61]. In the Netherlands, the set of minimal functionality requirements on smart meters is defined in the NTA 8130 standard [62] and the national reference architecture concerning smart metering in NTA 8150 standard [63], [64].

2.4.2 Distribution network automation

Distribution networks around the globe are currently passively operated and the penetration of distribution automation is low. As part of the future electricity system vision, more automation is expected to take place in the distribution network to improve reliability and efficiency of electricity distribution [13].

In the Netherlands, the distribution automation mainly aims to reduce the outage time of connected network users and to increase the utilization of distribution networks. The efforts with more distribution automation in the Netherlands resulted in a project focusing on an experimental MV/LV substation with new technologies applied to the distribution network [65], [66], [67].

2.5 Conclusions

Background information related to the developments in the distribution system in the Netherlands is provided in this chapter. The future demands and concerns related mainly to the proliferation of distributed generation and expected load increase present challenges on distribution network. However, the current distribution network was not designed to accommodate those new developments. The distribution network is nowadays passive and nearly no measurements are performed in the network.

Therefore, DSOs have to assess the future requirements on their network and search for applicable technological solutions to increase network flexibility.

Most of the network users in the Netherlands are currently provided with satisfactory quality of electricity supply, however this can be hard to maintain in the future. To provide a reliable connection to network users with required voltage quality, DSOs need to gain more insight into the performance of the distribution networks through measurements. Smart metering was expected to provide more insight into the operation of the distribution network, but the privacy concern can limit the expected benefits of it.

A DSO with more comprehensive information about the state of the distribution network is expected to be able to better manage the distribution network assets and to efficiently plan investment activities to the benefits of its network users.

Functionality of distribution networks

3.1 Introduction

Many developments take place nowadays in the power system including implications on distribution networks. To address correctly the requirements on future distribution networks, a set of functional criteria and a set of available technological alternatives are assessed in this chapter.

When the complexity of a problem or a system increases, the decision making related to it becomes also more complicated. Especially if the decision maker is biased, or decisions involve many interwoven variables to be considered and those variables are highly complex in their nature. Finding a suitable solution can be a very difficult task. Intuition could be used in cases, where the negative consequences of a decision would be tolerated. When the stakes are high, it is important to properly structure the problem, define criteria and apply reasonable techniques to obtain meaningful conclusions.

Techniques such as Multi-Criteria Decision Analysis (MCDA) can be very suitable exactly in the instances, where the problem complexity is high and when there are many conflicting criteria to be considered, and the decision makers can be biased by their environment or affiliation. As power systems are becoming increasingly complex, their operation and planning is also becoming increasingly complicated [68]. Therefore, also the decision-making process related to distribution networks requires more sophisticated tools such as MCDA to satisfy all the relevant considerations in distribution network operation and planning [69].

Since instrumenting all substations with all possible measuring devices and control techniques is not economically feasible, this chapter focuses on identifying and quantifying the expected functionality of distribution networks and on the priority quantification of distribution network operational aspects. The evaluation of the

expected functionality is important to identify the necessary measurements, among the distribution network, enabling and facilitating those expected network functions.

3.2 Analytic Hierarchy Process as a MCDA tool

The Analytic Hierarchy Process (AHP) is one of the MCDA tools used to organize and evaluate complex decisions [70]. Since the 1970s, the AHP methodology has been successfully applied to a variety of disciplines, especially for decisions with high complexity and where the criteria of making the decisions were not necessarily objective in nature [71].

The AHP methodology is developed to incorporate the subjectivity of decision makers into a mathematically sound objective priority ranking and alternative choices [70]. AHP allows simultaneous comparison of objective (quantitative) data with subjective (qualitative) judgements and simplifies complex decisions that involve many possible alternatives and decision makers. And, because the human mind has difficulty comparing the relative importance when confronted with many choices, AHP allows decision makers to compare only two items at a time via pairwise comparisons. The AHP methodology can derive priorities (dominance) based on paired comparison of decision elements with respect to a common objective for different levels of the AHP hierarchy. The AHP is supported by a mathematically sound framework to evaluate the consistency of provided judgements. Therefore, the judgement consistency can be improved if necessary. In doing so, it is argued that this methodology can draw out the true opinion of the decision maker [70].

The process of distribution network modernization can be associated mainly with network automation and increasing operational awareness. In the Netherlands, modernization efforts have resulted in MV/LV Intelligent Distribution Substation (IDS) pilot, as discussed in 2.4.2. The MV/LV substation is a highly important node in the distribution network as its design has to meet the expectations and requirements of both LV and MV networks. The familiarity with the IDS concept is used as a logical extension in addressing the distribution network functionality. Therefore, the evaluation takes the expected functionality of an IDS into consideration to obtain functionality expectations for the distribution network.

3.2.1 AHP applications in power systems

Numerous AHP applications to electrical and power engineering are known. The AHP methodology is applied as a decision making tool for energy mix planning [72]. But also for operation of electric power microgrids [73], where it proves its strengths to derive the best mix of resources available for the microgrid, their deployment, configuration and in defining the procedures to island a microgrid from the network [69]. And the AHP is applied for analysis of hidden failures (not apparent during normal system operation) in special protection schemes in power systems, where the least and the

most vulnerable parts of the system can be identified to assess their influence on system stability after a fault [74]. It is applied also for the automatic re-establishment (self-healing or self-reconfiguration) of power supply in more agile way after a contingency in the network, coordinating load transfers and power restoration using remote controlled switches [75]. Furthermore, the AHP methodology is successfully applied for remote switches allocation in distribution networks, where the subjective as well as the objective criteria for a potential switch location can be evaluated [76]. The AHP methodology was also utilized for the selection of suitable IT infrastructure for future power system applications, which is a very complex task including many interwoven variables, technical and non-technical criteria influencing the selection of plausible alternatives [77]. The selection of the most suitable electricity storage can be also addressed by AHP, based on multi-criteria decision making and evaluation (costs, efficiency, maturity, life-cycle, load management and power quality) [78]. Further applications of AHP include for instance the evaluation and routing of power transmission lines [79], generator fault diagnosis [80], load shedding schemes [81], post-evaluating of wind power [82] and others.

3.2.2 AHP methodology

AHP involves structuring a problem as a hierarchy of: a goal, the criteria affecting the goal with sub criteria as necessary and, finally all the possible alternatives. Individuals or groups of decision makers then compare, in a pairwise fashion, all the elements on each level of a hierarchy and the relative importance to each other and to the next highest level in the hierarchy. The process then generates a vector of overall preferences among the alternatives. The result is that the opinions of many decision makers, even if quite disparate, are incorporated in a final ranking of alternative choices.

The AHP methodology consist of the flowing steps [70]:

- Structure the problem in a hierarchy (see 3.2.2.1)
- Apply intensity scale to rank judgments importance (see 3.2.2.2)
- Create a judgment matrix (see 3.2.2.3)
- Evaluate the weight for each criterion (see 3.2.2.4)
- Rank available alternatives (see 3.4)

3.2.2.1 Structure the problem in a hierarchy

The problem is divided and decomposed into a multilevel structure, where we investigate the impact of higher level components in the hierarchy on the fulfilment of the goal and available alternatives. An absolute number can be assigned to either objective or subjective judgements for every pair compared. Therefore, the comparison of small more homogeneous clusters can be made as a subset of all relevant criteria.

The overall goal of the investigation in this dissertation focuses on the main question: *How to increase the performance of distribution networks?* and is presented in the first level of the AHP hierarchical structure in figure 3.1. The performance of distribution networks is defined based on the matrix of evaluated criteria presented in figure 3.1.

The second level of the AHP hierarchy represents the set of relevant criteria to achieve the defined goal. In total 10 criteria (noted as c.1,...,c.10) are selected as important aspects to be considered in the expected distribution network functionality assessment, as in figure 3.1. Four groups of criteria are identified, but evaluated separately to draw more detailed conclusions; criteria related to supply quality (c.1, c.2, c.3), criteria related to accommodation of new applications in the networks (c.4, c.5), criteria group related to demand response (DR) [83], (c.6, c.7) and criteria group related to other network functions (c.8, c.9, c.10).

The third level of the AHP hierarchy represents the group of alternatives (available technological options) for reaching the specified goal. Based on [66], [67], the set of possible technological alternatives to advance the current distribution network is defined, as third level in the AHP hierarchy in figure 3.1.

3.2.2.2 Intensity scale and importance judgements

A survey was constructed to solicit input form for the AHP methodology, with the aim to exploit the knowledge and experience of different stakeholders and experts in distribution network operation and planning. In total, 28 responders participated in the AHP survey in two groups; with an industrial affiliation and with an academic affiliation as detailed in table 3.2. An on-line questionnaire designed in Google Docs was used for the acquisition of expert responses (in the period of October and November, 2012). However, due to the limitation of the platform utilized here, the fundamental scale of comparative weights between alternatives from [70] was modified from nine comparison values to the five shown in table 3.3.

The responders were provided with criteria description (second level hierarchy) as presented in figure 3.1, and with a detailed description of the evaluated functionality aspects (criteria), to support their judgement decision with sufficient information as presented in table 3.1, based on EN 50160 standard [46].

3.2.2.3 Create a judgement matrix

The expert opinion from decision makers is drawn in form of a pairwise comparison for all considered criteria. The pairwise responses, based on comparing criteria in pairs to judge their preference, of each responder are organized in an answer matrix A . The answer matrix is $n \times n$ matrix, where n is the number of objective functions, ergo $n = 10$ for 10 evaluated criteria as in table 3.1. The equal importance in A is judged as $a_{i,j} = a_{j,i} = 1$, where $a_{i,j}$ is the intensity value from scale as in table 3.3.

To reduce the response time, the symmetric nature of the response matrix A is exploited such that $w_{i,j} = 1/w_{j,i} \quad \forall i,j \in NC$, where NC is the set of numbers

Table 3.1: Evaluated functionality aspects (criteria) in the AHP survey with detailed aspects considered in the survey, as outlined in figure 3.1.

Criteria	Description	Aspects considered in survey evaluation
c.1	Improve supply voltage (voltage level variations for connected LV network users)	Based on indices specified in EN 50160 [46], maintain $U_n \pm 10\%$ (nominal voltage magnitude), for all LV network users supplied. For 95 % of 10 minutes mean rms values over a week (or support even higher required voltage quality such as $U_n \pm 10\%$ over 99 % of the time)
c.2	Improve voltage quality for connected LV network users	Based on EN 50160 [46]: improve flicker indices for 95 % of the time, rapid voltage changes, voltage harmonics, voltage dips and unbalance
c.3	Improve reliability of power delivery	IDS can improve the reliability indices (SAIDI, SAIFI) for the connected network users. Self-healing (self-reconfiguration) after an outage can be implemented by IDS in MV networks and IDS can sense and report an outage in LV networks
c.4	Support seamless accommodation of DGs	IDS can actively alter the negative impact on voltage level in distribution network with high penetration of DG both in LV and MV network by means of OLTC or energy storage
c.5	Support accommodation of EVs	IDS can improve voltage level conditions and help to alleviate loading constraints in the LV network and can assist in local charging coordination at LV level
c.6	Enable DR - support distribution network operation (peak load reduction)	Facilitate DR with the focus on supporting operation of distribution networks (e.g., peak load reduction in LV and MV networks)
c.7	Enable DR - for other participants	IDS as a facilitator of LV DR programs for commercial purposes and enabler of market participation for active network users such as PowerMatcher (separated from network congestion management) [84]
c.8	Distribution network awareness (monitoring)	To enable (on-line) distribution network monitoring and to increase operational awareness of distribution network assets. Monitor operation with high penetration of new technologies such as EVs, heat-pumps or intermittent DGs
c.9	Theft detection	To monitor and reveal the theft in LV network. About 1200 GWh/year is expected to be stolen and tampering takes place at half of the (MV/LV) substations, with the loss for DNOs in NL to be about M€114/year [85]
c.10	Investment expenditure	Inventory in IDS can be a cost-effective alternative to other investment options and distribution network expansions

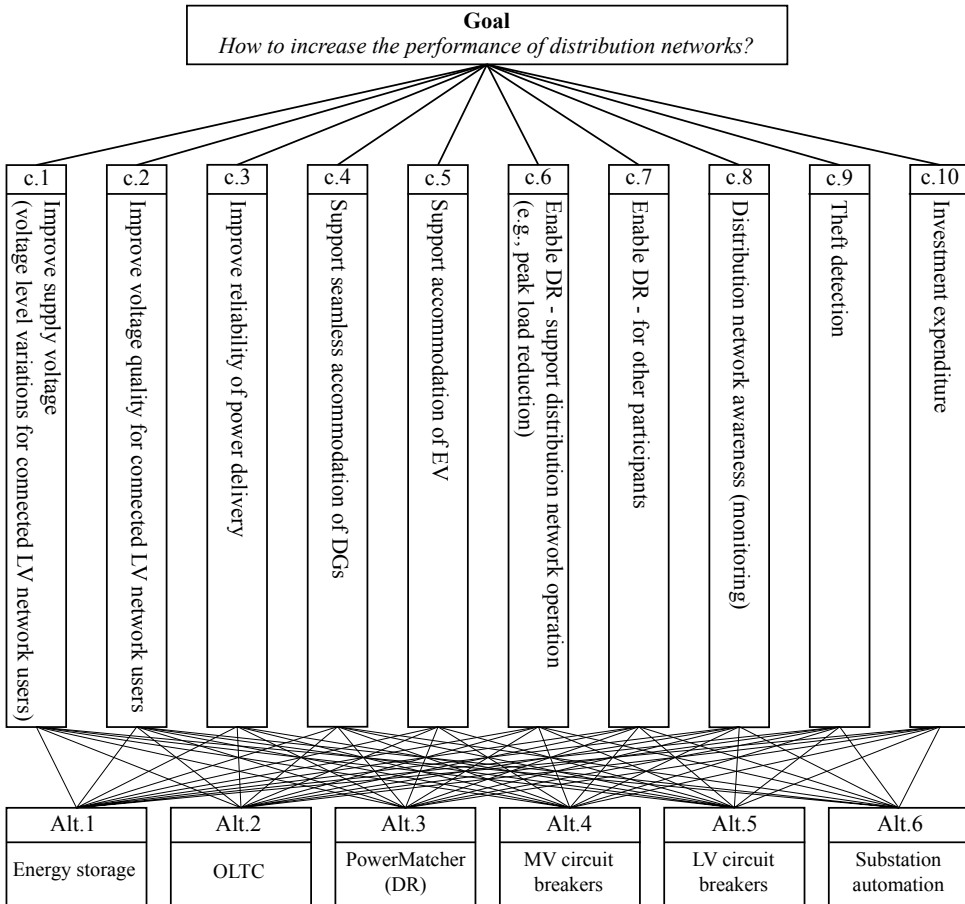


Figure 3.1: The AHP hierarchical structure for the evaluation of the expected distribution network functionality (second level of the hierarchy) and available technological alternatives (third level) to achieve the specified goal (first level).

representing the objective functions (choices), $NC = [1, \dots, n] \in \mathbb{Z}$. The responders were asked only the questions necessary to populate the upper triangular matrix for the second level of the hierarchy (criteria in table 3.1). Despite this time reduction effort, the average time per response was about one hour. In addition, some behavioural aspects, based on intuition, were implemented in the survey. The questions were not provided in the hierarchical order as presented in the AHP hierarchy, but in a mixed order to achieve higher objectivity of responses and to minimize answer bias.

Table 3.2: Responders affiliation by groups in the AHP survey.

Group description	Share	Responses received
Industry only	61 %	17
Academia only	39 %	11
All combined	100 %	28

Table 3.3: Modified intensity scale of importance for AHP evaluation [70].

Intensity scale	Description
1/8	Very strongly less important
1/4	Strongly less important
1	Equal importance
4	Strongly more important
8	Very strongly more important

It was intended for all responders to answer only their part of the survey, without the knowledge of previous results of other responders or current status of the survey.

3.2.2.4 Evaluate the weight for each criterion

Based on the responders judgements, the relative preferences can be estimated in a form of weight factors for each evaluated criterion. The priority weight of each criterion measures how much this specific criterion accounts for the overall goal.

The eigenvector W of the answer matrix A represents the relative dominance of each weight factor of A . This allows to estimate the resulting priorities for each alternative i , as in equation 3.1. The weight factors are normalized ($\sum_{i=1}^n w_i = 1$) for each level of the AHP hierarchy to provide relative judgement priority for preferences comparison across AHP levels (hierarchic composition principle) [70].

$$W = [w_1, \dots, w_n]^T \quad (3.1)$$

The resulting relative weights of each criterion can be compared among criteria and criteria clusters deriving their relative weights and to synthesize priorities for available alternative in a low level of the hierarchy, if present. This allows to add weighting global priority for each element or sub criteria on each level of hierarchy. As a consequence, ranking of all the stimuli at different AHP hierarchy levels is possible. The goal solving approach can be persuaded through developing a weighted structure of relations and influences, where the relative impact of one variable on another (criteria) can be evaluated [70].

3.2.2.5 Consistency improvements

Even with this guided decision-making process, people still frequently make inconsistent comparisons when confronted with many options. In an extreme example of this, a person might prefer choice A to B, and prefer B to C, but state that they prefer C to A, though deductive reasoning tells us that A should be preferred to C. Inconsistency is usually presented in more subtle forms.

The answer matrix A is considered as consistent if the individual judgement $a_{i,j}$ and the fraction of corresponding priority weights is in accordance with equation 3.2.

$$a_{i,j} = \frac{w_i}{w_j} \quad \forall i, j \in NC \quad (3.2)$$

The measure of answers inconsistency is expressed by a consistency ratio (CR) [70] defined by equation 3.3. Where λ_{max} is the largest eigenvalue of A and RI is the random index. The random index for $n = 10$ is $RI_{10} = 1.49$ based on [70]. As a consequence, the responses with CR values $< 0,10$ are acceptable as consistent answers for $n = 10$. The measure of inconsistency is an important aspect for the AHP methodology, because it allows to quantify the quality of responders replies and it admits a new knowledge to be added to their preference judgements.

$$CR = \frac{\left(\frac{\lambda_{max} - n}{n-1}\right)}{RI} \quad (3.3)$$

Multiple methods have been proposed to improve the consistency of personal judgements while retaining the opinion of a decision maker. The original method proposed by [70] is based on iterative process, which searches the most inconsistent judgement $a_{i,j}$ in A compared to the relative preference weight for selected i, j criteria w_i, w_j . The search for the most inconsistent judgement is based on equation 3.4.

$$\max |a_{i,j} - \frac{w_i}{w_j} \quad \forall i, j \in NC| \quad (3.4)$$

In the iterative process, the most inconsistent statements $a_{i,j}$ in A are replaced by relative weight $\frac{w_i}{w_j}$ until the inconsistency of decision maker responses decreases to acceptable level. As a consequence, the knowledge of a responder is extracted (selection priority is kept), while creating the response matrix consistent.

A more recent method in [86] presents a different methodological approach to improve answer matrix inconsistency. The problem is defined as finding a close consistent matrix Y_B , which is a consistent answer matrix with the same responders

preferences as in A . It is proven that the consistent matrix Y_B closest to B can be found based on Y_A (the closest consistent matrix to A) as in equation 3.5 [86].

$$Y_B = Y_A \odot (xy^T) \quad (3.5)$$

Where Y_A is the Hadamard (element by element) product (noted as \odot) of $x = [x_1, \dots, x_n]^T$ and $y = [y_1, \dots, y_n]$ such as the reciprocity and characteristics of the judgement answer matrix Y_B are kept. For more thorough explanation and mathematical proof, the interested reader is encouraged to consult [86]. The methodology presented in [86] is used to improve consistency of responses.

The responders in the conducted survey judged the criteria independently (without the previous knowledge other responders' preferences), for that reason the responses arrival based on time is not a relevant factor to be considered. The responses were evaluated based on their affiliation in three groups as in table 3.2.

To meaningfully synthesise the priorities of different group members and to arrive to a consensus, the application of arithmetic mean corresponding to individual criteria preferences is used [87]. Despite the limitations of the survey platform and available choices, the resulting judgement preferences can be as a consequence of this step refined to provide input for the expert $n \times n$ response matrix A .

The individual judgements are provided only for the upper triangular answer matrix and the remaining elements (the lower triangular part of the answer matrix) are calculated, as discussed in 3.2.2.3. For that reason, the average of the cumulative sum of the individual judgements provided in the upper triangular part of the individual judgement matrices is considered to construct the upper triangular part of the aggregated answer matrix A^{agg} . The A^{agg} with elements of $a_{i,j}^{agg}$ is constructed for selected number of responses $n.resp$ as in equation 3.6. The elements in the lower triangular part of A^{agg} are populated based on criteria presented in 3.2.2.3.

$$a_{i,j}^{agg}(n.resp) = \frac{\sum_{n=1}^{n.resp} a_{i,j}(n)}{n.resp}, \text{ where } i,j \in NC \wedge i \leq j \quad (3.6)$$

Assuming, the individual responses are sorted in descending order based on their individual CR , the weights factors and the CR of A^{agg} can be evaluated as a function of $n.resp$. If the consistency of provided responses is not satisfactory, the methods for consistency improvements shall be applied. The individual and the cum.sum average CR s for industry and academia related responses only are depicted in figure 3.2.

It is shown, that by constructing the A^{agg} for obtained responses in the survey, the combined response consistency improves to acceptable level compared to individual CR s. This is demonstrated on the comparison of individual CR s for all responses and their A^{agg} as depicted in figure 3.3. Despite the aggregation of numerous inconsistent individual responses (sorted in descending order by their CR s), the A^{agg} consistency

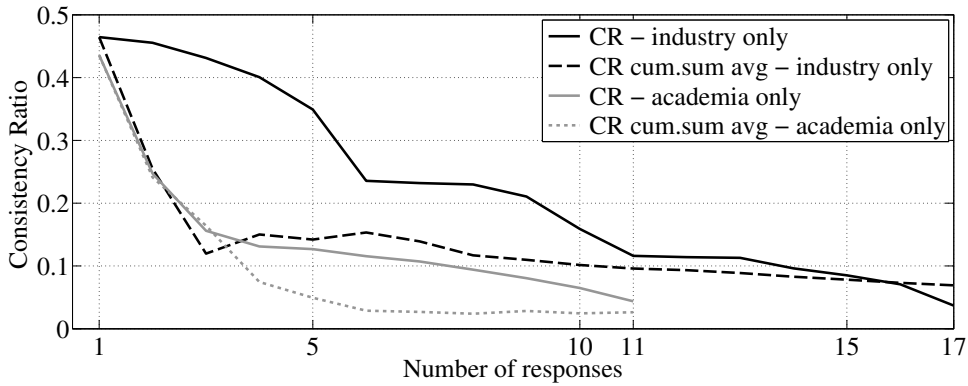


Figure 3.2: The comparison of the individual CR and their cum.sum average for responses received from academia (11) and industry (17) as in table 3.2 .

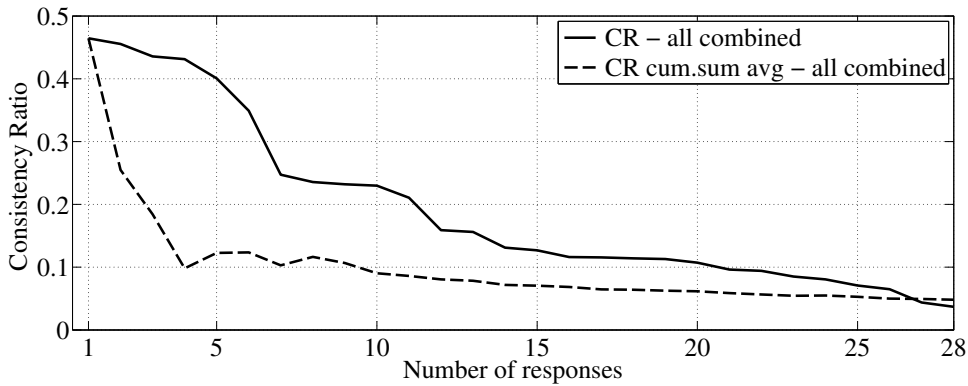


Figure 3.3: The comparison of the individual CR and their cum.sum average for all responses combined as in table 3.2.

significantly improves to acceptable level after aggregation of already 10 responses (36 % of all responses). Even with a significant number of responses with fairly bad consistency (approximately ten responses over 20 %), the averaged responses provided consistent judgement. Similar trend is also observed for the individual groups with industrial and academic affiliation of responders in figure 3.2.

The aggregating effect of A^{agg} on CR is studied in detail and the consistency improvements of A^{agg} as a function of $n.resp$ are evaluated for all $n.resp$, where the individual CR s are sorted in ascending order. The resulting CR s plots of A^{agg}

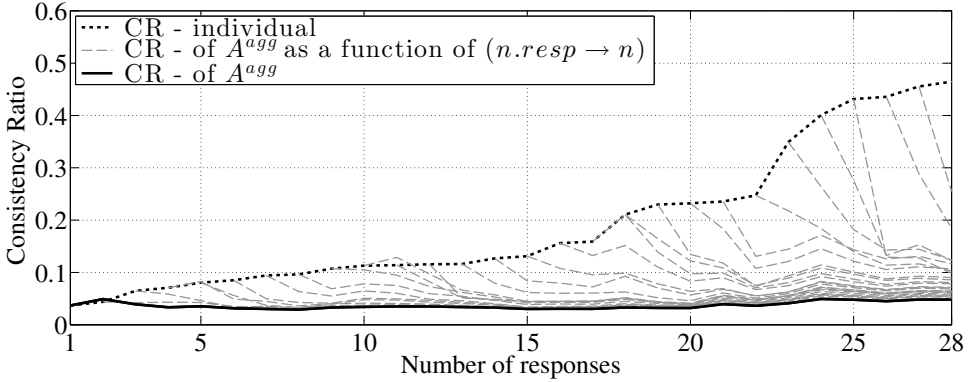


Figure 3.4: The comparison of the individual CR and their cum.sum average for all responses combined as in table 3.2, where $CR(n.resp)$ is estimated based on A^{agg} as a function of $(n.resp \rightarrow n)$.

constructed as a function of $n.resp$ are depicted in figure 3.4. It is observed that the A^{agg} mostly results in improved consistency for already small number of aggregated responses. However, for larger number of aggregated responses, the A^{agg} is considered as consistent for the result of this survey. In addition, it is observed that combinations of responses tend to converge to a A^{agg} with significantly lower CR than CR s of individual responses. This observation can support the argumentation that thanks to the survey structure, the individual inconsistency in judgements has more random characteristics and that most responders tend to provide complementary judgements with similar prioritization of evaluated criteria.

To support this argumentation, the development of criteria priorities as a function of $n.resp$ is depicted in figure 3.5. It can be observed that the criteria weights (relative priorities preference) are not changing significantly for higher numbers of responses received, see figure 3.5, for $n.resp \geq 10$. The turbulent criteria weights for $n.resp \leq 5$ are attributed to the combination of least consistent responses in the survey. The resulting CR s for all evaluated groups are presented in table 3.4

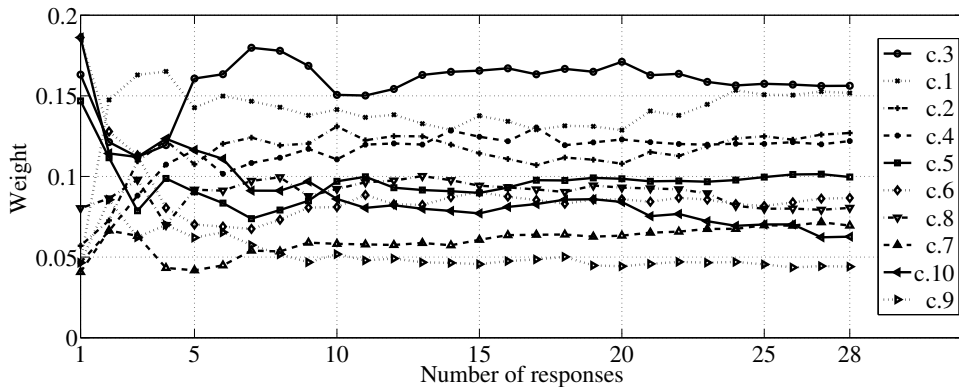
Judging from the results obtained, additional responses will most probably change the resulting priority weights only marginally. As a consequence, the obtained responses can be considered as a sufficient sample to yield representative results in this inquiry.

3.3 Functionality expectations of distribution networks

The AHP methodology was employed to derive the expected functionality of distribution networks. Based on the methodology presented in 3.2.2, the priority ranking of expected distribution network functions (criteria, as in table 3.1) can be estimated for

Table 3.4: Resulting CR factors by groups based on aggregated answers (A^{agg}).

Group description	CR
Industry only	0.069
Academia only	0.026
All combined	0.048

**Figure 3.5:** The comparison of criteria weights (priorities, from table 3.1) as a function of ($n.resp$) for all responses combined in table 3.2.

all evaluated groups from table 3.2. The resulting ranking of expected distribution network functionality is presented in figure 3.6. The three most important distribution network criteria for all responders can be seen in figure 3.6:

- Reliability
- Voltage level
- Other PQ aspects

The aspects of the most important criteria within the scope of this dissertation are addressed in detail for the LV networks in chapter 4 and for MV networks in chapter 5.

3.4 Alternatives selection

AHP methodology was applied for the evaluation of the expected functionality (criteria) to arrive with a quantification of the expert judgements. The extracted knowledge from the criteria ranking for the distribution network from 3.3 is applied to rank the

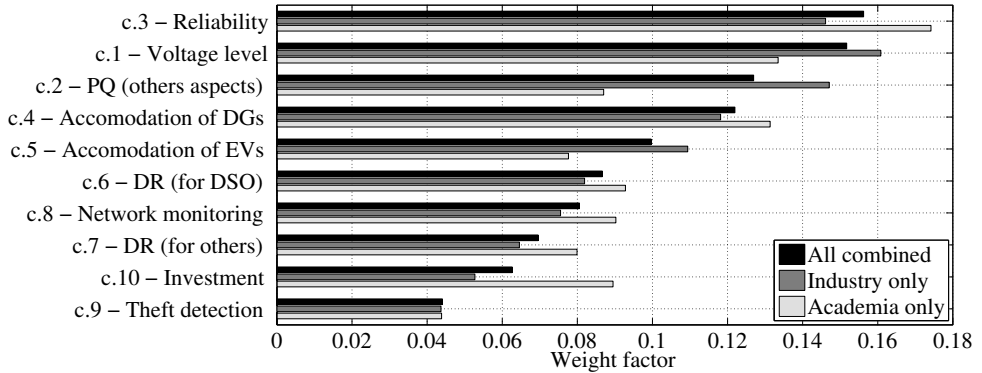


Figure 3.6: The comparison of the expected distribution network functionality criteria and their priorities for all groups, as outlined in table 3.2. The priorities are sorted in descending order based on weight factors of all responses combined.

applicable technological alternatives presented as the third level of AHP hierarchy in figure 3.1. Where each expected network function from figure 3.6 can be satisfied in certain share with one or more technological alternative listed in table 3.5.

Table 3.5: Alternative technologies available for distribution networks and for IDS, based on [66], [67].

Alternative	Description
Alt.1	Energy (battery) storage at LV bus-bar with bi-directional inverter
Alt.2	Smart MV/LV transformer with on-load tap changer (OLTC)
Alt.3	PowerMatcher for electricity markets and DR [84]
Alt.4	MV circuit breakers
Alt.5	LV circuit breakers
Alt.6	Substation instrumentation, communication and measurements

The comparison matrix for the alternatives i.e., the third level of the AHP hierarchy, is based on the qualified judgement of selected participants, which have a specific expert knowledge on the technical aspects of distribution networks and on IDS.

In a similar manner to the second level of the AHP hierarchy, the relative fulfilment of the selected alternatives is assessed as arithmetic mean of individual responses. To arrive at the alternative preferences, the results related to the functionality expectations and their priorities were combined with the expert judgements of relative contribution of each alternative to fulfil specified functionality (criteria). According to AHP, the resulting alternatives ranking is estimated as a product of normalized expert judgements

Table 3.6: Alternative technologies ranking and expert judgement evaluation of fulfilment for all criteria from table 3.1 (rounded).

Criterion	Alt.1	Alt.2	Alt.3	Alt.4	Alt.5	Alt.6
c.1	12 %	73 %	15 %	0 %	0 %	0 %
c.2	73 %	13 %	7 %	0 %	0 %	7 %
c.3	13 %	3 %	7 %	53 %	10 %	14 %
c.4	10 %	33 %	33 %	0 %	9 %	15 %
c.5	17 %	10 %	60 %	0 %	3 %	10 %
c.6	33 %	0 %	54 %	0 %	3 %	10 %
c.7	17 %	3 %	53 %	0 %	7 %	20 %
c.8	3 %	0 %	8 %	9 %	5 %	75 %
c.9	0 %	3 %	3 %	0 %	0 %	94 %
c.10	31 %	17 %	20 %	9 %	5 %	18 %

matrix, presented in table 3.6, and the weights factors for each evaluated criterion from figure 3.6. The combination of this judgements with criteria weights yields the final ranking and priorities of the technological alternatives in figure 3.7, presented in descending order for all three groupings. It is noted that despite obvious preferential differences in the criteria between the two groups - industry and academia - the overall technological alternatives ranking between the groups is consistent in alternatives preferences.

Notably, there are specific preferences indicative of operational practices in the Netherlands. As shown in figure 3.6, responses obtained mainly from the Dutch industry identified a preference to improving the voltage level and other power quality aspects over reliability; this may be due to them recognizing the already high power delivery reliability in the Dutch electrical system. Assuming this, the next concern for Dutch DSOs is the voltage level and power quality. Such a priori information can be used to selectively handle the ranked alternatives: here, the second ranked criterion in the combined group may be given first priority and the third ranked criterion may be given the second priority. Figure 3.7 also shows that the industry values voltage level and power quality over reliability, whereas the academic responders value reliability over all else.

Despite the preferences differences, figure 3.7 shows that both groups, in the same order, prefer technological alternatives such as PowerMatcher (with functions of power matching or power balancing [88]), followed by energy storage, to achieve the overall goal to increase the utility of distribution networks and IDS. The priority differences among the group are marginal and do not influence the resulting alternative preferences. However, Dutch DSOs in the current legal framework have to operate as unbundled utility and cannot be directly involved in energy trading, as this will be inherent to the two top ranked alternatives. The most preferable technological

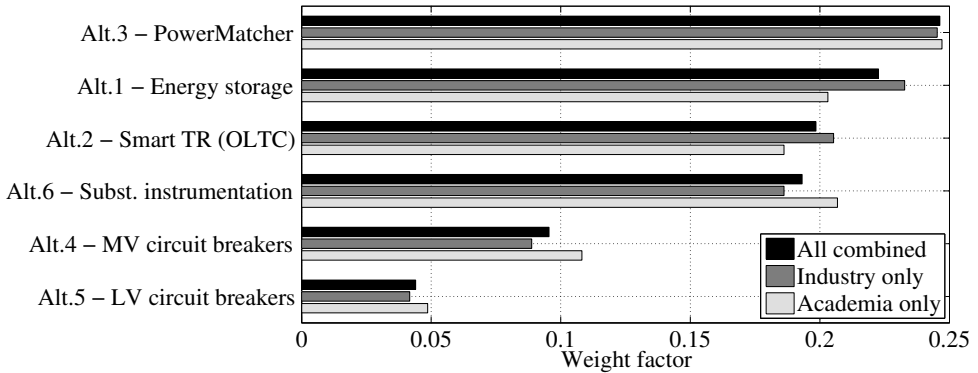


Figure 3.7: Weights factors of third level AHP hierarchy (alternatives ranking) for three groups of responders based on table 3.2.

alternatives might not be utilized due to this restrictions. Nevertheless, Dutch DSOs can already currently utilize the next highest ranked alternatives such as transformer with OLTC and substation instrumentation. Both those technological alternatives are already available to be deployed by DSOs in the Netherlands.

3.5 Conclusions

Many developments are predicted to happen in the distribution networks in the future. However, to reasonably reveal the plausible developments in the distribution network, the AHP methodology as a MCDA tool was applied.

Based on the hierarchy considered here - with the objective of achieving higher performance of distribution networks - the priorities of each criterion are evaluated. The responses and resulting priorities are divided in three groups: priorities based on replies from industry only, academia only, and all responses combined. By extracting the expert knowledge from responders, the criteria of expected distribution networks functionality are obtained and quantified. As a consequence, the expectations on the functionality level can be translated into ranking of suitable technological alternatives applicable to the distribution networks and especially to intelligent MV/LV substations.

In this chapter is also shown that with already approximately 36 % of received responses, the overall priority rankings stabilize and do not change significantly as more responses are considered. As a consequence, it is concluded that a sufficient sample of responses has been collected to provide satisfactory and representative results for evaluated group; and, the results are unlikely to change significantly with more responses. The application of the AHP methodology also allows to quantify the most

important criteria (expected network functions) for the distribution networks, which are consequently addressed in this dissertation.

The presented criteria priority ranking can also be applied for instrumenting the distribution network assets such as IDS and to resolving competing objectives during network operation.

Based on the functionality preferences, the resulting ranking of preferred technological alternatives is obtained. Despite some differences in the criteria weights and ranking among groups of responders, the resulting selection of preferred technological alternatives shares similarities in priority ranking for all groupings.

New technological alternatives should be subjected to a cost-benefits analysis and to the compliance check with the Dutch legal framework, before deployment at a DSO. Due to the constraints enforced by the Dutch legal framework for Dutch DSOs, the subset of available technological alternatives applicable to them is also identified. Notably, for the two top ranked alternatives, the benefits for a DSO can be ambiguous and might not be outweighed by the cost of acquiring and operating the assets, which might be technologically immature at a present time. The above mentioned limitations can make the deployment of a technologically preferable solutions prohibitive for a DSO, not only in economic sense.

As a consequence of the results presented in this chapter, the most important network functions (expected functionality) within the scope of this dissertation and the plausible technological alternatives applicable for Dutch DSO environment to enable this functionality are assessed in a greater detail in this dissertation. Especially the voltage level control with OLTC and substation instrumentation for PQ measurements in chapter 4 for LV networks and in chapter 5 for MV networks.

LV distribution networks

4.1 Introduction

The LV distribution networks have been designed to accommodate residential and small commercial network users (commonly labeled also as: consumers, end-entities, end-users or prosumers). In the Netherlands, the majority of the network users (≥ 6 millions) are residential or small business network users connected directly to the LV network. The LV networks can be seen as the end points in the traditional power system, where the electricity was generated centrally.

Nowadays, the connected network users are becoming more active in obtaining new types of appliances, which are connected via their residential installations to the LV network (both new loads and distributed generators are connected in increasing numbers and sometimes at rapid speed, as discussed in 2.3). The individual impact of a small network user on the whole network is minor, but the combination of network users appliances can consequently amplify their individual impact. This can create new challenges on the current distribution network, which have to be addressed by DSOs. Despite numerous developments on the network user side, a DSO is still responsible for delivering certain quality of supply voltage and service to the network users (or customers) and has to employ technical solutions to mitigate the impact of connected appliances on the distribution network within the responsibility of a DSO [28].

As a consequence of those developments, more insights and awareness about the operation of the LV distribution networks is required to increase the performance of the LV network. The voltage level and other PQ aspects are identified as one of the most important criteria for distribution network operation and are discussed in this chapter. The presented considerations are based on guidelines for required voltage quality outlined in international standards for supplied voltage quality applicable to DSOs [46].

4.2 Typical LV distribution network in the Netherlands

The estimated length of the LV circuits in the Netherlands was 122 124 km in 2009 [49] and almost all LV circuits consists of underground cables. Taking into consideration, that the new LV networks are solely underground cable networks, the model of a generic LV network in the Netherlands consist also of underground cables [27].

The key parameters of a typical LV network, as designed in the last decades in the Netherlands by Alliander, are:

- MV/LV transformer (10/0.4 kV, in general $S_n^{tr} = 400 \text{ kVA}$, Dyn connection type)
- 4 main feeders connected to the MV/LV substation (with $A = 150 \text{ mm}^2$ (Al), four-core (PEN), with length of 500 m per feeder)
- Radial layout of the LV network
- 240 LV customers supplied (single-phase or three-phase, connected to the main feeder with via a four-core (PEN) connection cable $A = 10 \text{ mm}^2$ (Cu) with 10 m length per cable)

The schematic topology of a typical LV network is depicted in figure 4.1. On average 240 LV network users are supplied by a single MV/LV transformer. The majority of network user connections are realized as single-phase, where an network user is connected via a connection cable to one of the main feeders. The connections are equally distributed among a feeder and phases. The interface of customer installation and the LV network is labelled as the point of connection (POC), indicated as the tip of the arrow in figure 4.1. The "Netcode Elektriciteit" defines that the connection to the network users with required power $\leq 60 \text{ kVA}$ shall be provided as a LV network connection (three-phase-connection), where the network users with required power $\leq 5,5 \text{ kVA}$ can be provided with a single-phase connection [47].

4.3 Electricity load profile characterization for residential LV network users

A suitable characterization of load profile is a necessary input for realistic simulations of the LV distribution network. The load profiles of connected network users depend on their appliances and time of use, which is strongly influenced by many factors such as geographic location, customers preferences and seasons.

4.3.1 Load characterization based on field measurements

One of the possible approaches to reconstruct LV load profile is the bottom-up approach, where the number of appliances and their time-of-use is evaluated (e.g., with a survey). The data obtained can be used to reconstruct individual or aggregated load profile of

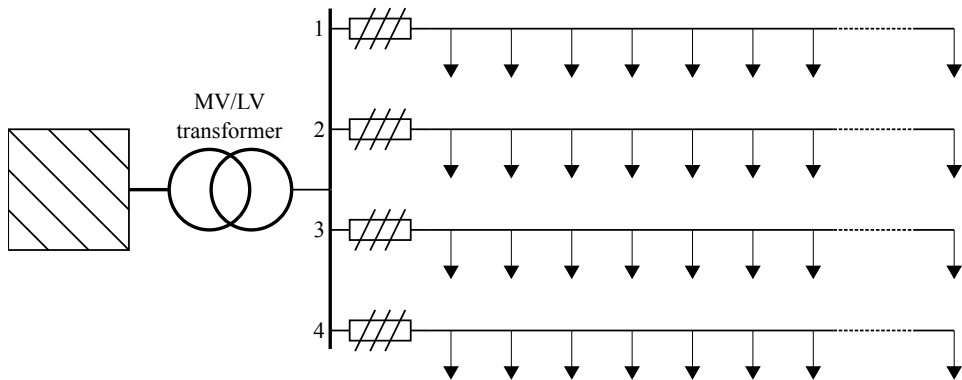


Figure 4.1: The schematic topology of a typical LV distribution network in the Netherlands. On average 240 equally distributed network users are connected via connection cable to main feeders. The MV/LV transformer supplies via the LV bus-bar 4 main feeders from the MV network.

an average household. This approach is time intensive and requires good knowledge of customer behaviour, socio-economics and demographics in the investigated area. In addition, commitment of participants and accuracy of their statements is necessary to derive representative load profiles. Nevertheless, the profiles obtained by this methodology can capture accurately only a share of all appliances connected, and are burdened by the time of conducted survey. Accurate load profiles over a longer period are difficult to obtain. Example of load profiles studies can be found in [89, 90, 91].

Extensive measurements are necessary to obtain an appropriate data set enabling characterization of residential load profiles. Measurements of residential electricity load profiles were conducted in a typical LV network in the Netherlands during several weeks in the winter period and during several weeks in the summer period. The average power measurements at customers POCs were obtained and reported in 15 min. intervals. An example of 5 measured load profiles is depicted in figure 4.2, which demonstrates the stochastic nature and differences present in individual load profiles. A high load peak (close to 7 kW) can be observed in measured data. The presence of high load peaks is acceptable due to the design of distribution networks. Nevertheless, the load peaks of similar amplitude are not currently considered in LV load models used for LV network design and planning [92].

The load at about 200 POCs was measured and the resulting aggregated load profiles over a week for the summer and the winter period are depicted in figure 4.3. The aggregated demand curves represent the load patterns, which could be observed at the substation level (including network losses). The high peaks caused by individual households are smoothed out.

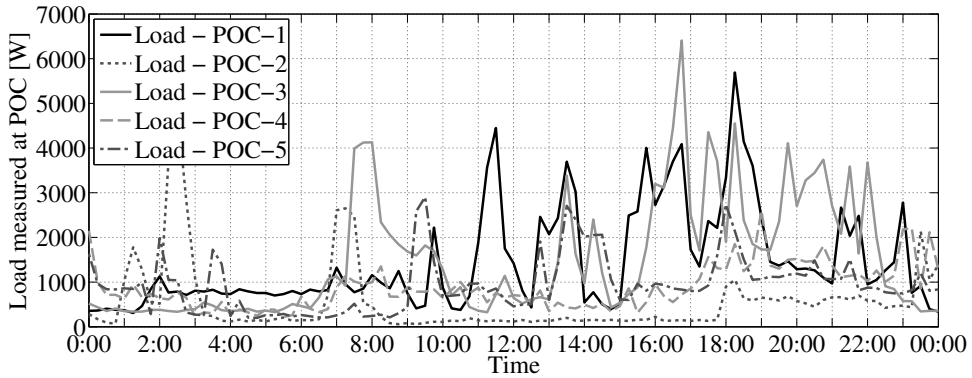


Figure 4.2: The load profiles of 5 measured LV network users during one winter day. The individual differences and stochastic nature of load profiles can be seen.

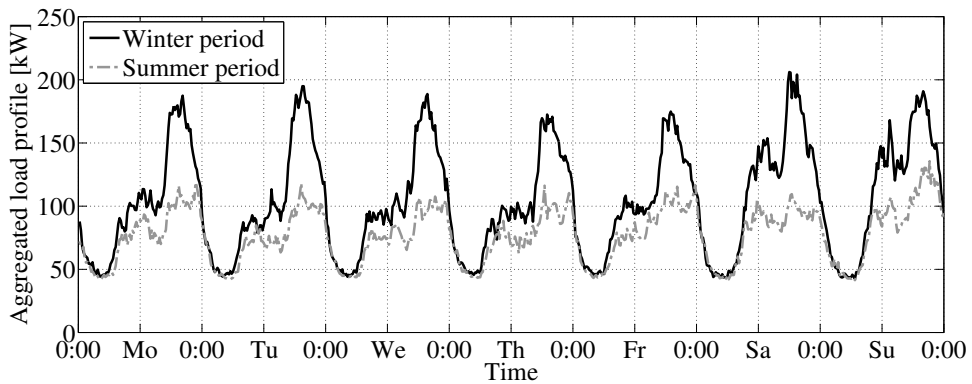


Figure 4.3: The aggregated load profiles of measured POCs during a week in the summer and in the winter period.

4.3.2 Generation of LV load profiles based on field measurements

As only a limited number of measurements is available for the research purposes, the different load profiles are characterized and a methodology for generation of similar load profiles (with the same key parameters) is presented in this section. The ability to generate additional network users load profiles enables more comprehensive simulations on the LV network.

The generated load profiles shall be compared with the measured data. The equality of two data sets (measured and generated load data) can be quantified based on

the Kolmogorov-Smirnov test (K-S test). The K-S test is based on the evaluation of the maximal absolute difference between empirical cumulative distribution functions (ECDF) of two data sets, as in equation 4.1. The K-S test can be used to assess the similarity of two data sets, or of one dataset and the ECDF of a selected reference probability distribution under test.

$$\max |F_{t1}(x) - F_{t2}(x)| \quad (4.1)$$

Where in equation 4.1, $F_{t1}(x)$ is the proportion of first tested data less than or equal to x (power measurements) and $F_{t2}(x)$ is the proportion of tested values less than or equal to x from either the second tested data set or from the reference distribution under test. The null hypothesis assumes that the two tested distributions are equal within defined significance level. The K-S test is repeated for each time instance (measurement) and the null hypothesis is rejected at 5 % significance level.

The application of the methodology based on the gamma distribution is regarded as suitable approximation to LV load profiles and was also tested on measured data [90]. Nevertheless, the K-S test rejected the null hypothesis for the measured data set compared with the set generated based on the gamma distribution, in 46 % of the time instances for the summer period and in 26 % of the time instances for the winter period. The measured data set contains numerous data points (e.g., with high load measurements), which are not sufficiently captured by the gamma distribution. Based on this equality assessment, it is concluded that the gamma distribution is an inaccurate (and inadequate for purposes of this study) distribution representing the measured data set and other, more accurate methodology, needs to be employed for load data generation.

The proposed methodology to generate LV load profiles is based on a random selection from the ECDF and is described by the following steps:

- Estimate ECDF of measured data set for every time instance separately
- The random selection (with uniformly distributed pseudo-random numbers) from the estimated ECDF yields the required number of generated load profiles for every time instance
- The equality of the generated load profiles is compared with the original data set
- The load generation procedure is repeated over the required number of time instances (e.g., to obtain one week of generated data for arbitrary number of network users)

The resulting set of generated load profiles was compared with the measured data on basis of following criteria:

- Compliance with the two-sample K-S test

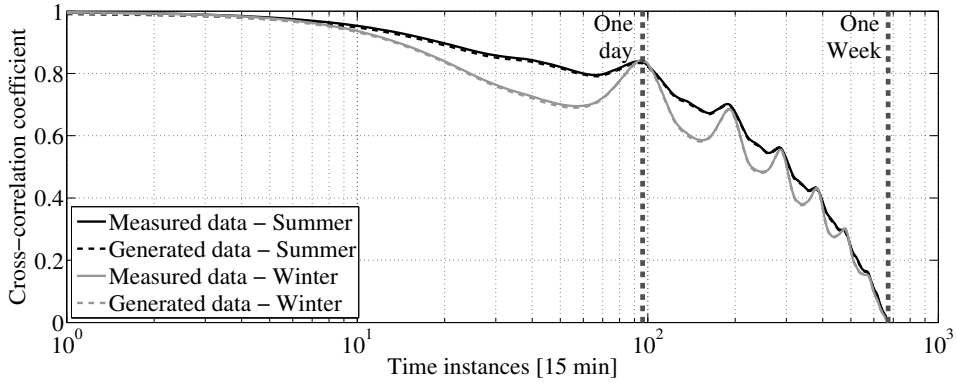


Figure 4.4: The cross-correlation coefficients of aggregated network users load profiles from measured and generated data sets during one week, for the summer and the winter period. The one day and the one week differences in the sliding window between the evaluated data sets are depicted as dashed vertical lines.

- Presence of similar daily and weekly patterns in both data sets

The data evaluation and generation was implemented in MATLAB environment. In the two-sample K-S test, the null hypothesis that the distributions are similar was rejected in less than 0.5 % of evaluated time instances for both the summer and the winter period. The mismatches of both distributions are only minimal compared with the data generated based on gamma distribution. The differences can be attributed to stochastic nature of data selection process and to the size of the measured data set.

Despite the stochastic nature of the data generation process, the characteristic daily and weekly load patterns shall be also preserved in the generated data sets. To validate this assumption, load profiles of 240 LV residential network users in duration of one week for the summer, and for the winter, period were generated.

The cross-correlation, as a function of the time lag applied to two signals (sliding dot product), is commonly used as a measure to compare the similarity of two signals. The aggregated load data, based on generated and measured network users load profiles, are used as input signals for the cross-correlation assessment. The resulting cross-correlation coefficients of aggregated profiles for both data sets are depicted in figure 4.4, where one day and one week differences in the sliding window between the evaluated data sets are depicted as dashed vertical lines. The cross-correlation of both signals exhibits strong similarities with simultaneously occurring patterns, which can be observed in both data sets on daily and weekly basis.

The proposed approach enables to generate load profiles in accordance with the observed distribution in the measured data. The key parameters of the load profiles

Table 4.1: The key characteristics of measured network users load profiles.

Period	Peak load observed at a POC	Average peak load for all network users	Average load of all network users
Summer	7 896 W	710 W	407 W
Winter	6 892 W	1 015 W	518 W

are preserved also in the generated data. The values of the average load, the average peak load and the maximal peak load are listed in table 4.1. The average peak load is a parameter important for distribution network planning and the maximum value (for the winter period) in table 4.1 is close to the commonly used value of 1.1 kW in the Netherlands.

The presented methodology enables generation of an arbitrary number of stochastic LV network users load profiles for more realistic simulations on LV network. This methodology is applied for the simulations on the typical LV network in the Netherlands.

Nevertheless, some limitations of the proposed methodology shall be noted. The evaluated measurements were only available for a limited number of POCs and only in 15 min. intervals. Whereas, this is sufficient for characterization of LV load profiles, network planning and for design purposes, it is not sufficient for evaluation of power quality phenomena in detail. If the measurements at POCs were available at a higher sampling rate, the same methodology can be applied for load profile characterization and network users load profiles generation. The applied methodology also emphasizes on the stochastic data generation and suppresses conditional probability to generate more diversified load profiles.

Nowadays, the apparent approach to obtain reliable load profiles is the utilization of smart metering infrastructure, which can provide accurate input data for large number of network users over long period. However, the application of this approach is significantly limited by the privacy concerns and access restrictions to the data.

4.4 Voltage deviations in distribution networks

Improving and maintaining the acceptable voltage level for all connected network users is ranked as the most important criterion (quality aspect) in distribution networks from the DSO perspective, as addressed in 3.3.

The quality of supplied voltage is defined as the set of minimum requirements on the supplied voltage for connected network users, which has to be provided by the DSO at their POC, if not contracted otherwise. In the Netherlands, the requirements on the supply voltage level are specified in EN 50160 [46] and in the Dutch "Netcode Elektriciteit" [47].

The voltage level is related to the nominal voltage U_n , for which the supply network is designed. The standard nominal voltage is 230 V [46], which is measured between

Table 4.2: The requirements on supply voltage level for network users connected to LV network (with nominal voltage $U_n \leq 1 \text{ kV}$).

Specifications (U_c within)	Description	Test methodology
$U_n \pm 10 \%$	Defined by EN 50160 [46] and by "Netcode Elektriciteit" [47] for all network users	Applicable for 95 % of the measurements (measured as 10 min. mean rms values over one week period)
$U_n + 10 \% \wedge U_n - 15 \%$	For special situations, defined by EN 50160 [46] for not interconnected networks with the transmission system or special remote areas	All measurements shall be within $U_n + 10 \% \wedge U_n - 15 \%$

phase and neutral (in the four-wire three-phase system). A different supply voltage U_c can be also agreed between a DSO and a network user. Generally $U_c = U_n = 230 \text{ V}$ in public low voltage networks [46]. The set of minimal requirements regarding the voltage level for network users connected at LV network (with nominal voltage $U_n \leq 1 \text{ kV}$) is presented in table 4.2.

A voltage deviation in the network ΔU or a voltage deviation ΔU_g due to a generator g supplying current I_g (or apparent power S_g) with the phase angle between current and voltage φ , in the LV network with impedance Z_{net} (with resistance R_{net} and reactance X_{net}) can be determined with equation 4.2 [27].

$$\Delta U_g \approx I_g (R_{net} \cdot \cos\varphi + X_{net} \cdot \sin\varphi) = \frac{R_{net} \cdot P_g + X_{net} \cdot Q_g}{U_g} \quad (4.2)$$

The voltage deviation ΔU_{cs} (e.g., voltage drop or rise), as the difference between two end voltages \vec{U}_1 , \vec{U}_2 , across each cable or feeder section in the LV network depends on active P_{cs} and reactive power Q_{cs} transferred across the cable section and on cable parameter Z_{cs} (with R_{cs} and X_{cs}). The voltage deviation can be estimated based on 4.3 for each cable and feeder section in the LV network. Similarly, also the voltage drop or rise across the MV/LV transformer can be estimated.

$$\Delta U_{cs} = |\vec{U}_1 - \vec{U}_2| \approx \frac{(R_{cs} \cdot P_{cs} + X_{cs} \cdot Q_{cs})}{U_1} \quad (4.3)$$

The distribution networks supply mostly single-phase residential network users or commercial network users with a three-phase connection. Therefore all simulations on

the LV network are based on the four-wire unbalanced load flow. The unbalanced three-phase currents, due to asymmetrical loading, result in non-zero neutral current I_N in the LV network, which is also considered in LV simulations.

The resulting voltage conditions in the LV network can be estimated with an iterative process based on Newton-Raphson solution finding method. The network simulation methodology is corresponding to the presented approaches in [27] and [24].

4.5 Voltage level conditioning with OLTC

The LV distribution networks are designed to accommodate network users loads. However, the increasing amount of small DGs (e.g., PVs with certain output patterns) connected directly to the LV network changes the voltage level conditions in the LV network. A DG installation at premises of one user influences not only voltage level at his POC, but also the voltage level in the LV network, as detailed in [93]. In addition, EVs can operate also as electricity source in the V2G mode. Both EVs and DGs can create new challenges for LV network operation, as mentioned in 2.3.

As shown in the table 4.2, the target for Dutch DSOs is to maintain the voltage level variations within $U_n \pm 10\%$, for all LV network users connected. Although the current standards defines this limit only for 95 % of the weekly values, it is anticipated that the future will extend the requirements for 99 % or 100 % of measured values [94].

In the context of Dutch environment, a DSO has limited options to address voltage level conditioning in the LV networks during their operation. The preferable technical solution to improve the LV voltage level conditions is the application of a MV/LV transformer with OLTC, as discussed in 3.4. The voltage level control based on reactive power control is not suitable alternative for Dutch LV underground cable network due to prevailing resistive character of the LV networks, as pointed out in [27].

Therefore, the application of OLTC with the MV/LV transformer to improve voltage level conditions in LV networks is investigated. The assessment focuses on finding of the most suitable control strategy for OLTC and considers also the required data acquisition from the LV network.

4.5.1 OLTC at MV/LV transformer

The current LV networks are supplied by a traditional MV/LV transformer with an off-load tap changer, which is adjusted off-line during the installation or after a topology change in the network. The off-line tap position is typically set to $10/0.4\text{ kV} + 2.5\%$ to offset the voltage drop in LV and MV network due to loads considered. The varying voltage conditions in the network will require in the future (independent) voltage level conditioning of LV networks during their operation, especially when MV voltage level control is not possible [27].

The so called "smart transformer" is a traditional MV/LV transformer equipped with a power electronic tap changer on the MV side, which is capable of adjusting the

secondary voltage on-line (continuous operation of tap changing) [95], [96]. An OLTC installed at the MV/LV substation offers applications for [97]:

- LV networks, where OLTC can mitigate voltage level fluctuations due to presence of DGs [98]
- MV networks, where OLTC can reduce the propagation of MV voltage level fluctuations to the supplied LV network, as discussed in 5.3 and in [99]

With a MV/LV transformer equipped with OLTC, the voltage level at the LV side is no longer directly linked to the voltage level at the MV side and the LV bus-bar voltage is not directed by the load conditions in the network.

4.5.2 OLTC at MV/LV transformer - case studies on Dutch LV network

A set of case studies is presented to assess the possibilities of voltage level conditioning with OLTC equipped MV/LV transformer in LV networks. Three different operational approaches of OLTC control are discussed and evaluated. The requirements on measurements among the LV network to enable the desired operation goals of an OLTC are also considered.

The case studies were performed on a typical LV network in the Netherlands, as discussed in 4.2. The LV network users loading profiles were generated based on field measurements in 15 min. resolution over one week period, as presented in 4.3. An additional DG generation profile was added to the load profiles of network users connected, to simulate the output of PV installations connected to the LV network. Especially the voltage level increase due to the presence of DGs is investigated in detail during the low-load and high-generation period (summer period). The PV profile (as DGs output) is based on measured PV profiles in the Netherlands and an example of the normalized power output for the summer period is depicted in figure 4.5.

The maximum power output (rating) of individual DGs is set to be related to the nominal rating of the MV/LV transformer supplying the LV network. The maximal DG generation in the LV network is assumed to be up to the nominal transformer rating. Certain diversity of DGs allocation in the LV network is assumed to represent realistic and more challenging conditions for OLTC operation. The DGs are simultaneously operating (PV installations) and are connected only to 3 out of 4 LV feeders.

The evaluated case studies differ in the sizing of DGs connected in the LV network. The ratio of DGs in the LV network (DG_{ratio}) is the share of the sum of maximum power outputs of all (n) DGs in the LV network over the nominal MV/LV transformer rating, as in equation 4.4.

$$DG_{ratio} \approx \frac{\sum_{i=1}^n (P_{max}^{DG}(i))}{S_n^{tr}} \quad (4.4)$$

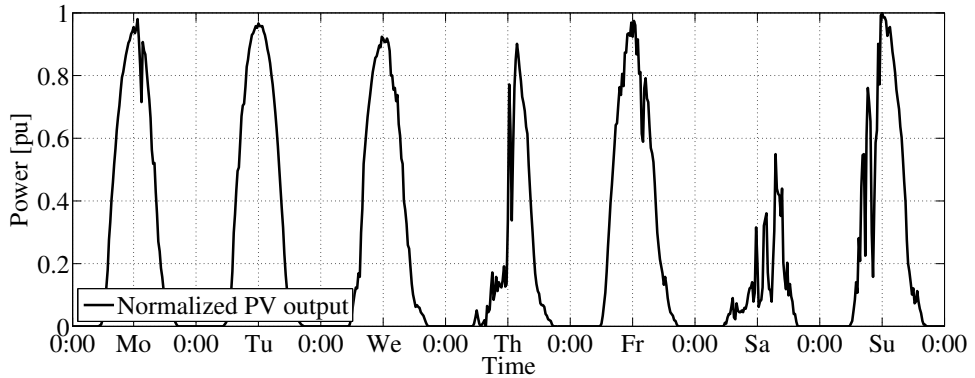


Figure 4.5: The measured PV profile (normalized output) over a week in the summer period in the Netherlands.

Based on the DG_{ratio} for each case study, the maximum power output of P_{max}^{DG} of individual DGs is estimated. The constant distribution of DG rating among feeders is kept for all simulations such, that feeder 2 and 3, with larger DG installations, have each 43 % of all DG installations connected ($0.43 \cdot \sum_{i=1}^n (P_{max}^{DG}(i))$). Feeder 1, with smaller DG installations, has the remaining 14 % of all DG installations connected ($0.14 \cdot \sum_{i=1}^n (P_{max}^{DG}(i))$). The last feeder 4 is assumed to be without DG installations. The small business PV installations or PV installations on a farm are simulated by 4 larger three-phase DGs (PV installations, each with maximum power output of $P_{max}^{DG} = 14.3 \text{ kW/phase}$ for $DG_{ratio} = 100 \%$), which are connected to the last 4 POCs at main feeders 2 and 3. The residential PV installations are simulated as 20 smaller DGs (PV installations connected to single-phase at 20 POCs, each with $P_{max}^{DG} = 2.9 \text{ kW/phase}$ for $DG_{ratio} = 100 \%$) connected to feeder 1.

The voltage level conditions are evaluated for every POC independently, but the results are grouped for 3 neighbouring POCs for better representation. The connection of DG installations to the LV network, and their grouping, is schematically depicted in figure 4.6. Five case studies are investigated with a different DG_{ratio} , covering the cases with highest DG penetration in the LV network to the base case without DGs. The rating of DGs per feeder (f_1, \dots, f_4) for each case study is detailed in table 4.3.

The evaluated voltage level conditions for each case study are assessed based on the following control strategies for OLTC [98]:

- Control strategy A - the OLTC is adjusted to keep the LV bus-bar voltage in the MV/LV substation at a constant value ($U_n = 230 \text{ V}$). This control strategy requires only local measurements of voltage level at the LV bus-bar in the MV/LV substation

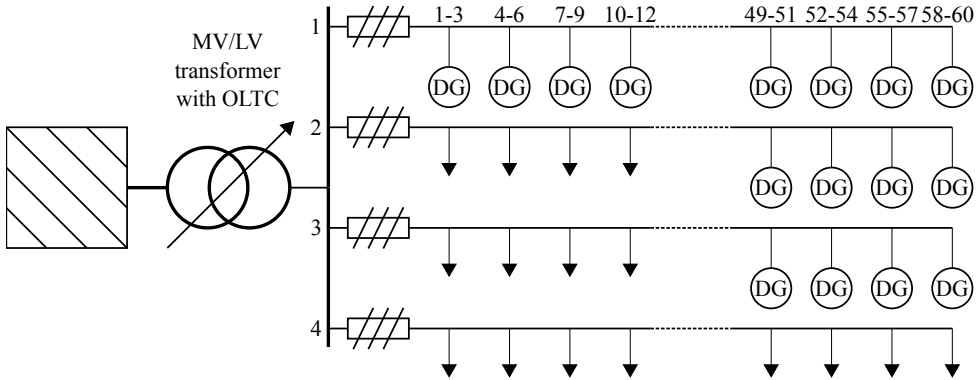


Figure 4.6: The schematic topology of investigated LV distribution network based on the typical LV network in the Netherlands as in figure 4.1. 240 equally distributed network users are connected via connection cable to 4 main feeders resulting in 60 network users connected to each main feeder. The network users POCs are labelled in ascending order from the MV/LV substation, where 3 neighbouring network users are schematically grouped. The allocation of DGs is indicated; feeder 1 accommodates DGs distributed along the whole feeder, feeder 3 and 4 accommodate DGs connected to the last POC's and feeder 4 is without DGs, as detailed in table 4.3.

- Control strategy B - the OLTC is adjusted to maintain the average voltage level at the end of the feeders ($U^{POC(60)}$) at constant value ($U_n = 230 V$), as in equation 4.5. The typical LV network topology has 4 main feeders

Table 4.3: The rating of DGs per feeder, as depicted in figure 4.6, for all investigated case studies based on their DG_{ratio} .

Case study with DG_{ratio}	Feeder 1 $\sum(P_{max}^{DG,f1})$	Feeder 2 $\sum(P_{max}^{DG,f2})$	Feeder 3 $\sum(P_{max}^{DG,f3})$	Feeder 4 $\sum(P_{max}^{DG,f4})$	Total rating of all n DGs $\sum_{i=1}^n (P_{max}^{DG}(i))$
100 %	57 kW	171.5 kW	171.5 kW	0 kW	400 kW
80 %	46 kW	137 kW	137 kW	0 kW	320 kW
60 %	34 kW	103 kW	103 kW	0 kW	240 kW
40 %	23 kW	68.5 kW	68.5 kW	0 kW	160 kW
20 %	12 kW	34 kW	34 kW	0 kW	80 kW
0 %	0 kW	0 kW	0 kW	0 kW	0 kW

($n.feeders = 4$), as in figure 4.6, and the average voltage is maintained at U_n .

$$\frac{\sum_{f=1}^{n.feeders} U^{POC(60)}(f)}{n.feeders} = U_n \quad (4.5)$$

This control strategy requires measurements from POCs at the end of each main feeder ($U^{POC(60)}$), which could be obtained by a smart metering infrastructure and communicated to the MV/LV substation. The tap position in the MV/LV substation is selected to offset the voltage drop in the MV network and the voltage deviations due to the loads and generations present in the LV network

- Control strategy C - the OLTC is adjusted to keep the desired voltage level for all POCs at all connected feeders at constant value ($U_n = 230 V$) on average, as in equation 4.6. The typical LV network topology has 60 POCs on each main feeder ($n.POCs = 60$), as depicted in figure 4.6.

$$\frac{\sum_{f=1}^{n.feeders} \sum_{POC=1}^{n.POCs} U^{POC}(f, n.POCs)}{n.feeders \cdot n.POCs} = U_n \quad (4.6)$$

This control strategy is the most demanding on data acquisition and communication, as it requires measurements from all POCs in the LV network to be communicated to the MV/LV substation for OLTC positioning. The resulting tap position in the MV/LV substation is selected based on the evaluation of the voltage level conditions in the whole LV network

The voltage level magnitudes were estimated in MATLAB for each OLTC control scenario and for each case study. The results for $DG_{ratio} = 100\%$ are presented in detail. The results are depicted as box plots for groups of POCs or whole network, where the central marks of boxes are the median values, the edges of the boxes are the 25th and 75th percentiles and the outliers are plotted individually. In accordance to the requirements on supply voltage level in EN 50160, as discussed in 4.4, the voltage limits ($U_n - 10\%$ and $U_n + 10\%$) are plotted in figures as dashed lines.

As the base case, the voltage level deviations as a function of DG_{ratio} are estimated for all case studies, from table 4.3, for scenario with no OLTC control applied in MV/LV substation. The results are depicted in figure 4.7. Without the MV level fluctuations, increasing share of DGs connected to the network (higher DG_{ratio}) results in larger voltage deviations for network users. Two case studies with high DG_{ratio} represent situations, where the voltage level is not complying with the EN 50160 standard [46].

The detailed voltage level deviations for the investigated LV network, where $DG_{ratio} = 100\%$ as in table 4.3 and no control action is taken on OLTC in the MV/LV substation, is depicted in figure 4.8. It can be observed that network users connected

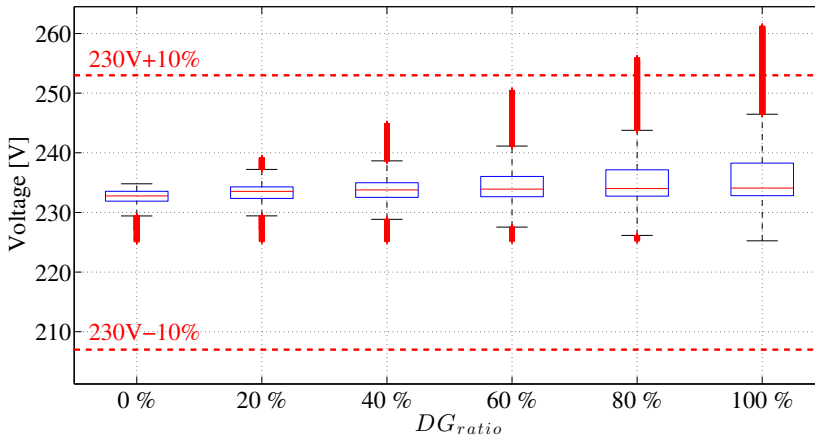


Figure 4.7: The voltage deviations in the investigated LV network as a function of DG_{ratio} from table 4.3 for no OLTC control strategy applied in the MV/LV substation and without MV voltage variations.

at more distant POCs from the MV/LV substation will experience higher voltages than allowed by the EN 50160 standard. This situation is unacceptable and the DSO will have to take corrective actions to improve the voltage level for supplied network users.

The voltage level in the investigated LV network is assessed for all the different OLTC control strategies. For LV network with $DG_{ratio} = 100\%$, as in table 4.3, with OLTC control strategy A applied are the results of voltage levels for all POCs depicted in figure 4.9. The voltage level condition improves such that all network users are supplied with an acceptable voltage level based on EN 50160 standard. By the virtue of the control strategy, the smallest voltage deviation from U_n can be observed at POCs closest to the MV/LV substation.

The voltage level conditions for the investigated LV network with $DG_{ratio} = 100\%$ as in table 4.3 and OLTC control strategy B applied, are depicted in figure 4.10. The voltage level condition for all network users are acceptable considering the EN 50160 standard. The control strategy B emphasises the voltage level conditioning based on voltage level at the end of the main feeders, which can be also observed in figure 4.10.

Similarly, the voltage level conditions for the investigated LV network with $DG_{ratio} = 100\%$ as in table 4.3, with OLTC control strategy C applied, are depicted in figure 4.11. Also for this OLTC applications, the voltage levels for all network users are acceptable considering the EN 50160 standard. The control strategy C gives importance to keeping the average voltage level at desired value for all network users, which can be seen in figure 4.11, where the median values for the POCs in the middle of the feeders

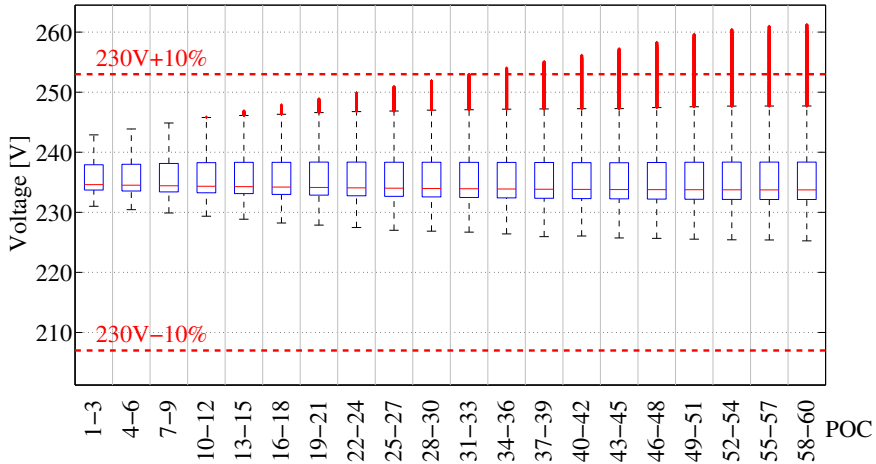


Figure 4.8: The voltage deviations in the investigated LV network for all connected network users for $DG_{ratio} = 100\%$ as in table 4.3, without the application of the OLTC in the MV/LV substation.

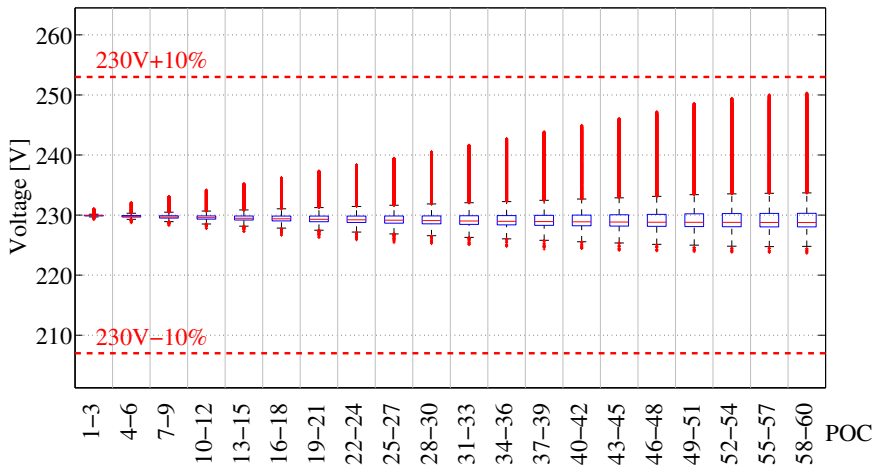


Figure 4.9: The voltage deviations in the investigated LV network for all connected network users for $DG_{ratio} = 100\%$ as in table 4.3. The control strategy A is applied to control the OLTC in the MV/LV substation.

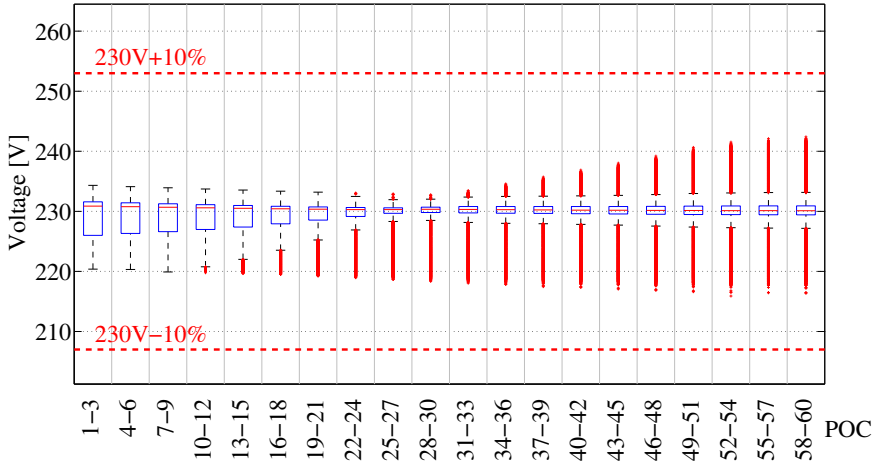


Figure 4.10: The voltage deviations in the investigated LV network for all connected network users for $DG_{ratio} = 100\%$ as in table 4.3. The control strategy B is applied to control the OLTC in the MV/LV substation.

are close to desired U_n value.

For $DG_{ratio} = 100\%$, the voltage level conditions for all investigated control strategies A, B and C are contrasted with the situation, where no OLTC control is applied, as depicted in figure 4.12. All evaluated control strategies improve the supplied voltage level for LV network users to acceptable levels according to EN 50160 standard [46]. Nevertheless, control strategy B and C require data acquisition from POCs in the LV network for their operation, which can be difficult and costly to obtain in a reliable manner. Therefore, the OLTC control strategy A, based only on local measurements in MV/LV substation, shall be the preferable solution for voltage level conditioning.

The importance of voltage control in the LV network is demonstrated in this section. A high penetration of DGs in LV network can cause voltage level deviations, which are unacceptable according to the EN 50160 standard. Moreover, the voltage fluctuations in the MV network can amplify the voltage deviations in connected LV networks. The OLTC was identified as preferable technical solution for DSO deployment in 3.4. Therefore, the concept of OLTC operating in the MV/LV substation is applied to attenuate the unwanted voltage deviations in the LV network. The results are compared for different penetration levels of DGs and contrasted with the current situation, where no OLTC control strategy is applied. The application of OLTC improves the voltage conditions for all connected network users and as a consequence facilitates accommodation of more DGs in the LV networks. It is concluded that the OLTC control strategy A (keeping the

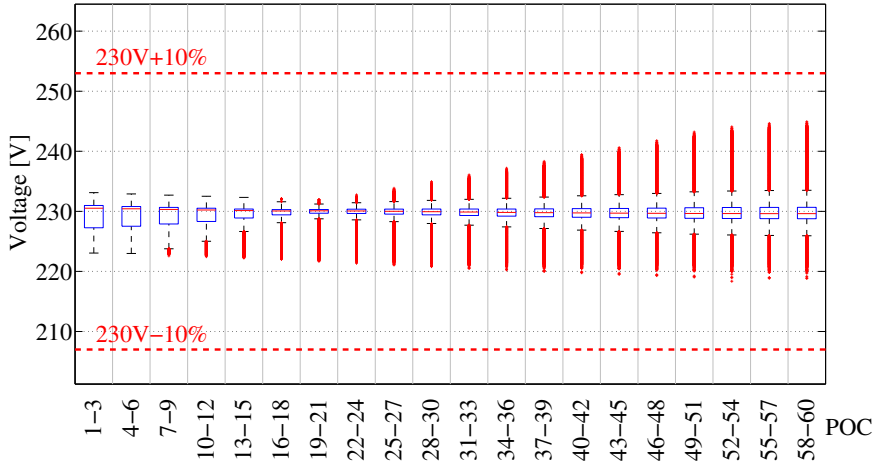


Figure 4.11: The voltage deviations in the investigated LV network for all connected network users for $DG_{ratio} = 100\%$ as in table 4.3. The control strategy C is applied to control the OLTC in the MV/LV substation.

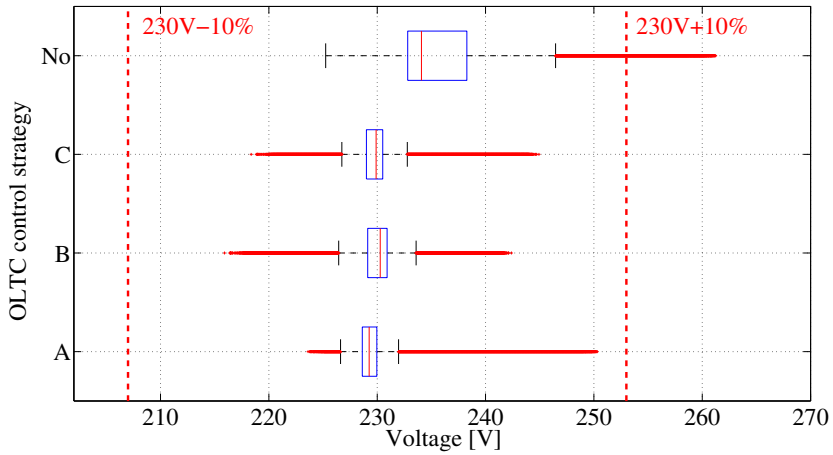


Figure 4.12: The voltage deviations in the investigated LV network for $DG_{ratio} = 100\%$, as in table 4.3. All control strategies are contrasted with the case, where no OLTC control is applied in the MV/LV substation (labelled 'No').

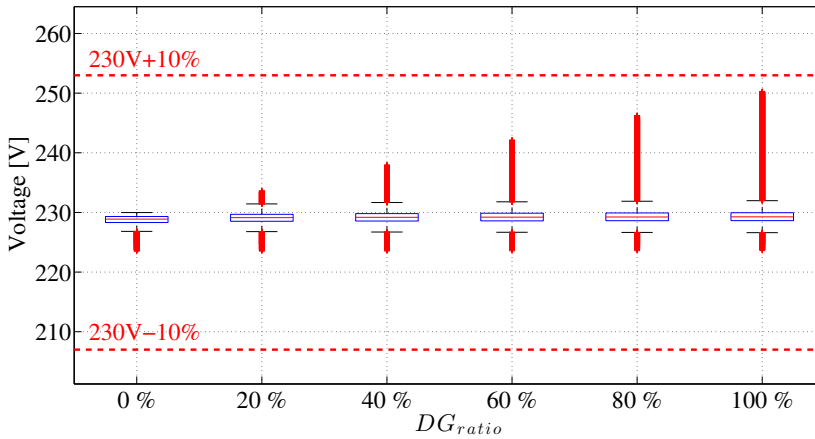


Figure 4.13: The voltage deviations in the investigated LV network as a function of DG_{ratio} from table 4.3 for OLTC control strategy A applied in the MV/LV substation.

bus bar voltage at constant value U_n) is the most suitable for implementation in current distribution networks. The voltage level conditions for all evaluated case studies from table 4.3 presented for the control strategy A in figure 4.13. With the control strategy A, the acceptable voltage level are maintained for all case studies evaluated.

The control strategy A represents also a compact solution (measurements, communication and control included within the MV/LV substation) for refurbishment of current MV/LV substations, where no measurements in the LV network are available.

4.6 Power quality measurements and data

The propagation of harmonic distortion and flicker in the LV network is discussed in this section. The goal of this assessment is to derive the most suitable locations for measurements in the LV network, which will provide a good insight about the PQ aspects to the DSO operating the LV network.

4.6.1 Flicker distortion in LV networks

Flicker can be described as annoying sensation of varying illumination intensity of light sources. Nevertheless, the perception of flicker and the annoying flicker sensation depends on personal sensitivity level. The flicker is a common reason for network users complaints and about 36 % of complaints from residential network users in the

Netherlands are associated to flicker (56 % of complaints are related to the voltage level) [27].

The intermittent and irregular power consumption or production can cause voltage fluctuations in the network, which can result in flicker related problems in the network (e.g., switching off and on of devices). Nowadays, only a small set of PQ related measurements is conducted at random locations in LV networks in the Netherlands, as discussed in 2.3.3. The flicker related measurements in a specific LV network are conducted only after a complaint of an network user. To oversee if the LV network users are supplied with sufficient voltage quality and with acceptable flicker levels, a set of measurements will be necessary in the LV network. Therefore, the evaluation of suitable locations for flicker related measurements to provide an overview about the flicker levels in the LV network is addressed in this section.

Flicker observed in LV network can originate from a source in the LV network, or can propagate to the LV network from MV network, where it can originate also from HV network [100]. The common sources of flicker in LV networks are induction motors with high inrush currents such as in elevators, heat-pumps, air-conditioners, but also welding machines, photocopying machines, or heavy irregular loads connected to LV [27].

The flicker severity is measured by a flicker meter (more details can be found in IEC 61000-4-15 and in [101]), which is a device to estimate an objective flicker value from measured voltage variations [102]. The P_{st} index is measured over a period of 10 min. and the P_{lt} index is calculated from a sequence of 12 P_{st} measurements over a 2 hour period, as in equation 4.7 [46].

$$P_{lt} = \sqrt[3]{\sum_{i=1}^{12} \frac{P_{st}(i)^3}{12}} \quad (4.7)$$

The permissible flicker limits for LV distribution networks are set in EN 50160 [46] standard. The limits for contribution to the flicker level for network users are addressed in standard IEC 61000-3-3 and adopted in the "Netcode Elektriciteit" [47]. The overview of the flicker related requirements for a DSO is presented together with limits on network users contribution to the flicker in table 4.4.

The P_{st} flicker level at a POC in the LV network is determined based on the relative voltage change at the POC caused by the flicker source, noted as $\frac{\Delta U^{POC}}{U_n^{POC}}$ (in [%]). The voltage deviation in the LV network is estimated based on network impedance and flicker source current, similarly as in equation 4.2. The P_{st}^{POC} flicker severity for a POC in the network can be determined with equation 4.8 [27].

$$P_{st}^{POC} = 0.337 \cdot F \cdot r^{\frac{1}{3.2}} \cdot \left(\frac{\Delta U^{POC}}{U_n^{POC}} \right) \cdot 100 \quad (4.8)$$

Where the P_{st}^{POC} value in equation 4.8 is estimated based on the shape factor F and on the repetition rate factor r . The shape factor corresponds to the waveform shape

Table 4.4: The requirements on flicker indexes for network users connected to the LV network in the Netherlands (with nominal voltage $U_n \leq 1$ kV).

Specifications	Description	Test methodology
$P_{lt} \leq 1$	Long-term flicker severity limit, defined by EN 50160 [46] and "Netcode Elektriciteit" [47]	Under normal operating conditions, during each period of one week for 95 % of values
$P_{lt} \leq 5$	The long-term flicker severity index, defined by "Netcode Elektriciteit" [47]	For all measured values during one week period
$\Delta U_n \leq 10 \%$	Fast voltage variations, defined by "Netcode Elektriciteit" [47]	For all measured values
$\Delta U_n \leq 3 \%$	Fast voltage variations, defined by "Netcode Elektriciteit" [47]	During a normal operation without a loss of generation, disconnection of heavy loads or a fault
$\Delta P_{st} \leq 1$ and simultaneously $\Delta P_{lt} \leq 0.8$	Contribution by the network user to the flicker level, defined by "Netcode Elektriciteit" [47]	Measured at POC, based on the reference impedance of the network at POC (283 Ω as in IEC 61000-3-3)

change and $F = 1$ is considered in simulations to represent the worst case [27]. The r factor (in [$number\ of\ repetitions \cdot min.^{-1}$]) represents the repetition rate of distorting source, for instance motor start-ups. When n multiple flicker sources are present in the network, the resulting aggregated flicker level for a POC in the network $P_{st,agg}^{POC}$ can be estimated based on equation 4.9 [103].

$$P_{st,agg}^{POC} = \sqrt[3]{\sum_{i=1}^n P_{st}^{POC,i}{}^3} \quad (4.9)$$

4.6.2 Flicker propagation in LV networks

Next to the absolute value of flicker severity levels for each POC, the flicker propagation in the LV network can be expressed based on the flicker transfer coefficients $T_{P_{st}}$. The flicker transfer coefficients from a $POC(1)$ to $POC(2)$ $T_{P_{st}}^{POC(1) \rightarrow POC(2)}$ is defined as the share of P_{st} values for both locations, as in equation 4.10. The principle governing the flicker propagation from the flicker source downstream or upstream in the radial network is

based on the propagation of voltage changes caused by the flicker source.

$$T_{P_{st}^{POC(1) \rightarrow POC(2)}} = \frac{P_{st}^{POC(2)}}{P_{st}^{POC(1)}} \quad (4.10)$$

Suppose the typical LV network in the Netherlands, as depicted in figure 4.1, with a flicker source connected in the middle of the feeder 1, $POC(30)$. The flicker from the source will propagate upstream and downstream throughout the network. The flicker transfer coefficient from a POC to the upstream LV bus-bar in the MV/LV substation (labelled $T_{P_{st}}^{POC \rightarrow LV_{bus-bar}}$) is proportional to the relative voltage change caused by the flicker source at the LV bus-bar considered, as expressed in equation 4.11. The flicker propagation throughout the radial network can be estimated based on the network impedances. The MV network impedance Z_{MV} , the MV/LV transformer impedance Z_{tr} and the network impedance from the MV/LV transformer to the POC $Z_{net}^{POC \rightarrow LV_{bus-bar}}$ are considered in this evaluation, as can be seen in equation 4.11 [104].

$$\begin{aligned} T_{P_{st}}^{POC \rightarrow LV_{bus-bar}} &= \frac{\frac{\Delta U^{LV_{bus-bar}}}{U^{LV_{bus-bar}}}}{\frac{\Delta U^{POC}}{U^{POC}}} \\ &= \left| \frac{Z_{MV} + Z_{tr}}{Z_{MV} + Z_{tr} + Z_{net}^{POC \rightarrow LV_{bus-bar}}} \right| \end{aligned} \quad (4.11)$$

The flicker propagation upstream from a POC in the network to the LV bus-bar in the MV/LV substation can be estimated based on the network parameters of the LV network. The propagation in the network depends on the observation point and on the location of the flicker source. The transfer coefficients for the flicker propagation upstream to the LV bus-bar $T_{P_{st}}^{POC \rightarrow LV_{bus-bar}}$ are estimated for the typical LV network, described in 4.2, as a function of flicker source location in the LV network for all POCs. The resulting transfer coefficients are depicted for all POCs in figure 4.14, where the LV bus-bar in the MV/LV substation is denoted as SS-LV. The detailed network parameters are provided in Appendix A.

It can be observed, that the transfer coefficient $T_{P_{st}}^{POC \rightarrow LV_{bus-bar}} = 1$ for the flicker source location at the LV bus-bar. With the increasing distance of the flicker source from the MV/LV substation (and increasing Z_{net}), the flicker propagation towards the LV bus-bar is attenuated and $T_{P_{st}}^{POC \rightarrow LV_{bus-bar}} < 1$. An example of P_{st} propagation upstream in the LV network is estimated based on a load start-up with inrush current $3 \cdot I_n = 3 \cdot 16$ [A], e.g., induction motor, located at the end of the feeder at $POC(60)$. As presented in Appendix A, the $P_{st}^{POC(60)} = 0.65$ is estimated. The resulting contribution of the flicker source to the $P_{st}^{POC(60 \rightarrow LV_{bus-bar})}$ levels at upstream POCs in the network are

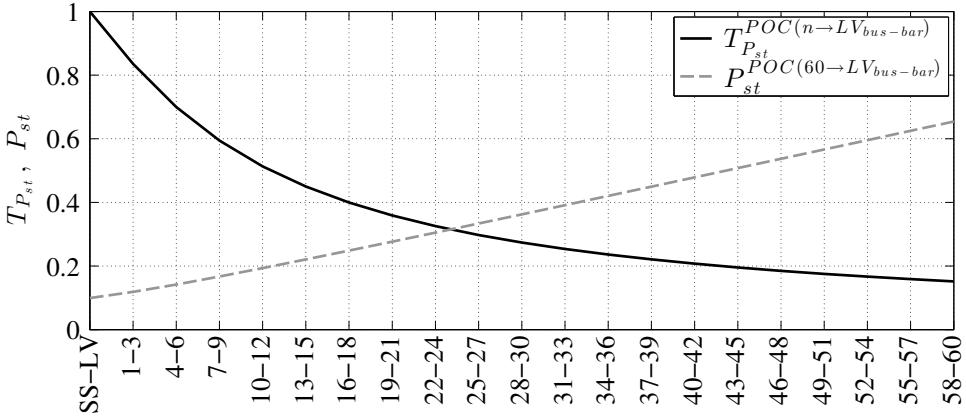


Figure 4.14: The flicker transfer coefficients $T_{P_{st}}^{POC \rightarrow LV_{bus-bar}}$ from a POC in the LV network towards the upstream LV bus-bar in the MV/LV substation together with the propagation of a flicker distortion $P_{st}^{POC(60 \rightarrow LV_{bus-bar})}$, originating at POC(60), upstream in the LV network towards the LV bus-bar. The values for the LV bus-bar in the MV/LV substation are denoted, among POCs, on the x-axis as SS-LV.

depicted in figure 4.14. The flicker propagation upstream is attenuated proportionally to the decreasing network impedance and results in $P_{st}^{LV_{bus-bar}} < P_{st}^{POC(60)}$.

The flicker transfer coefficient from the LV bus-bar in the MV/LV substation downstream to a POC in the LV network (labelled $T_{P_{st}}^{POC \leftarrow LV_{bus-bar}}$) is proportional to the relative voltage change at the LV bus-bar and the relative voltage change observed at a POC. The flicker propagation in downstream radial network also depends on impedances of connected loads (Z_{load}). The transitional voltage variations, causing flicker, affect in principle rather dynamic impedances of loads connected (Z'_{load}) and shall be considered especially in simulations for large machines with known parameters. However, the dynamic and static impedances are approximately equal for static loads ($Z_{load} \approx Z'_{load}$), which can be commonly found in LV networks. Nevertheless, for some industrial loads such as induction motors, the $|Z'_{load}| < |Z_{load}|$, which will affect flicker propagation [104]. Similarly to the upstream flicker propagation, as in equation 4.11, the downstream flicker transfer coefficient can be estimated based on the relative voltage change in the LV network due to flicker source located upstream in the network. The downstream flicker propagation is governed by the loads impedances

in the LV network and $T_{P_{st}}^{POC \leftarrow LV_{bus-bar}}$ can be estimated, as in equation 4.12.

$$\begin{aligned}
 T_{P_{st}}^{POC \leftarrow LV_{bus-bar}} &= \frac{\frac{\Delta U^{POC}}{U^{POC}}}{\frac{\Delta U^{LV_{bus-bar}}}{U^{LV_{bus-bar}}}} \\
 &= \left| \frac{Z'_{load}}{Z_{net}^{POC \rightarrow LV_{bus-bar}} + Z'_{load}} \cdot \frac{Z_{load} + Z_{net}^{POC \rightarrow LV_{bus-bar}}}{Z_{load}} \right|
 \end{aligned} \tag{4.12}$$

In a radial LV network structure, voltage at the LV bus-bar is directive for downstream connected POCs in the network and as a consequence, the flicker can propagate unattenuated in the LV network, which results in $T_{P_{st}}^{POC \leftarrow LV_{bus-bar}} = 1$ for $Z_{load} = Z'_{load}$. The load response to the flicker depends on particular parameters of every single load, flicker source parameters and on the combined load composition. In addition, the load parameters can be frequency dependent in the range of frequencies causing flicker. But the variations, can be small and the measured values for an example of induction motor indicate only a small variations in range of $T_{P_{st}} \subset (0.85, 1)$, as presented in [105]. Therefore $T_{P_{st}}^{POC \leftarrow LV_{bus-bar}} = 1$ can be assumed and the complete flicker propagation from a flicker source downstream in the LV network can be considered, similarly such as concluded in [27] and in [104].

It is demonstrated that the flicker propagation upstream in the LV network is limited and is attenuated by increasing impedance between the flicker source and the LV bus-bar in the MV/LV substation. On the contrary, the flicker distortion from an upstream source propagates throughout the LV network unattenuated. Therefore, the most severe flicker severity levels in LV network can be observed at the end of a LV feeder (at the last POC). Based on figure 4.14, the measurements at the ends of LV feeders $POC(60)$ and at the LV bus-bar in the MV/LV substation will provide satisfactory information about the flicker level in observed LV network to the DSO. In addition, if the $P_{st}^{POC(60)} > P_{st}^{LV_{bus-bar}}$, the origin of the flicker can be found among the POCs in the LV network connected to the investigated feeder.

Further detection of the flicker source location inside the LV network can be based on additional measurements in the LV network. Assume that a flicker source is placed downstream from the observation point, than the flicker contribution (based on the voltage amplitude) to the total voltage deviation observed will be relatively smaller during the low load period compared to the high load period in the network. However, if the loads behave only as constant power loads, this assumption can lead to misrepresentation, nevertheless this is very seldom in practice. The detailed methodology for the above mentioned flicker source detection and for the detection of the major flicker source in the network are presented in [106], [107].

As a consequence of presented evaluation and results, it is suggested that 10 min. P_{st} measurements at LV bus-bar and at $POC(60)$ for all feeders are conducted. Those

measurements will provide sufficient insight about the flicker levels in the LV network for the DSO operating the observed network.

4.6.3 Harmonic distortion in LV networks

The harmonic distortion is generally related to voltage and current distortions. The term harmonic mostly defines higher frequencies observed in the system, which are superimposed integer multiples of the fundamental system frequency. The harmonic distortion is an important aspect in power system operation, because it can have an adverse effect on electrical equipment of connected network users and DSO assets. Among common problems associated to harmonic distortion are equipment malfunctioning, overheating and shorter life-time [27]. The non-linear behaviour of power system components, together with the interaction of non-linear loads connected at premises of LV network users, can cause current distortion and induce voltage harmonic distortions. The common sources of harmonic distortion in the LV network are for instance adjustable drive systems, switching mode power supplies, computers, fluorescent lighting, wind and solar generators [108]. The harmonic distortion that propagates throughout the LV network, is influenced by system non-linearities and it influences network users equipment at different locations.

The harmonic analysis of the LV network is not a simple task as many different non-linear loads can be connected and can operate at different times. Certain load or generator characterization can be made based on, so called, harmonic fingerprints [27]. More insights on the complexity of evaluation of combined harmonic distortion in the network, the harmonic summations, can be found for instance in [109].

A DSO has to make sure, that all LV network users are supplied with certain voltage quality within acceptable levels of harmonic distortion. Therefore, the evaluation of suitable locations for measurements of harmonic distortion in the LV network is addressed in this section. The goal is to provide an overview about the harmonic distortion in the LV network for DSO purposes.

The notation of harmonics is related to the multiples of the fundamental frequency $f = 50 \text{ Hz}$ (in Europe) and individual harmonic orders are denoted by the subscript h (additional number can indicate specific harmonics). Based on EN 50160, the *THD* is defined on the principle of individual voltage harmonics summation up to u_{h40} , as in equation 4.13, where u_h are evaluated individually by their relative amplitude to the voltage at the fundamental frequency $\frac{u_h}{u_{h1}}$ [46].

$$THD = \sqrt{\sum_{h=2}^{40} (u_h)^2} \quad (4.13)$$

The responsibility of a DSO is to provide certain quality of supplied voltage in accordance with the EN 50160 standard [46] and with the "Netcode Elektriciteit" [47], where the indicators for supplied voltage quality are defined. Therefore, the harmonic

Table 4.5: The requirements on harmonic distortion for LV network in the Netherlands (with nominal voltage $U_n \leq 1 \text{ kV}$).

Specifications	Description	Test methodology
$THD \leq 8 \%$	Total harmonic distortion limit of voltage, defined by EN 50160 [46] and by "Netcode Elektriciteit" [47]	Applicable for 95 % of the measured 10 min. mean rms values over one week period
$u_{1,\dots,25}$	Limits for individual harmonics defined as the relative value of the fundamental voltage in EN 50160 [46]	
For $u_h \notin u_{1,\dots,25}$ applies $u_h < \min(u_{1,\dots,25})$	Limits for individual harmonics u_h not defined in EN 50160. The smallest value from EN 50160 applies, as defined by "Netcode Elektriciteit" [47]	
Individual harmonics shall be $< 5.5 \cdot u_h$	Limits for individual harmonics shall be < 5.5 than indicated percentage in EN 50160 [46], as defined in "Netcode Elektriciteit" [47]	Applicable for 99.9 % of the measured 10 min. mean rms values
$THD < 12 \%$	Total harmonic distortion limit for u , defined by "Netcode Elektriciteit" [47]	

distortion of supplied voltage is evaluated and term harmonics refers to the voltage harmonics here if not indicated otherwise. The limits for harmonic currents emission for network user appliances are indicated for instance in IEC61000-3-2 standard for devices up to 16 A. The limits for harmonic distortion applicable to the LV networks in the Netherlands are presented in table 4.5.

4.6.4 Propagation of harmonic distortion in LV networks

The individual harmonics or the THD value can be estimated under certain assumptions (e.g., sources of harmonic distortion) for all POCs in the LV network. Nevertheless, the propagation evaluation based on transfer coefficients is presented to better demonstrate the propagation of harmonic distortion in LV networks. The principle governing the propagation of harmonic distortion from a source downstream or upstream in the radial network is based on harmonic load flow, which governs the propagation of harmonics voltages in the LV network. Assume the typical LV network structure as presented in 4.2.

The transfer coefficient characterizing the propagation of harmonic distortion T_{u_h} from a $POC(1)$ to $POC(2)$ in the LV network $T_{u_h}^{POC(1) \rightarrow POC(2)}$ is defined as the contribution of harmonic distortion from $POC(1)$ to $POC(2)$ ergo, the ratio of u_h for both locations, as in equation 4.14.

$$T_{u_h}^{POC(1) \rightarrow POC(2)} = \frac{u_h^{POC(2)}}{u_h^{POC(1)}} \quad (4.14)$$

Similarly such as for the flicker propagation in 4.6.2, suppose the typical LV network in the Netherlands from figure 4.1, where a source of harmonic distortion is connected in the middle of the feeder 1, $POC(30)$. The harmonic distortion will propagate upstream and downstream throughout the network from the source. The transfer coefficient of harmonic distortion from a POC to the upstream LV bus-bar in the MV/LV substation (labelled $T_{u_h}^{POC \rightarrow LV_{bus-bar}}$) is proportional to the harmonic distortion observed at the LV bus-bar $\frac{\Delta u_h^{LV_{bus-bar}}}{u_h^{LV_{bus-bar}}}$ due to the source of harmonic distortion located at a POC $\frac{\Delta u_h^{POC}}{u_h^{POC}}$, as in equation 4.15. The propagation of harmonics throughout the radial network depends on network impedances, which are frequency dependent. Assume the impedances of the typical LV network from Appendix A for $h = 1$ and $h = 5$, the MV network impedance $Z_{MV,h}$, the MV/LV transformer impedance $Z_{tr,h}$ and the network impedance $Z_{net,h}^{POC \rightarrow LV_{bus-bar}}$ are considered, similarly as in equation 4.11 [104].

$$\begin{aligned} T_{u_h}^{POC \rightarrow LV_{bus-bar}} &= \frac{\frac{\Delta u_h^{LV_{bus-bar}}}{u_h^{LV_{bus-bar}}}}{\frac{\Delta u_h^{POC}}{u_h^{POC}}} \\ &= \left| \frac{Z_{MV,h} + Z_{tr,h}}{Z_{MV,h} + Z_{tr,h} + Z_{net,h}^{POC \rightarrow LV_{bus-bar}}} \right| \end{aligned} \quad (4.15)$$

The transfer coefficients for harmonic distortion propagation upstream from a POC towards the LV bus-bar can be estimated as a function of location in the LV-network. Based on equation 4.15, the resulting $T_{u_h}^{POC \rightarrow LV_{bus-bar}}$ are depicted in figure 4.15. The parameters used to estimate the values in figure 4.15 are presented in Appendix A.

Similarly to the upstream harmonic propagation, the downstream harmonics transfer coefficient $T_{u_h}^{POC \leftarrow LV_{bus-bar}}$ is defined as the transfer coefficient from the LV bus-bar in the MV/LV substation downstream to a POC in the LV network. The coefficient $T_{u_h}^{POC \leftarrow LV_{bus-bar}}$ is proportional to the relative harmonic distortion at the LV bus-bar and at observed POC. A source of harmonic distortion in the network will cause a harmonic voltage distortion observed at the LV bus-bar, which is normative for the LV network.

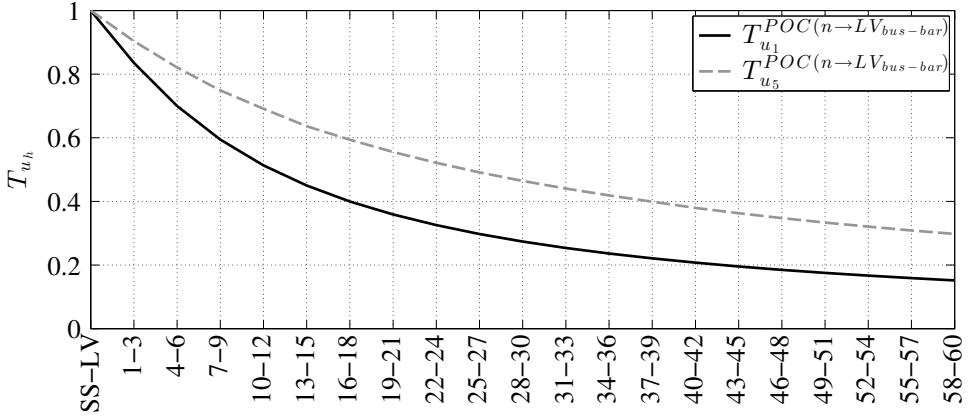


Figure 4.15: The transfer coefficients of harmonic distortion $T_{u_1}^{POC \rightarrow LV_{bus-bar}}$ and $T_{u_5}^{POC \rightarrow LV_{bus-bar}}$ from a POC located in the LV network towards the upstream LV bus-bar in the MV/LV substation. The values for the LV bus-bar in the MV/LV substation are denoted, among POCs, on the x-axis as SS-LV.

In the worst case of reduction, the harmonic distortion will completely propagate throughout the network and $T_{u_h}^{POC \leftarrow LV_{bus-bar}} \approx 1$ can be assumed as in [27].

To identify the source of harmonic distortion in the LV network, the factor of total current harmonic distortion THD_i^{POC} can be established. The THD_i^{POC} is defined on principle of summation of individual harmonic currents up to i_{h40} , which are relative to fundamental current i_{h1} at the network user facility as in equation 4.16.

$$THD_i^{POC} = \sqrt{\sum_{h=2}^{40} (i_h^{POC})^2} \quad (4.16)$$

The THD_i^{POC} evaluates the harmonic current injections of individual network users to the LV network, which can be used to identify the users contributing most to the distortion in the LV network. The identification is feasible if THD_i^{POC} are measured at POCs (e.g., by smart meters).

Note that the summation and detailed propagation of harmonic distortion in networks is a complex topic, as harmonics can be different by their frequency, amplitude and phase and they propagate in network with many non-linear components. More information can be found for instance in [109], [110] or [111], [112].

The modelling of harmonic loads is sensitive to load representation in frequency domain, which influences the propagation of harmonics. The detailed models of LV equipment are commonly unknown as well as models of LV appliances from

manufacturers, which are not interested to divulge detailed description of their appliances. In addition, when the system changes (e.g., switching of appliances), the current injection in the LV network changes as well and new levels of harmonic distortion can be observed. Models such as the CIGRE load model for bulk load representation based on experimental measurements can assist in approximate estimation of harmonic propagation [108], [113], [114]. Despite efforts to derive realistic load models for harmonic simulations, the LV distribution system is a set of not-quantified interacting load, which make the detailed evaluation of harmonic propagation complex and infeasible in detail.

In a radial LV network structure, the sources of harmonic distortion contribute to the harmonic distortion at the LV bus-bar, which is directive for downstream connected POCs in the network. The harmonic propagation in the LV network is in practice more complex, as it is influenced by numerous LV loads with different frequency and time dependent impedances, which are not known to the DSO. Similarly to the flicker propagation, load composition can reduce the harmonic propagation in the LV network, but generally the harmonic distortion propagates unattenuated in the LV network downstream from a source of harmonic distortion in the LV network. Therefore, it is concluded that the most severe levels of harmonic distortion in LV network can be mostly observed at the end of a LV feeder (at the last POC). Based on figure 4.15, the measurements at the ends of LV feeders $POC(60)$ and at the LV bus-bar in the MV/LV substation can provide satisfactory information about levels of harmonic distortion in observed LV network to the DSO.

As a consequence of presented evaluation and results, it is suggested that the individual harmonics and THD values are recorded as 10 min. measurements (average values) in accordance to required standards at the LV bus-bar and at last POCs in the LV network for all conducted feeders. Those measurements will provide sufficient insight about levels of harmonic distortion in the LV network for the DSO operating the observed network. If advanced measurements were available at POCs to the DSO, THD_i^{POC} values can be measured to indicate the source of harmonic distortion in the LV network.

4.7 Conclusions

The operation and power quality aspects of LV distribution networks are addressed in this chapter. Firstly, the particular characteristics of LV distribution networks in the Netherlands are presented and the model of the typical LV network is defined. The currently applied load characterization approaches are assessed against the measured load profiles from LV network. It is concluded that the currently used methodology for characterization of LV residential load profiles can be improved. Therefore, a more suitable methodology is proposed and a set of LV residential load data, similar to measured ones, is generated and compared with the original data.

It is demonstrated on the typical LV network in the Netherlands, that the LV voltage

level control will be necessary to accommodate a high penetration of DGs in the network. Based on the conclusions of chapter 3, the solution derived from OLTC application in the MV/LV substation is assessed. Three OLTC control strategies are proposed and evaluated based on their capabilities to mitigate the voltage deviations in the network. The measurement requirements for the OLTC control strategy operation are also considered. The most suitable OLTC control strategy is proposed with no measurements required from POCs in the LV network. Nevertheless, a DSO shall make sure that all POCs in the LV network are supplied with voltage level in accordance to prescribed limits. A smart meter installed at a POC at the end of each feeder can measure and communicate 10 min. average voltage measurements to provide an overview about the voltage conditions in the LV network. The voltage measurements can be also utilized to enhance the OLTC control strategy, if required for local voltage level conditioning.

As PQ aspects are of DSO concern in the distribution networks, aspects related to the propagation of harmonic distortion and flicker in the LV are presented. The propagation phenomena in LV network are investigated and the conclusions about the most suitable measurement locations in the LV network are drawn. The measurements at those locations will provide a DSO with overview about the power quality levels in the LV network.

The DSO shall provide all connected network users with certain quality of supplied voltage. Therefore, the set of measures to assess the quality of supplied voltage and to improve the voltage level of LV networks is presented.

MV distribution networks

5.1 Introduction

The MV distribution system is designated to provide a cost-effective connection between the transmission and LV distribution networks, where the majority of network users is connected. The MV network also accommodates medium-size network users, commonly labeled also as: consumers, end-users, end-entities and connected parties.

Nowadays, next to the developments in the LV network, many developments take place also in MV distribution. In the MV network, numerous industrial network users participate on power generation, e.g., with co-generation units used for greenhouse farming. In some parts of the distribution network the penetration of DGs is rather high and causes voltage level problems [21]. The system load in the Netherlands is envisioned to increase in the coming years [38], which will have implications also on the load in the MV network and on the operation of the distribution network, as discussed in 2.3. The developments at HV and LV levels have impact also on the MV network and its operation. In this chapter different MV network topologies are described and discussed.

As a consequence of the developments in the distribution network, more awareness and insights will be required also in the MV network to increase the distribution network performance. The propagation of power quality phenomena is studied on them to evaluate the most suitable locations for observation of the distortion levels in the network. The implications related to the application of OLTC in the MV/LV substation are assessed and the capability to mitigate the propagation of MV voltage level fluctuations to the LV network is evaluated.

5.2 MV networks in the Netherlands

The transmission system operator (TSO) in the Netherlands (TenneT TSO) operates the transmission network with voltage levels ≥ 110 kV. After the independent grid administration act passed the Dutch Parliament in the year 2006, the networks at the voltage levels 110 kV and 150 kV were integrated under the Dutch TSO. The integration was accomplished in the year 2011 [17]. DSOs in the Netherlands operate the networks with high, medium and low voltage levels below the lowest transmission network voltage level. The networks with the voltage level > 1 kV and ≤ 36 kV correspond to the MV distribution in the Netherlands [46]. The most common MV voltage level in the Netherlands is 10 kV. Nevertheless, distribution networks with voltage levels of 6, 12, 20, 25 and 50 kV can be found in a limited scale in the assets of Dutch DSOs [25].

The Netherlands has the largest share of underground MV networks (with the total circuit length 110 398 km in the year 2009) among the European countries [49]. Based on [24], all MV networks in the Netherlands are underground cable networks which is exceptional, but it helps Dutch DSOs to deliver a very reliable electricity connection to its network users. The MV networks are designed as three-phase, delta operated networks without a neutral. Because, the MV winding (primary winding) of MV/LV transformers are delta operated and the secondary winding of the MV/LV transformers are star operated, the asymmetrical load from LV network is not transferred to the MV network.

The networks operated by Dutch DSOs serve to:

- Deliver electricity to network users (consumers) or take the electricity from network users (producers) directly connected at the MV voltage level (e.g., industrial network users) or at the LV voltage level via a MV/LV substation
- Transport electricity at voltage levels operated by DSOs (MV transmission) to efficiently connect usually remote parts of the MV network. In this case, several parallel cables are commonly used to transport bulk electricity to other MV substations, eventually with a boost transformer to correct for the unwanted voltage deviations, from where MV distribution takes place to other MV/LV substations

The MV network with the MV distribution and MV transmission functionality is schematically depicted in figure 5.1. The MV transmission part of the MV network can increase the hosting capacity of connected MV distribution.

The direct connection to the MV network has economical benefits for some, usually industrial, network users, which use their own MV/LV transformers to supply industrial processes at required voltage level. However, the majority of connected network users in the Dutch distribution network is supplied at the LV voltage level via MV/LV substations. Approximately 75 % of MV/LV substations in the Netherlands supply LV residential network users [20].

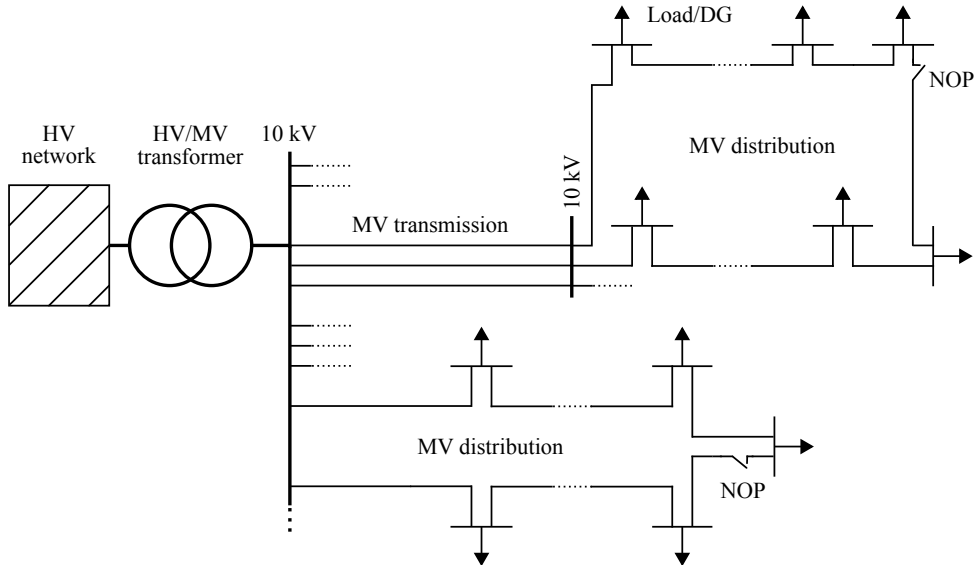


Figure 5.1: The schematic topology of a MV network in the Netherlands with MV transmission and MV distribution parts.

5.2.1 Current MV network topology

The majority of MV distribution networks in the Netherlands is designed as a ring topology. However, MV network rings are normally operated as radial networks (open ring structures). The MV distribution network ring structure is electrically divided by the normally open point (NOP) in a MV/LV substation, which is usually located somewhere close to the middle of the MV ring structure. In a case of disturbance on the MV ring (e.g., MV cable failures due to excavation works), the configuration of the MV network can be changed with switching operations at MV/LV substations and at the substation with NOP, to enable electricity rerouting. After the isolation of the faulted part in the MV network (done mostly manually), the remaining parts of the MV network can be re-energized [25].

The distribution network is extensive, because it has to supply a large number of network users, but standardized equipment and straight forward design practices are used to achieve cost-efficiency. A typical HV/MV substation of Alliander in the Netherlands supplies about 15 MV feeders, where on average a MV feeder supplies about 15 to 25 MV/LV substations [20]. The number of MV/LV substations per a MV ring structure can vary, as it is influenced by location specifics and by the DSO best practices. A MV/LV substation can be connected in the main ring, in a sub-ring or in a stud-end of the MV network structure [25]. The topology of the typical MV distribution

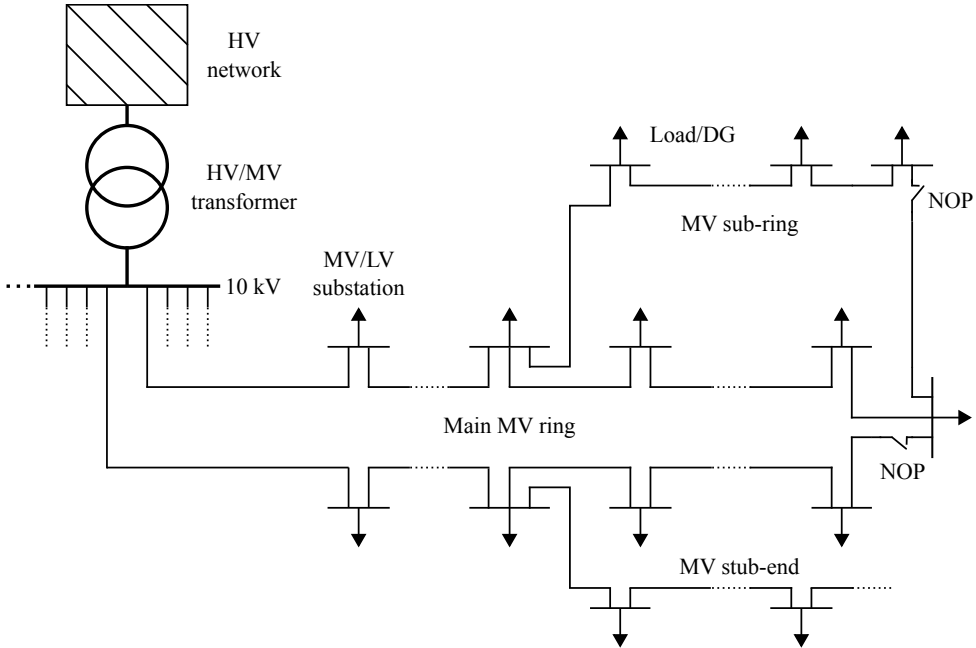


Figure 5.2: The schematic topology of the typical MV distribution network in the Netherlands, where the main MV ring, a MV sub-ring and a MV stub-end are depicted.

network is schematically depicted in figure 5.2.

The typical 10 kV MV distribution structure nowadays uses MV $3 \times 240 \text{ mm}^2$ Al three-phase cables for main feeders with the current rating of $I_{max} = 360 \text{ A}$ [20]. The MV network is designed for $I \leq 0.5 \cdot I_{max}$ during normal operation to facilitate energy rerouting in a case of an outage in the MV ring structure.

5.2.2 New MV network topology

As the current MV network topology has a limited capacity to accommodate the challenges envisioned for the MV network, a new concept of mixed 20/10 kV MV network is proposed. It is developed by Alliander and perceives this concept of MV transmission and distribution as an economically sensible solution to increase the hosting capacity of current MV networks. The 20 kV transmission is more cost efficient per unit of power transported than 10 kV transmission. This concept shall help to alleviate concerns related to the envisioned load increase and higher penetration of DGs in the future distribution networks, as discussed in 2.3. The proposed structure shall also allow a higher hosting capacity for accommodation of

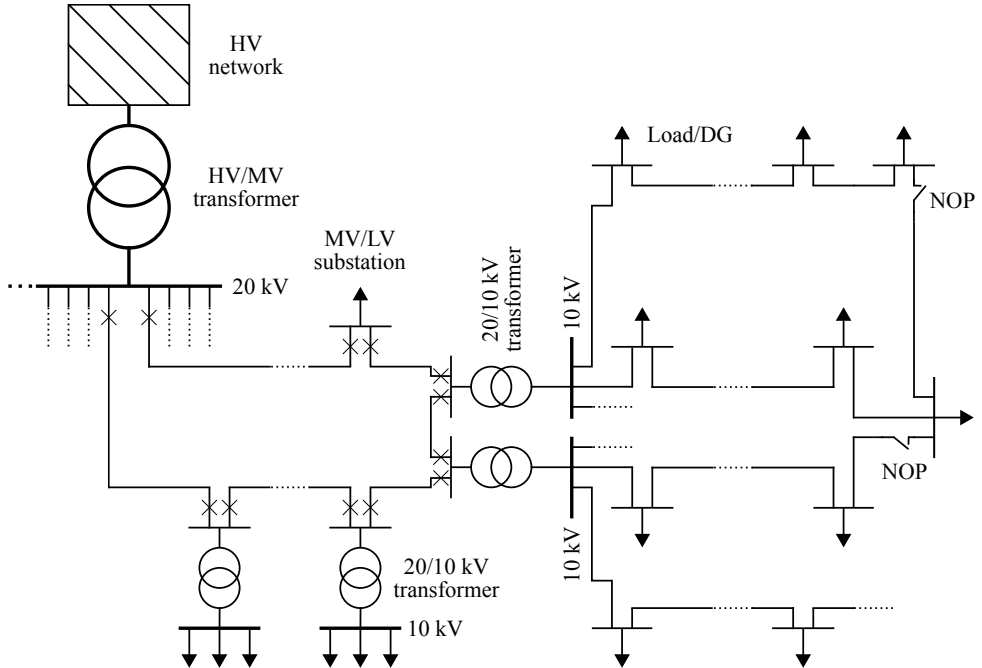


Figure 5.3: The schematic topology of a proposed new 20/10 kV MV network structure in the Netherlands. The new 20 kV part of the MV network with remotely operated circuit breakers is integrated into the current 10 kV MV network, which is depicted in figure 5.2.

DGs in the distribution network and it shall better facilitate complex power flows in the MV network [24], [115].

The new 20 kV MV transmission ring structure is proposed to be incorporated into the current 10 kV distribution network. The 20 kV transmission structure is expected to increase reliability of power delivery, to reduce the customer minutes lost for supplied network users and to offer more flexibility in accommodation of more load and DGs in the network. The topology of the MV network with the new 20/10 kV ring structure is schematically depicted in figure 5.3.

The main characteristics of the mixed 20/10 kV structure are [24], [115]:

- The 20 kV ring structure will have mainly transmission functionality with remotely operated circuit breakers to facilitate automatic reconfigurations
- The current 10 kV structure will become part of the new 20 kV structure, where:
 - The length of 10 kV feeders will be reduced in comparison to the current situation

- More interconnections of the 10 kV structure with the new 20 kV structure are expected, because the current 10 kV structure will be divided into smaller (shorter) 10 kV parts connected at more connection points to the new 20 kV structure
- The reduced length of 10 kV circuits shall enable a higher hosting capacity also at the 10 kV level
- More voltage control shall be possible in the distribution network, as some MV/MV substations (20/10 kV) and some MV/LV substations are expected to be equipped by OLTC in the future. Therefore, the voltage level conditions in the 10 kV MV distribution and consequently in the LV network would be better controllable

The proposed 20 kV MV transmission is a concept with several design alternatives [24], [115]. Different levels of substation automation and monitoring are considered for the 20 kV MV transmission and 10 kV MV distribution to empower a DSO with different levels of control and sensing capabilities.

5.3 MV supply voltage conditioning

In this section are firstly presented the requirements on the supplied voltage level for network users connected at DSO network with voltage level > 1 kV and secondly, the assessment of MV voltage fluctuations and the implications of OLTC control strategies are presented.

5.3.1 MV supply voltage characteristics

Network users with a high electricity demand, which exceeds the capacity of LV network, are connected to the MV network. The magnitude of supply voltage for MV network users is given by declared supply voltage U_c . The network user with a power demand $S_{max}^{POC} \in (0.3, 3)$ MVA shall be connected to the MV network at the declared supply voltage level $U_c \in (1, 25)$ kV according to the Dutch "Netcode Elektriciteit" [47]. The network user with even higher power demand $S_{max}^{POC} \in (3, 100)$ MVA shall be connected in the distribution network at $U_c \in (25, 50)$ kV, if available in DSO service area [47].

The characteristics of declared supply voltage U_c for MV network users are characterized in EN 50160 standard [46] and in "Netcode Elektriciteit" [47]. The overview of required characteristics of declared supply voltage for MV network users is presented in table 5.1. The international standard EN 50160 presents a minimum requirements on the supplied voltage quality. The authorities of each country can add additional requirements in their national grid code. The differences in terminology of MV voltage level and required quality of declared supply voltage level can be seen in table 5.1.

Table 5.1: The requirements on supply voltage level for network users connected to network at voltage levels operated by DSOs in the Netherlands.

Specifications (U_c within)	Description	Test methodology
$U_c \pm 10 \%$	Defined by EN 50160 [46] for MV network users with $U_c \in (1, 36)$ kV	Applicable for at least 99 % of the measurements (measured as 10 min. mean rms values over one week period)
$U_c \pm 15 \%$	Defined by EN 50160 [46] for MV network users with $U_c \in (1, 36)$ kV	Applicable for all measurements (measured as 10 min. mean rms values over one week period)
$U_c + 10 \% \wedge U_c - 15 \%$	For special situations or on a temporary basis, defined by EN 50160 [46] for not interconnected networks with the transmission system or special remote areas for MV network users with $U_c \in (1, 36)$ kV	All measurements shall be within $U_n + 10 \% \wedge U_n - 15 \%$ (measured as 10 min. mean rms values over one week period)
$U_c \pm 10 \%$	Defined by "Netcode Elektriciteit" [47] for MV network users with $U_c \in (1, 35)$ kV	Applicable for at least 95 % of the measurements (measured as 10 min. mean rms values over one week period)
$U_c + 10 \% \wedge U_c - 15 \%$	Defined by "Netcode Elektriciteit" [47] for MV network users with $U_c \in (1, 35)$ kV	Declared for all measurements (measured as 10 min. mean rms values over one week period)
$U_c \pm 10 \%$	Defined by "Netcode Elektriciteit" [47] for network users with $U_c \geq 35$ kV	Applicable for 99.9 % of the measurements (measured as 10 min. mean rms values over one week period)

5.3.2 Voltage level conditioning with OLTC in MV networks

It is envisioned, that the future distribution network will require more voltage control actions due to the presence of DGs connected at the LV and at the MV voltage level. The OLTC at the MV/LV substation is identified as a viable technological alternative applicable by DSOs to improve the voltage level conditioning in the distribution network, which is the top ranked expected functionality of distribution networks from industrial perspective, as discussed in 3.4. The analysis of the OLTC impact on the LV network is presented in 4.5.2. The implications of different OLTC control schemes applied at MV/LV substation on the MV network are assessed in this section to provide a

comprehensive evaluation of this technology on distribution networks. The simulations presented in this section follow up on the work addressed in 4.5.2 and they are used to assess the implications of different OLTC control schemes on MV network operation and to assess the capabilities of OLTC control schemes to simultaneously mitigate the propagation of MV voltage level fluctuations.

Nowadays, off-line tap position adjustments are done at the MV/LV substation to offset voltage fluctuations in the LV and MV network due to loads considered. On-line tap adjustments are done at the HV/MV level. However, as more DGs will be connected to the future distribution network, more varying voltage conditions in the MV network can be expected. Without the tap control, the voltage control at the MV network is possible also by means of reactive power control and active power control of connected DGs [116]. The presence of OLTC in a MV/LV substation decouples voltage levels in the MV network with the LV network and the propagation of voltage level fluctuations to the LV network can be reduced. Therefore, higher MV voltage fluctuations in a certain range can be allowed without their propagation to network users in the LV network, if the OLTC is used at the MV/LV substation.

5.3.3 Implications of MV/LV OLTC control on MV network - case studies

The capabilities to attenuate MV voltage fluctuations are assessed for all OLTC control strategies presented in section 4.5.2:

- Control strategy A - the OLTC is adjusted to keep the LV bus-bar voltage in the MV/LV substation at a constant value ($U_n = 230 \text{ V}$)
- Control strategy B - the OLTC is adjusted to maintain the average voltage level at the end of the feeders at constant value
- Control strategy C - the OLTC is adjusted to keep the desired voltage level for all POCs at all connected feeders at constant value ($U_n = 230 \text{ V}$) on average

At every time instance t , the tap position on the MV side of the MV/LV transformer is adjusted to meet the control objectives required by the selected control strategy in LV network, e.g., to maintain U_n at LV bus-bar for the control strategy A. The OLTC tap position can be expressed by $U_{tap}(t)$, which respects the selected control strategy and the voltage drop across the MV/LV transformer. The $U_{tap}(t)$ can operate only within the OLTC operation limits $\langle U_{TR,min}; U_{TR,max} \rangle$, given by the design as $\langle U_n - 5 \%; U_n + 5 \% \rangle$ [95]. As $U_{tap}(t)$ follows its selected control objective, range of voltage variations from the MV network can be mitigated without violating this objective. The maxima of voltage level mitigation capabilities for a positive voltage deviations $U_{MV,max}(t)$ in the MV network (voltage increase) can be defined per-unit (pu), as in equation 5.1.

$$U_{MV,max}(t) = U_n + U_{tap}(t) - U_{TR,min} \quad (5.1)$$

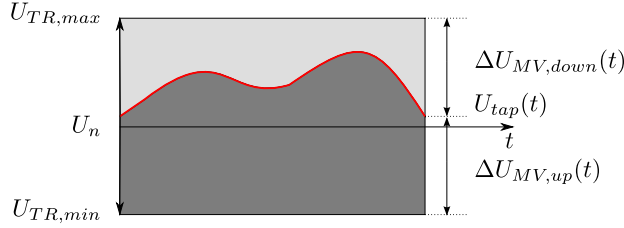


Figure 5.4: The schematic limits and variations of the MV voltage mitigation capabilities of OLTC at a MV/LV substation.

The minima of the negative voltage deviations $U_{MV,min}(t)$ in the MV network (voltage decrease), which propagation to the LV network can mitigated with the OLTC, can be defined pu as in equation 5.2.

$$U_{MV,min}(t) = U_n + U_{tap}(t) - U_{TR,max} \quad (5.2)$$

The maxima and the minima of MV voltage define the limits of the voltage range $\Delta U_{MV,down}$; $\Delta U_{MV,up}$, in which the MV voltage fluctuations propagation to LV network can be suppressed. Where, the propagation of voltage increases in the MV network to the LV network can be mitigated within $\Delta U_{MV,up}(t) = \langle U_n; U_{MV,max}(t) \rangle$ and the voltage decreases can be mitigated within $\Delta U_{MV,down}(t) = \langle U_{MV,min}(t); U_n \rangle$ for every time instance t . The voltage range $\Delta U_{MV,down}(t)$; $\Delta U_{MV,up}(t)$ changes over time, as $U_{tap}(t)$ is adjusted to follow the load in the network. The variations of the available voltage range over time are schematically depicted in figure 5.4.

The variations of the OLTC tap position depend on the selected control strategy and differences can be observed for a high penetration of DGs in the LV network, where the control strategies adjusting the OLTC tap position based on measurements from POCs in the LV network require a wider range of U_{tap} . Based on assumptions about DG penetration in the LV network in 4.5.2, variations of $U_{tap}(t)$ for all control strategies can be estimated for $DG_{ratio} = 100\%$. The results for one week period are depicted in figure 5.5. It can be seen in figure 5.5, that the control strategies governed by measurements from POCs utilize a wider range of U_{tap} and as a consequence, OLTC capabilities to mitigate the propagation of MV voltage fluctuations are more time dependent. For some time instances, $U_{tap}(t)$ can reach its technical limits $\langle U_{TR,min}; U_{TR,max} \rangle$ for control strategies B and C. Therefore, the mitigation of MV voltage level fluctuations propagation will be not possible for those time instances. As a consequence, the available voltage range $\Delta U_{MV,down}(t)$, $\Delta U_{MV,up}(t)$ is limited for those strategies and strongly time dependent.

The control strategy A requires the smallest deviations of $U_{tap}(t)$ from the nominal voltage at the MV/LV substation. Consequently, $\Delta U_{MV,down}(t)$ and $\Delta U_{MV,up}(t)$ vary less over time for the OLTC control strategy A than for control strategies B and C. The

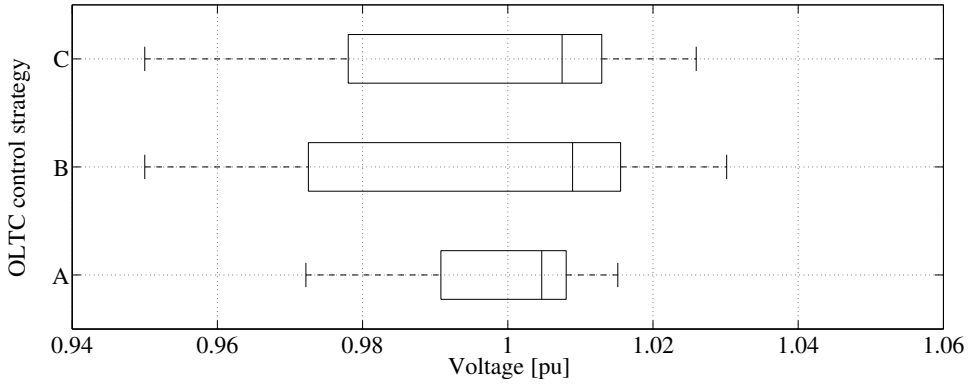


Figure 5.5: The comparison of OLTC tap positions U_{tap} variations at a MV/LV substation for evaluated control strategies. The results are estimated for $DG_{ratio} = 100\%$ over one week period as discussed in 4.5.2.

Table 5.2: The capabilities of evaluated OLTC control strategies to mitigate the propagation of MV voltage fluctuations for $DG_{ratio} = 100\%$.

Variables estimated	OLTC control strategy		
	A	B	C
$\Delta \bar{U}_{MV,down} \pm \sigma [pu]$	(0.94, 0.96)	(0.93, 0.98)	(0.93, 0.98)
$\bar{U}_{MV,down}, \bar{U}_{MV,up} [pu]$	(0.95, 1.05)	(0.95, 1.05)	(0.95, 1.05)
$\Delta \bar{U}_{MV,up} \pm \sigma [pu]$	(1.04, 1.06)	(1.03, 1.08)	(1.03, 1.08)
σ	0.012	0.026	0.023

estimated available $\Delta U_{MV,down}(t)$ and $\Delta U_{MV,up}(t)$ is depicted for one week period in figure 5.6. As the control strategy A maintains the LV bus-bar voltage at U_n , $U_{tap}(t)$ is lower when DGs in the LV network are active then at times when DGs are inactive if the load is the same. Consequently, a higher voltage range $\Delta U_{MV,up}$ can be mitigated during the periods, where DGs in LV network are active, as depicted in figure 5.6. This can have a profound impact on MV network operation, because higher MV voltage levels could be acceptable during periods, where DGs in many LV networks operate simultaneously to supply electricity (e.g., PV based DGs).

The available range of voltages $\Delta U_{MV,down}$ and $\Delta U_{MV,up}$ can be estimated for all values of DG_{ratio} , as assumed in 4.5.2. For the OLTC control strategy A can be observed, that with significantly increasing penetration level of DGs in the LV network, the available voltage ranges for mitigation of MV voltage level fluctuations do not change significantly. The available ranges of voltages $\Delta U_{MV,down}$ and $\Delta U_{MV,up}$ for the OLTC control strategy A is estimated for all considered DG_{ratio} over one week period and the

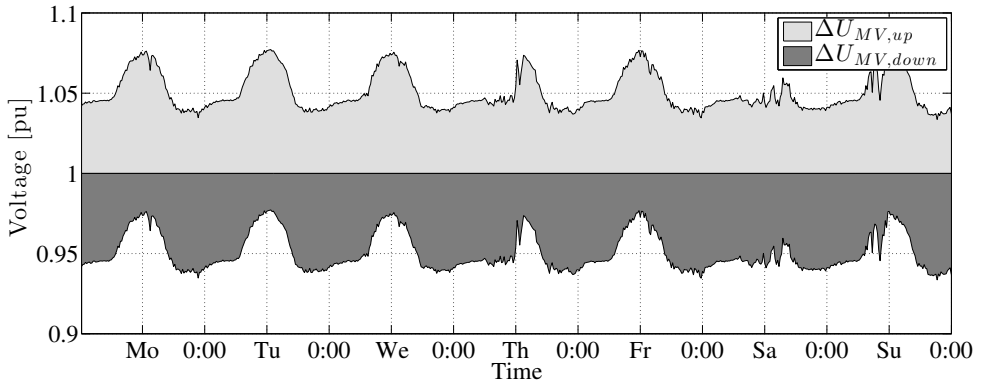


Figure 5.6: The available range of MV voltages $\Delta U_{MV,down}$ and $\Delta U_{MV,up}$, which can be mitigated by the OLTC with the control strategy A over one week period. The results are estimated for $DG_{ratio} = 100\%$ and based on assumptions presented in 4.5.2.

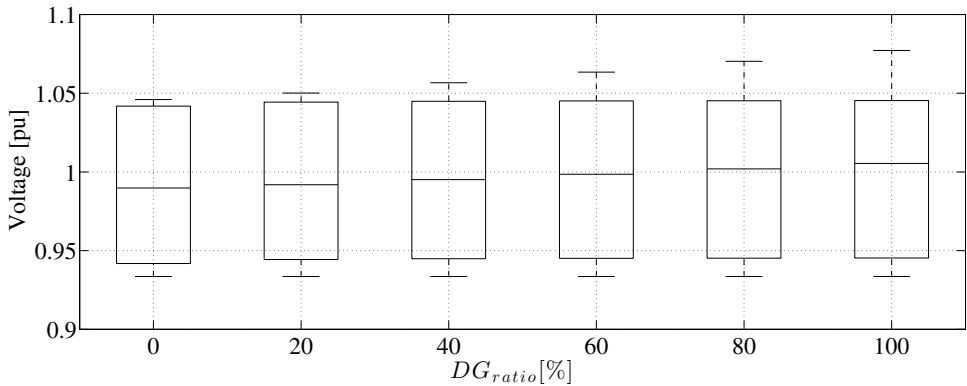


Figure 5.7: The available range of MV voltages $\Delta U_{MV,down}$ and $\Delta U_{MV,up}$, which can be mitigated by the OLTC with a control strategy A over one week period. The results are estimated for all values of DG_{ratio} presented in 4.5.2.

results are depicted in figure 5.7.

The numeric results of the mitigation capabilities for all evaluated OLTC control strategies are presented in table 5.2, where it can be seen that the OLTC control strategy A exhibits the lowest variations of available voltage range $\Delta U_{MV,down}(t); \Delta U_{MV,up}(t)$, ergo the standard deviation σ of the values from their mean is the smallest for this control strategy. As a consequence of this small variations

of U_{tap} , the capability to mitigate the voltage fluctuations in the MV network is the least time dependent for the OLTC control strategy A. Additionally, the mitigation capabilities of the OLTC control strategy A will change only marginally with increasing penetration of DGs in the LV network, as is shown in figure 5.7.

In this section is shown and quantified, that the OLTC control applied for LV networks has a positive impact on MV network as it allows to mitigate the propagation of MV voltage fluctuations in a certain range. Similarly to the presented evaluation, the assessment of the mitigation capabilities of the OLTC applied within the mixed 20/10 kV concept structure could be made.

5.4 Power quality measurements and data

In this section, the propagation of flicker and harmonic distortion in the MV network is assessed to evaluate the most suitable locations for the measurements of those aspects in the MV network. This work is complementary to the work presented in [27] and in [28]. The investigation is divided in two sections; for the current MV network structure in 5.4.1 and for the 20/10 kV MV network structure in 5.4.2.

5.4.1 PQ phenomena propagation in current 10 kV MV networks

The flicker limits for HV, MV and LV voltage levels are considered in the planning process. The limits for flicker emissions at each voltage level are set to make sure that the LV compatibility level for flicker of $P_{lt}^{LV} = 1$ can be achieved. The flicker propagation throughout the different voltage levels in the distribution network can be characterized by flicker transfer coefficients. The flicker originating in the HV network is attenuated as it propagates through the system. The transfer coefficients indicate the portion of flicker emission propagating from one bus to other bus. For instance, the transfer coefficients from HV to MV network are estimated based on corresponding P_{st}^{HV} and P_{st}^{MV} values, as in equation 5.3. Similarly, $T_{P_{st}}^{MV \rightarrow LV}$ and $T_{P_{st}}^{MV \leftarrow LV}$ can be estimated.

$$T_{P_{st}}^{HV \rightarrow MV} = \frac{P_{st}^{MV}}{P_{st}^{HV}} \quad (5.3)$$

The propagation of flicker in MV networks is in reality rather complex, but $T_{P_{st}}$ values can be approximately estimated based on the ratio of network impedances of investigated buses [117].

If more sources of flicker are contributing to the distortion on that bus, the aggregated value of $P_{st,agg}$ at the bus or a POC can be estimated based on the combination of all flicker sources, as discussed in section 4.6.1 and shown in equation 4.9.

The requirements on flicker level in the MV and HV networks in the Netherlands are presented in table 5.3.

Table 5.3: The requirements on flicker indexes for network users connected to MV and HV networks in the Netherlands (with $U_c \geq 1$ kV).

Specifications	Description	Test methodology
$P_{lt} \leq 1$	Long-term flicker severity limit, defined by EN 50160 [46] and "Netcode Elektriciteit" [47]	Under normal operating conditions, during each period of one week for 95 % of values
$P_{lt} \leq 5$	Long-term flicker severity limit, defined by "Netcode Elektriciteit" [47]	For all measured values during one week period
$\Delta U_c \leq 10 \%$	Fast voltage variations, defined by "Netcode Elektriciteit" [47]	For all measured values
$\Delta U_c \leq 3 \%$	Fast voltage variations, defined by "Netcode Elektriciteit" [47]	During a normal operation without a loss of generation, disconnection of heavy loads or a fault

Transfer coefficient for flicker propagation from HV to MV network is commonly set to $T_{P_{st}^{HV \rightarrow MV}} = 0.9$ and for propagation from MV to LV network set to $T_{P_{st}^{MV \rightarrow LV}} = 1$ [27]. Therefore, to conform with the compatibility level in LV networks, $P_{st}^{LV} = 1$ from table 4.4, the limits at MV network shall be $P_{st}^{MV} \leq 1$. To estimate the limits in MV network, the planning level at LV network is usually set to the compatibility level ($P_{st}^{LV} = 1$), the maximal global contribution from LV network users $G_{P_{st}^{LV}} = 0.65$ is assumed and the cubic summation is used [118]. The flicker limit for the MV network P_{st}^{MV} can be estimated as in equation 5.4 [103].

$$P_{st}^{MV} = \sqrt[3]{\frac{(P_{st}^{LV})^3 - (G_{P_{st}^{LV}})^3}{(T_{P_{st}^{MV \rightarrow LV}})^3}} \approx 0.9 \quad (5.4)$$

In this situation, the resulting limit at MV network is estimated to $P_{st}^{MV} \approx 0.9$.

The main sources of flicker in MV networks are generally large industrial applications with repetitive or irregular cycles such as motors, welding machines or arc furnaces [28]. Flicker is also the main source of complaints of small industrial network users (with contracted power > 50 kVA) in the Netherlands, while 53 % of all complaints are associated with flicker [27].

A set of case studies on MV network is performed to demonstrate the propagation of flicker distortion in current MV structure and in the concept of the mixed 20/10 kV

Table 5.4: The loads considered in the 10 kV MV network for investigation of PQ phenomena in the Netherlands (see figure 5.8).

Description	Location (MV nodes)	Specification
Industrial load (I)	10-2, 10-6, 10-13	With $S = 250$ kVA and $PF = 0.95$ (<i>ind.</i>), each supplied via 400 kVA MV/LV transformer
Residential load (R)	10-4, 10-5, 10-7, 10-10, 10-11, 10-14, 10-15, 10-16, 10-17	With $S = 200$ kVA and $PF = 0.9$ (<i>ind.</i>), each supplied via 400 kVA MV/LV transformer
Combined industrial and residential load (I+R)	10-8, 10-9, 10-12, 10-18	Residential part as a load with $S = 100$ kVA and $PF = 0.9$ (<i>ind.</i>), industrial part as a load with $S = 100$ kVA and $PF = 0.95$ (<i>ind.</i>), both supplied via 400 kVA MV/LV transformer
Larger industrial load (LI)	10-3	With $S = 400$ kVA and $PF = 0.95$ (<i>ind.</i>), supplied via 630 kVA MV/LV transformer

MV network structure in the Netherlands.

The typical MV network structure, as presented in 5.2.1 and in [20], is adapted for simulations related to propagation of flicker and harmonic distortion. Assume a main 10 kV MV feeder in the main MV ring with length of 12 km, which supplies 10 equally distributed MV/LV substations with the typical value of the short-circuit power for a MV network in the Netherlands $S_q'' = 300$ MVA. The details of loads considered in the investigated 10 kV MV network are presented in table 5.4.

The schematic topology of the MV network used for investigation of flicker propagation is depicted in figure 5.8. The MV network model was developed in DlgSILENT PowerFactory [119].

As the common sources of flicker in MV networks are for instance industrial motors [28], in each case study motor startups are simulated and their impact on the flicker level propagation throughout the MV network is estimated for all other nodes. The locations of the distorting loads (DL), which are the sources of flicker in the 10 kV MV network are depicted in figure 5.8. The following case studies are considered in the investigating of flicker propagation in the 10 kV MV/LV network, as in figure 5.8:

- 10 – BB - distortion propagation from upstream HV/MV network, the distorting load (AM motor, $P_m = 400$ kW startup) is connected at node 10 – BB
- 10 – 6 - distortion propagating from middle of the MV network, the distorting load (AM motor, $P_m = 400$ kW startup) is connected at node 10 – 6

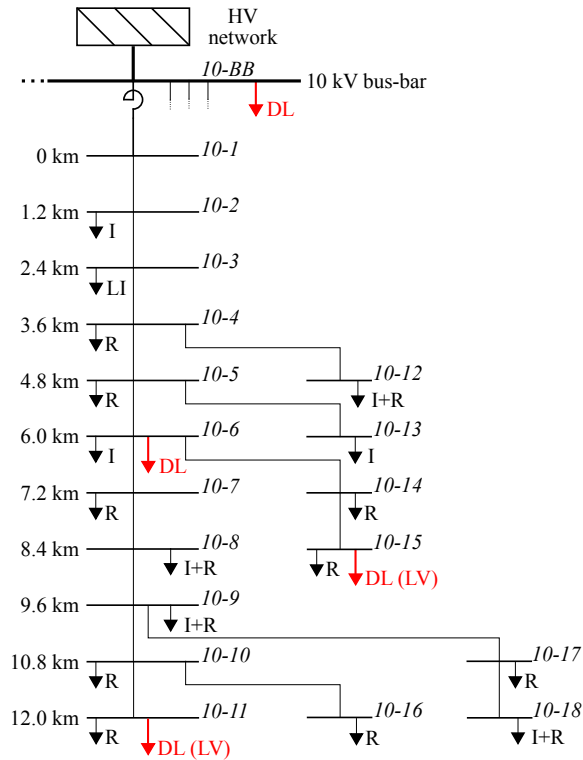


Figure 5.8: The topology of the 10 kV MV network structure used for assessment of PQ phenomena propagation. The notation *voltage-node number* is used for bus-bars, where residential (R), industrial (I), large industrial (LI) or mixed (I+R) loads connected. The distorting loads (DL) are connected to the 10 kV bus-bar or to the LV network.

- 10 – 11 - distortion propagation from end of the main MV feeder, the distorting load (AM motor, $P_m = 18.5 \text{ kW}$ startup) is connected at the LV part of the node 10 – 11
- 10 – 15 - distortion propagation from a MV branch, the distorting load (AM motor, $P_m = 18.5 \text{ kW}$ startup) is connected at the LV part of the node 10 – 15

For each case study is estimated the flicker level at the MV node with the distorting load and the flicker propagation towards upstream and downstream located MV nodes (MV) is estimated. The flicker transfer coefficients $T_{P_{st}}$ are defined as the share of P_{st}

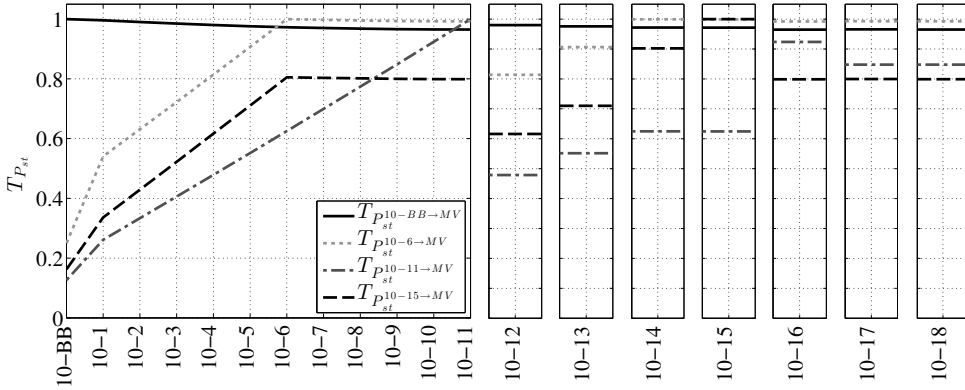


Figure 5.9: The flicker transfer coefficients for investigated case studies on the 10 kV MV network.

values at two locations in the MV network, $MV(1)$ and $MV(2)$, as in equation 5.5.

$$T_{P_{st}^{MV(1) \rightarrow MV(2)}} = \frac{P_{st}^{MV(2)}}{P_{st}^{MV(1)}} \quad (5.5)$$

The flicker transfer coefficients are estimated for all case studies and for all nodes in the investigated MV network. The estimated transfer coefficients are depicted in figure 5.9

Similarly, to the flicker propagation, the propagation of harmonic distortion in the 10 kV structure is investigated. The limits for harmonic distortion in HV and MV networks in the Netherlands are presented in table 5.5.

The propagation of harmonic distortion in the MV network is demonstrated on a set of case studies. The location of sources of distortion is identical with the locations of distorting loads in the 10 kV MV network structure, as in figure 5.8. The sources of harmonic distortion are simulated as current sources with $\frac{u_5}{u_1} = 1$ and $u_5 = 100$ A in following case studies, as in figure 5.8:

- 10 – BB - distortion propagation from upstream HV/MV network, the source of harmonic distortion connected at node 10 – BB
- 10 – 6 - distortion propagating from middle of the MV network, the source of harmonic distortion connected at node 10 – 6
- 10 – 11 - distortion propagation from end of the main MV feeder, the source of harmonic distortion connected at LV side at node 10 – 11

Table 5.5: The requirements on harmonic distortion for network users connected to the MV and HV network in the Netherlands (with $U_c \geq 1 \text{ kV}$).

Specifications	Description	Test methodology
$THD \leq 8 \%$	Total harmonic distortion limit of voltage, defined by EN 50160 [46] and by "Netcode Elektriciteit" [47]	Applicable for 95 % of the measured 10 min. mean rms values over one week period
$u_{1,\dots,25}$	Limits for individual harmonics defined as the relative value of the fundamental voltage in EN 50160 [46] and by "Netcode Elektriciteit" [47]	
Individual harmonics shall be $< 5.5 \cdot u_h$	Limits for individual harmonics shall be < 5.5 than indicated percentage in EN 50160 [46], as defined in "Netcode Elektriciteit" [47]	Applicable for 99.9 % of the measured 10 min. mean rms values
$THD \leq 12 \%$	Total harmonic distortion limit for u , defined by "Netcode Elektriciteit" [47] for networks with $U_c < 35 \text{ kV}$	
$THD \leq 6 \%$	Total harmonic distortion limit of voltage, defined by "Netcode Elektriciteit" [47] for HV networks with $35 \text{ kV} \leq U_c < 150 \text{ kV}$	Applicable for 95 % of the measured 10 min. mean rms values over one week period
$THD \leq 7 \%$	Total harmonic distortion limit of voltage, defined by "Netcode Elektriciteit" [47] for HV networks with $35 \text{ kV} \leq U_c < 150 \text{ kV}$	Applicable for 99.9 % of the measured 10 min. mean rms values

- 10 – 15 - distortion propagation from a MV branch, the source of harmonic distortion connected at LV side at node 10 – 15

Similarly to the propagation of flicker distortion in equation 5.5, the transfer coefficients can be estimated. The level of harmonic distortion is estimated for each MV node, where the source of harmonic distortion is located in the particular case study. The propagation towards MV nodes (MV) located upstream and downstream in the 10 kV MV network structure is estimated and the transfer coefficients are derived. The propagation of harmonic distortion depends on load composition and especially

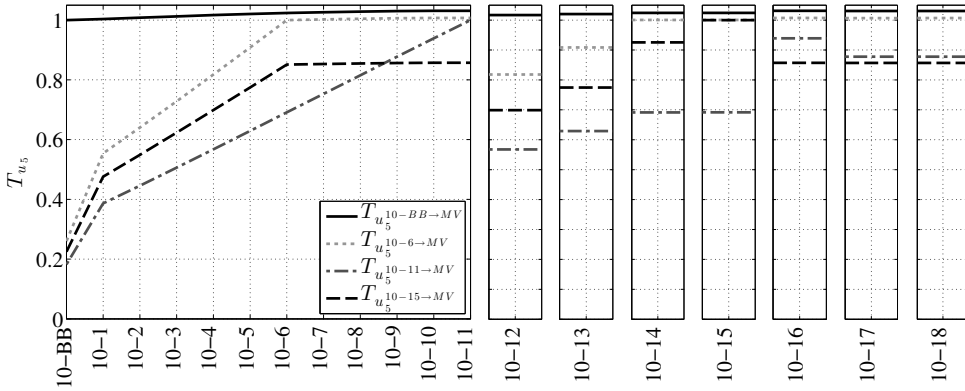


Figure 5.10: The transfer coefficients for propagation of harmonic distortion T_{u_5} , for all investigated case studies on the 10 kV MV network.

for a higher order harmonics can be significantly attenuated by certain loads in the network. The harmonic distortion u_5 is currently the most prominent in MV networks in the Netherlands. The transfer coefficients for harmonic distortion T_{u_5} are defined as the share of harmonic distortion at two locations in the MV network, $MV(1)$ and $MV(2)$, as in equation 5.6.

$$T_{u_5}^{MV(1) \rightarrow MV(2)} = \frac{u_5^{MV(2)}}{u_5^{MV(1)}} \quad (5.6)$$

The transfer coefficients for propagation of harmonic distortion are estimated for all case studies and for all nodes in the investigated MV network and the results for T_{u_5} are depicted in figure 5.10

In figure 5.9 and in figure 5.10 can be observed that flicker and harmonic distortion are attenuated in its propagation to upstream nodes in the 10 kV MV network structure. On the contrary, the propagation to MV nodes located downstream from the location with a source of distortion is only marginally attenuated. The propagation from LV network to MV network is strongly attenuated.

Therefore, the most suitable locations for a DSO to oversee the levels of harmonic distortion and flicker in the 10 kV MV network are the locations at the beginning of the MV feeder (location 10 – BB in figure 5.8), at its end (location 10 – 11) and at the end of all MV branches (locations 10 – 12, 10 – 13, 10 – 15, 10 – 16 and 10 – 18). The measurements shall be conducted in line with presented requirements given by the international and the national standards.

Table 5.6: The loads considered in the 20/10 kV MV network for investigation of PQ phenomena, as presented in figure 5.11.

Description	Location (MV nodes)	Specification
MV load on 20 kV feeder (L)	20-1, 20-2, 20-3	With $S = 2 \text{ MVA}$ and $PF = 0.99 \text{ (ind.)}$, each supplied via 20/10 kV transformer
Industrial load (I)	10-2, 10-9	With $S = 250 \text{ kVA}$ and $PF = 0.95 \text{ (ind.)}$, each supplied via 400 kVA MV/LV transformer
Residential load (R)	10-1, 10-3, 10-6, 10-7, 10-10, 10-11, 10-12, 10-13	With $S = 200 \text{ kVA}$ and $PF = 0.9 \text{ (ind.)}$ each, supplied via 400 kVA MV/LV transformer
Combined industrial and residential load (I+R)	10-4, 10-5, 10-8, 10-14	Residential part as a load with $S = 100 \text{ kVA}$ and $PF = 0.9 \text{ (ind.)}$, industrial part as a load with $S = 100 \text{ kVA}$ and $PF = 0.95 \text{ (ind.)}$, both supplied via 400 kVA MV/LV transformer
Larger industrial load (LI)	10-BB	With $S = 400 \text{ kVA}$ and $PF = 0.95 \text{ (ind.)}$, supplied via 630 kVA MV/LV transformer

5.4.2 PQ phenomena propagation in 20/10 kV MV network

The propagation of continuous fast PQ phenomena is assessed in this section for the concept of the 20/10 kV MV network structure described in 5.2.2, similarly to the investigation presented in 5.4.1 for the 10 kV MV network structure. The schematic topology of the considered 20/10 kV MV network used for investigation of flicker and harmonics propagation is depicted in figure 5.11. The MV network model was developed in DIGSILENT PowerFactory [119] and the loads considered in the 20/10 kV MV network structure are presented in table 5.6.

To evaluate the flicker propagation in the 20/10 kV MV structure, a set of case studies with distorting loads is presented. Consistently with the simulation on the 10 kV MV network structure, as in 5.4.1, motor startups are simulated in each case study and their impact on the flicker level propagation throughout the MV network is estimated for all remaining nodes. The locations of all distorting loads (DL), which are the sources of flicker in the 20/10 kV MV network are depicted in figure 5.11. The following case studies are considered in the investigating of flicker propagation, as in figure 5.11:

- 20 – BB - distortion propagation from upstream HV network, the distorting load (AM motor, $P_m = 400 \text{ kW}$ startup) is connected at node 20 – BB

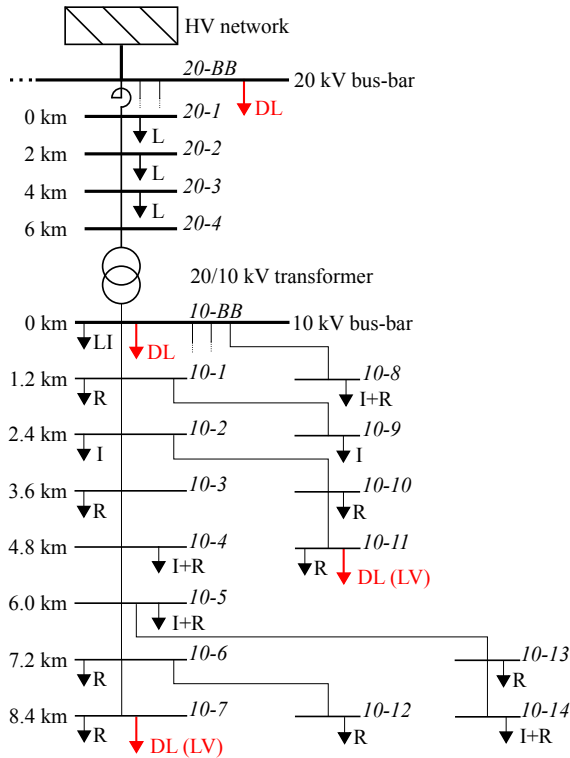


Figure 5.11: The topology of the 20/10 kV MV network structure used for assessment of PQ phenomena propagation. The notation *voltage-node number* is used for bus-bars, where residential (R), industrial (I), large industrial (LI) or combined (I+R) loads connected. The distorting loads (DL) are connected to the 10 kV bus-bar, 20 kV bus-bar or to the LV network.

- 10 – BB - distortion propagating from the beginning of the 10 kV MV network, the distorting load (AM motor, $P_m = 400 \text{ kW}$ startup) is connected at node 10 – BB
- 10 – 7 - distortion propagation from end of the main 10 kV MV feeder, the distorting load (AM motor, $P_m = 18.5 \text{ kW}$ startup) is connected at the LV part of the node 10 – 7
- 10 – 11 - distortion propagation from a 10 kV MV branch, the distorting load (AM motor, $P_m = 18.5 \text{ kW}$ startup) is connected at the LV part of the node 10 – 11

The flicker level is estimated for each case study and for all MV nodes. The flicker propagation towards upstream and downstream located MV nodes (*MV*) from the node with distorting load (DL) is estimated as in equation 5.5.

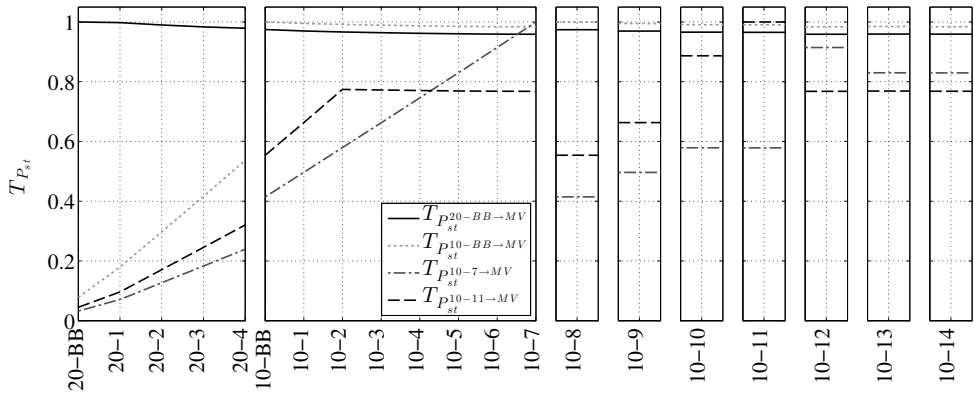


Figure 5.12: The flicker transfer coefficients for investigated case studies on the 20/10 kV MV network structure.

The flicker transfer coefficients are estimated for all case studies and for all nodes in the investigated MV network. The estimated transfer coefficients are depicted in figure 5.12. It can be observed in figure 5.12 that the flicker propagates downstream in the MV network structure with $T_{P_{st}} \approx 1$. The flicker propagation upstream is attenuated.

Next to the propagation of flicker, the propagation of harmonic distortion in the 20/10 kV structure is investigated on a set of case studies. The location of sources of harmonic distortion is identical with the locations of distorting loads for flicker propagation, as in figure 5.11. The sources of harmonic distortion are simulated as current sources with $\frac{u_5}{u_1} = 1$ and $u_5 = 100$ A in following case studies, as in figure 5.11:

- 20 – BB - distortion propagation from upstream HV network, the source of harmonic distortion connected at node 20 – BB
- 10 – BB - distortion propagating from the beginning of the 10 kV main feeder, the source of harmonic distortion connected at node 10 – BB
- 10 – 7 - distortion propagation from end of the main 10 kV feeder, the source of harmonic distortion connected at LV side at node 10 – 7
- 10 – 11 - distortion propagation from a 10 kV MV branch, the source of harmonic distortion connected at LV side at node 10 – 11

The level of harmonic distortion is estimated for each MV node, where the source of harmonic distortion is located in the particular case study. The propagation towards

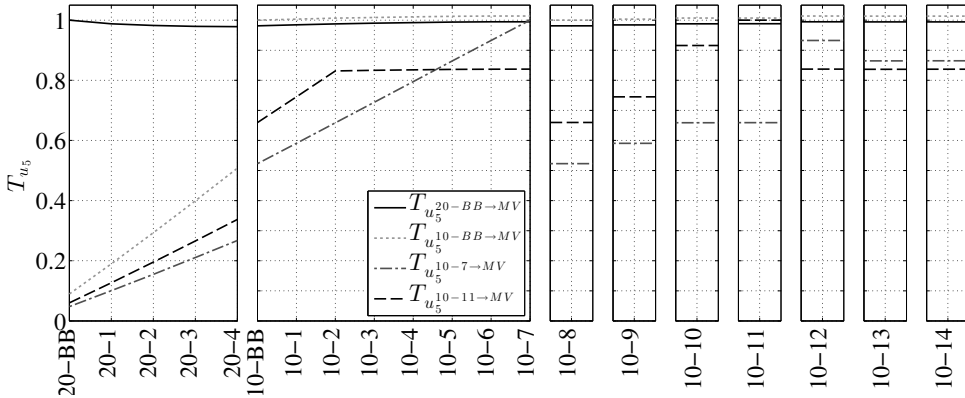


Figure 5.13: The transfer coefficients for propagation of harmonic distortion T_{u_5} , for all investigated case studies on the new 20/10 kV MV network structure.

MV nodes located upstream and downstream in the 20/10 kV MV network structure is estimated and the transfer coefficients are derived as in equation 5.6.

The transfer coefficients for propagation of harmonic distortion for all case studies in the investigated 20/10 kV MV network structure are depicted in figure 5.13.

The propagation of distortion is attenuated in its propagation to upstream nodes in the MV network structure and between different voltage levels. On the contrary, the propagation to downstream located nodes from the location with a source of distortion is only marginally attenuated.

Similarly to the 10 kV MV network structure, the most suitable locations for a DSO to oversee the levels of harmonic distortion and flicker in the 20/10 kV MV network are the locations at the beginning of MV feeders (locations 20 – BB and 10 – BB in figure 5.11), at its end (location 10 – 7) and at the end of all MV branches (locations 10 – 8, 10 – 9, 10 – 11, 10 – 12 and 10 – 14).

5.5 Conclusions

The operational and power quality aspects of MV distribution networks are presented in this chapter. A typical MV network structure and the concept of a mixed 20/10 kV MV distribution and MV transmission network are introduced. The mixed 20/10 kV structure is proposed by one of the network operators in the Netherlands mainly to improve the reliability of power delivery and to increase the MV network hosting capacity.

In chapter 4, the application of the on-line voltage tap changer for MV/LV substations is proposed. In this chapter the implications of different controls

strategies for voltage control in the LV network on the MV voltage network are assessed. The capabilities to mitigate the propagation of MV voltage variations, taking into account the different control strategies, are investigated and quantified. This capability can be used additionally in MV networks with a high penetration of DGs, where the currently used voltage control at the HV/MV substation will not yield satisfactory results and connected network users would experience high voltage fluctuations.

The requirements on power quality phenomena measurements and the propagation of power quality aspects in investigated MV network structures are presented. The propagation of power quality aspects in the MV network is demonstrated on a set of case studies for the typical MV network structure and for the concept of a mixed 20/10 kV MV network structure. It is shown, that the distortion is attenuated in its propagation to upstream nodes in the network. In the 20/10 kV structure, elements of the 10 kV network will be connected to the 20 kV ring and the propagation will be further attenuated. Therefore, a lower levels of distortion can be expected in the 20/10 kV structure compared to the 10 kV distribution.

It is concluded, that for a DSO to oversee the flicker levels and levels of harmonic distortion in the MV network, measurements at ends of MV network feeders shall be conducted at each voltage level. Knowledge of the propagation of harmonic distortion and flicker in the MV network can assist DSOs delivering power supply to network users in required quality.

Data applications

6.1 Introduction

The data needed for operation and power quality assessment of distribution networks are presented in chapters 4 and 5. Some of the developments in data management and distribution automation can unlock new functionalities at the distribution level. Therefore, some applications of data, measurements and operating assets in the distribution network are presented in this chapter:

- The application of OLTC control is utilized to unlock a demand-side management functionality at the distribution level, which resembles demand response (DR). The concept of DR induced via a voltage control at the IDS is presented in section 6.2. The availability of the proposed DR is evaluated and the application using the available DR to support system balancing is proposed. The implications on system imbalances are assessed and presented on a case study for the Dutch power system
- In section 6.3 is presented an application of measurement data from the LV network to detect and to locate the illegal abstraction of electricity within the LV network. The proposed application exploits measurement data available from the smart metering infrastructure and from the MV/LV substation
- In section 6.4 is presented the application of heavy loading assessment in distribution networks, which is based on exploitation of measurement data from smart metering infrastructure in LV network. This concept can enable monitoring of network components, which are not directly measured, but are likely to be exposed to heavy load conditions, which can be outside their operational limits

6.2 Application of OLTC for demand side management

At the distribution level, the DSO strives to achieve a well-functioning distribution system with high reliability and economic operation. Ergo, new developments in the distribution network automation are undertaken. However, some developments can expand the boundaries of intended applications for distribution networks only, and can facilitate new services traditionally attributed to the transmission system operator. A DSO implements active voltage control to improve power quality, to defer network investments and to increase distribution network assets utilization. However, simultaneously new services, such as supporting power system balancing, can emerge with active voltage control, without affecting the initial goal of improving supplied voltage quality to network users.

The aim of this section is to present an application of active voltage control, as a new service provided at the distribution level, which can be enabled by distribution automation. The proposed application can enable demand-side management which resembles demand response (DR) induced by voltage control, which can be used, for instance for supporting power system balancing.

The demand-side management encompasses functions directing mostly demand activities to influence customers load [120]. DR schemes are mainly used to lower electricity costs and to support power system at times, when the power system reliability is jeopardized (e.g., direct load control) and when the system is stressed [121], [122]. Nowadays, the real-time demand response schemes are proposed to reflect on actual electricity prices and to provide an incentive to change network users behaviour [123], [124], [125]. The proposed DR mechanism in this section is based on utilization of DSO equipment to induce real-time load changes and belongs to the demand-side management scheme, where DR is realized via a direct control through utility equipment.

The on-line voltage control can be applied in distribution networks to accommodate new technologies such as DG, as discussed in 4.5.1. However, on-line voltage control through on-line tap changing (OLTC) can simultaneously induce DR. This functionality was tested in a field test and results are presented in 6.2.1. The accessible voltage range can be quantified as a function of supplied load, as presented in 6.2.2, and the available DR can be estimated as in 6.2.3. The impact of the proposed application on power system balancing is assessed in 6.2.4. The evaluation of the distribution network losses related to the proposed service provision is presented in 6.2.5. The technologies enabling the proposed DR application are discussed in 6.2.6.

6.2.1 Field test with OLTC

Every load responds in a certain way to changes in supplied voltage. The load response to a voltage change was explored in several voltage reduction applications, which aimed to use the load response effect for electricity consumption reduction or for lowering the system peak load [126] and it is known as the conservation voltage reduction (CVR)

technique. Although with some controversy about the magnitude of achievable load response, CVR has been used to achieve energy saving objectives and to conserve energy [127], [128], [129], [130]. Voltage level control has also been applied by vertically integrated utilities to reduce cost of peak generation, before the unbundling of electricity sector took place [131]. With the unbundling of the electricity sector [132], interest in CVR as a tool for load control has diminished. The entities, which can apply the voltage control actions in the network (DSOs and TSOs), are not substantially benefiting from load reduction as they do not participate on electricity generation. But for balancing the power system active voltage control might still be an interesting application.

The MV/LV transformer with OLTC tested is a conventional 10/0.4 kV MV/LV transformer equipped with power-electronic tap-changer on its primary side (without mechanical tap adjustments). The OLTC allows fast and on-line voltage level control [95] [96], which mitigates voltage fluctuations in the distribution network.

Assume that a control action is taken by OLTC to change the voltage level at the LV bus-bar. The voltage level change will consequently result in alternation of power demanded by supplied LV network (with all LV network users). The load response to the voltage change depends on load composition, but in general, if the voltage decreases, the power drawn by supplied loads reduces and vice versa. Therefore, at any time instance t , if a voltage control is requested, the voltage level (e.g., at the LV bus-bar of the transformer) can be either increased by ΔU_{up} , or decreased by ΔU_{down} . If applied, a voltage change will have impact on network users in the supplied LV network and will result in alternation of demanded power by the LV network. For instance, if at time t_0 , the supplied voltage level can change from U_0 to U_1 , the power demanded (e.g., by the LV network) will alter from P_0 to P_1 as a consequence of induced voltage change. The principle of voltage control actions, which can be applied for alternation of demanded power is depicted in figure 6.1. Where in case of the positive voltage change ΔU_{up} applied, the demanded power is expected to increase by ΔP_{up} , as depicted in figure 6.1b, and vice versa for ΔU_{down} and ΔP_{down} , as depicted in figure 6.1a.

The change of power demanded ΔP , as a response to the applied voltage change ΔU , can be expressed per unit with the load response ratio PU_{ratio} , as in equation 6.1.

$$\begin{aligned}
 PU_{ratio} &= \frac{\frac{|P_0 - P_1|}{P_0}}{\frac{|U_0 - U_1|}{U_0}} \\
 &= \frac{\Delta P}{\Delta U}
 \end{aligned} \tag{6.1}$$

A field test was conducted in the network of Allinader (Dutch DSO) to estimate the PU_{ratio} of a real LV network in the Netherlands [133]. As more loads with a power

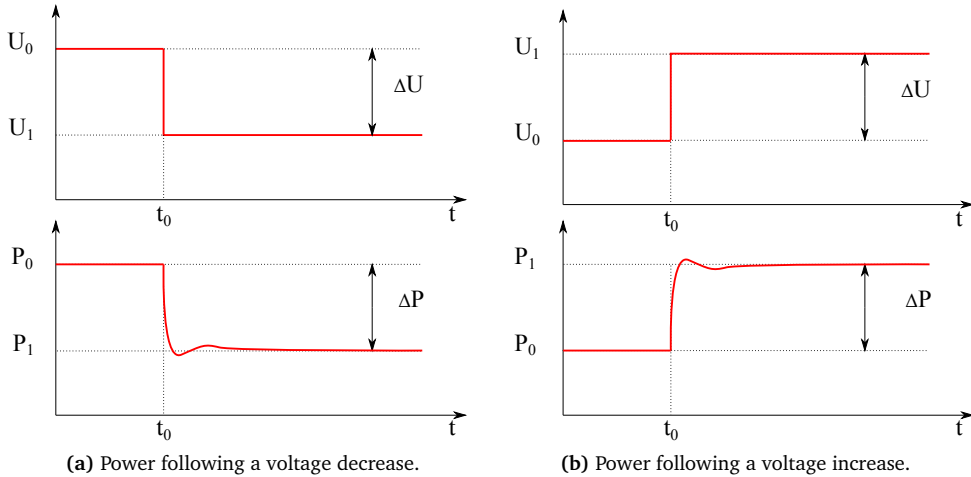


Figure 6.1: The principle of voltage control to achieve response in supplied loads; for a voltage decrease 6.1a and for a voltage increase 6.1b.

electronic interface can be nowadays expected in LV networks supplying residential network users and as those loads can behave as constant power loads, the motivation for the field test was to evaluate if a load response can be still observed in nowadays LV network. The aim of the field test was also to examine the possibilities of voltage control with the installed transformer with OLTC and to validate the feasibility of the proposed concept. The field test had to respect the standard for supplied voltage quality and the limits set for deviation from U_n , as discussed in 4.4. Although higher voltage deviation would be possible, only the voltage range of $\approx 4\% U_n$ was allowed to avoid any violations of supplied voltage level for connected network users. In addition, due to the experimental conditions, the voltage level steps had to be manually set by controlling the OLTC on the primary side (10 kV) of the MV/LV transformer. Due to the practical constraints, the field test had a demonstration purpose and only a limited duration [133].

Among other variables, the voltage level and the active power values at the LV busbar were measured during the field test. To compare all measurements; the active power and the voltage level at the beginning of each voltage step are compared against the active power and the voltage level at the end of each voltage step. The relative values are estimated, as the difference from the actual voltage and power level before and after the applied voltage step. The average duration of the applied voltage step was ≈ 8 s. The results from the field test, as measured voltages versus the measured active power at the beginning and the end of each voltage steps, are depicted in figure 6.2. Consequently, the average load response ratio was

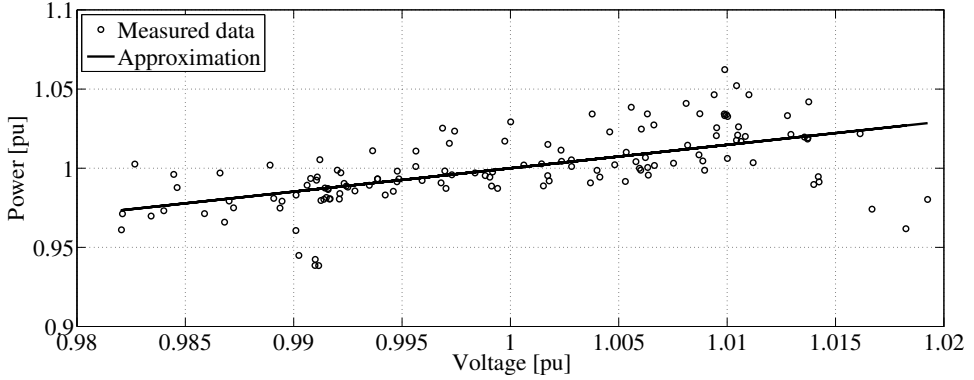


Figure 6.2: The measured active power versus the measured voltage at the secondary side of the transformer about the time, when a voltage change was applied with OLTC during the field test. The first-order approximation of the results with slope of the PU_{ratio} is depicted as solid line.

estimated $PU_{ratio} = 1.5$. As insufficient number of measurements is available for reliable higher-order approximations, the first-order approximation of measured results is used. The approximation of the average load response ratio is presented also in figure 6.2 as a solid line with the slope corresponding to the estimated PU_{ratio} .

Although the field test has some limitations, it demonstrated the potential and the feasibility of the proposed application. The results of the field test are comparable with CVR studies, as presented in an overview in table 6.1 for available information based on expected energy and power reductions. However, the impact on the long-term energy consumption of network users could differ from the values presented and was not the aim of the conducted field test. Note, that despite some controversy about CVR technique applicability nowadays, considerable benefits can be achieved with the application of CVR technique in modern power systems, as presented in a recent work [134].

6.2.2 The available voltage range to induce DR

In comparison to the voltage control applied at the HV/MV substations, IDS offers voltage control, which can be applied locally for a single LV network. Therefore, higher voltage variations can be achieved, in comparison to the control scheme applied at the HV/MV substation, without jeopardizing the supplied voltage quality of connected network users. To correctly assess the full potential of proposed DR, the technically possible and the available (allowable) voltage range have to be distinguished. Whereas, the technically possible voltage range is limited only by the OLTC constraints, the available (or allowable during normal operation) voltage range reflects also on the

Table 6.1: The overview of CVR studies and the load response coefficients estimated (CVR results presented as equivalent to PU_{ratio}).

Source	Load response (PU_{ratio} equivalent)	Note
Pacific Northwest National Laboratory [134]	0.5 to 4	Report about the national wide benefits of CVR for the USA
Khurmy et al. [135]	3	Maximum energy saving potential with the CVR technique
Scalley et.al. [126]	0.5 to 4	Values range based on 22 CVR related studies
Krupa et.al. [136]	0.96 to 1.11	Based on values of the annual average change of real power for residential loads

voltage level conditions in the LV network and limits the technically possible range to maintain the supplied voltage quality for all LV network users.

The OLTC adjustments in the HV/MV substation actively offset the voltage drop among the distribution network and moderate voltage level fluctuations. The MV voltage level fluctuations resulting in $\pm 5\% U_n$ in the LV network are commonly accepted in the Netherlands. The actual voltage level in the MV network is location specific and depends on the substation location in the MV network. The position of IDS will have implications on the available voltage range for provision of proposed DR. In a real application the available voltage range to induce DR could differ for different locations of IDS in the MV network. Therefore, to evaluate the potential of the proposed DR application in general, the nominal voltage at the MV side of IDS is used and the OLTC adjustments are undertaken to satisfy the control objective of maintaining the LV bus-bar voltage at U_n , as discussed in 4.5.

The transformer with OLTC (on MV side) in the IDS can adjust the secondary voltage (LV side) within the range $\langle U_{TR,min}; U_{TR,max} \rangle$, given by the design as $\langle U_n - 5\%; U_n + 5\% \rangle$ [95]. The actual tap position, expressed by the OLTC voltage $U_{tap}(t)$, reflects the OLTC adjustments to maintain the control objective of LV bus-bar voltage at U_n . The OLTC control strategy A is assumed. Therefore, the available voltage range to induce DR varies over time due to load variations. As the OLTC operates within $\langle U_{TR,min}; U_{TR,max} \rangle$, the remaining voltage range can be accessed to perform voltage control for DR purposes. For each time instance t , the available maximal voltage increase $U_{up,max}(t)$ can be defined as in equation 6.2. To perform voltage control for DR purposes, the available (allowable) voltage increase $U_{up,max}(t)$ shall respects the voltage level conditions in the LV network. Therefore, control actions, which will induce a voltage at any POC $U_{max}^{POC}(t) > U_n + 10\%$, shall be avoided, as discussed in 4.4.

This limitation due to voltage level maxima, observed in the LV network at POCs, is introduced with $U_{max}^{POC}(t)$ in equation 6.2.

$$U_{up,max}(t) = U_n + \min \left(U_{TR,max} - U_{tap}(t), (U_n + 10\%) - U_{max}^{POC}(t) \right) \quad (6.2)$$

Similarly, the available maximum voltage range for voltage decrease $U_{down,max}(t)$ can be defined, as in equation 6.3. Any control action, which will result in a voltage level decrease at any POC, such that $U_{min}^{POC}(t) < U_n - 10\%$ shall be avoided, as discussed in 4.4.

$$U_{down,max}(t) = U_n - \min \left(U_{tap}(t) - U_{TR,min}, U_{min}^{POC}(t) - (U_n - 10\%) \right) \quad (6.3)$$

The limit of declared supply voltage variation (at POCs of connected network users) introduces limitations on the available control range, which can be utilized at the IDS for the proposed DR application. Therefore, the voltage conditions of all connected LV network users in the typical LV network in the Netherlands, as presented in 4.2, were evaluated. The load profiles were generated on weekly basis for a week in the summer period and for a week in the winter period to cover both load extremes and to utilize available data. The network user load profiles were generated based on the measured data to provide a realistic input, as discussed in 4.3. The voltage drop in the network depends on the network users behaviour and on the power demanded at every time instance. As the load allocation and its time dependency has random characteristics, the voltage conditions were assessed based on a Monte Carlo simulation with 10 000 week iterations, simulating the possible conditions in the LV network and different load-behaviours of network users. This approach enables the evaluation of the voltage conditions in the whole LV network and the occurrence probability estimation for each time instance. The time resolution of 15 min. is applied throughout the simulation.

The results from the Monte Carlo simulation allow the estimation of the cumulative distribution function of all supply voltages in the investigated LV network for every time instance t . By selecting the limit values, the share of supply voltages within a defined range of probability occurrence can be estimated. The voltage conditions in the complete LV network can be assessed as a function of time and required probability of declared supply quality deviation from U_n . The results for the summer period are depicted in figure 6.3 and for the winter period in figure 6.4.

It can be seen in figure 6.3 and in figure 6.4, that if a larger voltage range for DR purposes was allowed, by accepting that network users will be supplied with $U_n \pm 10\%$ with certain probability $< 100\%$, extended control actions would be possible. For instance, consider the differences in voltage conditions in the investigated LV network in figure 6.3 and in figure 6.4, if a occurrence probability of $< 99\%$ or $< 99.9\%$ would be acceptable.

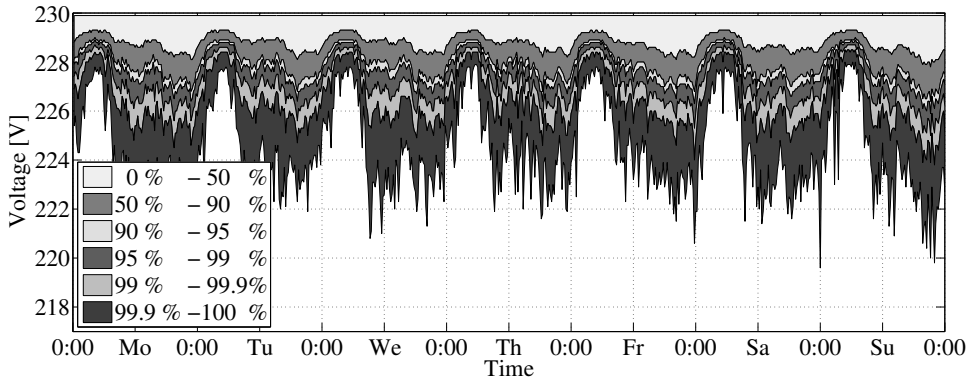


Figure 6.3: The estimated supply voltage levels at all POCs in the investigated LV network as a function of occurrence probability within the defined range of one week period in the summer time.

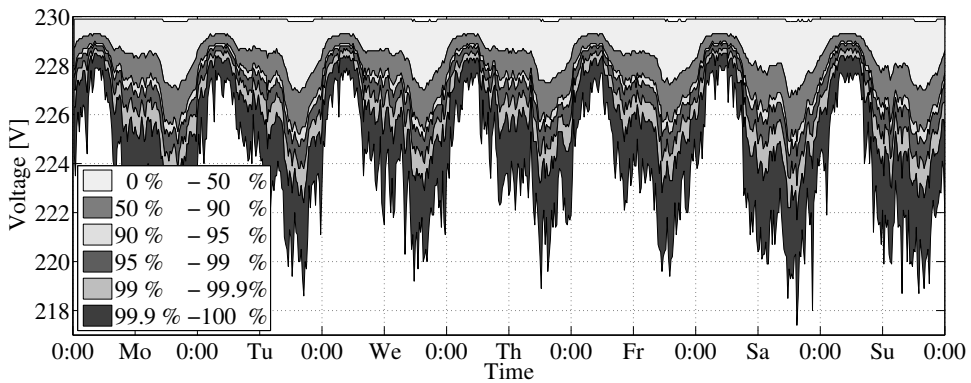


Figure 6.4: The estimated supply voltage levels at all POCs in the investigated LV network as a function of occurrence probability within the defined range of one week period in the winter time.

The currently applied standard for quality of supply voltage EN 50160 defines allowed supply voltage variations for LV network users as $U_n \pm 10\%$ for 95% of 10 min. mean rms values measured over one week period, as discussed in 4.4. However, extended voltage control actions could be possible in some situations or when larger supply voltage variation ($U_n - 15\% < U_{min}^{POC} \leq U_n - 10\%$) would be acceptable.

The estimated voltage limits $U_{min}^{POC}(t)$ and $U_{max}^{POC}(t)$, with a certain probability, can be utilized as limiting factor for the evaluation of the available voltage range for OLTC control in time, as in equation 6.2 and in equation 6.3. The voltage level limits $U_{min}^{POC}(t)$

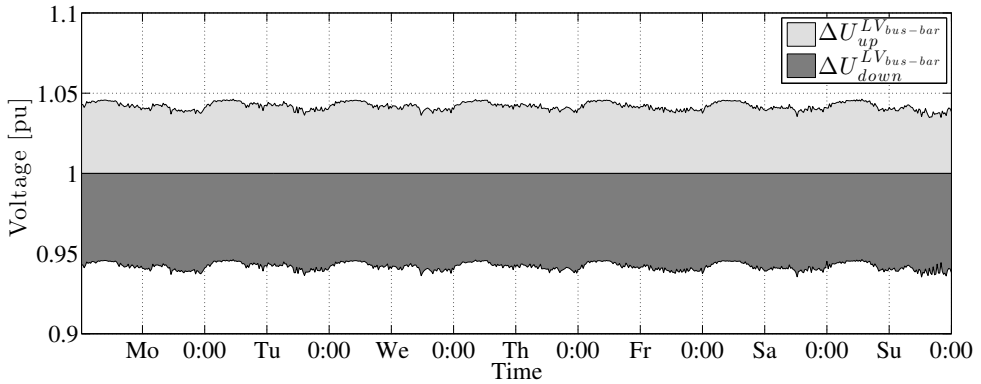


Figure 6.5: The available voltage control range for the investigated LV network over one week period in the summer time.

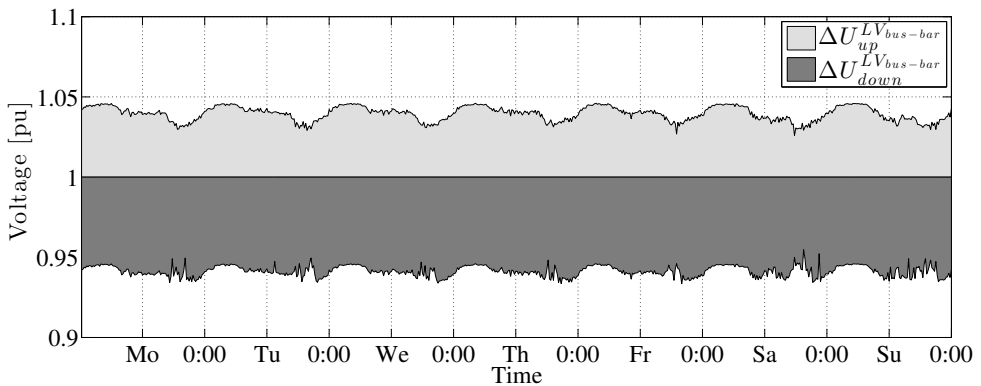


Figure 6.6: The available voltage control range for the investigated LV network over one week period in the winter time.

and $U_{max}^{POC}(t)$ from the Monte Carlo simulation, that ensure 100 % of supply voltages within $U_n \pm 10\%$ are used for estimation of the available voltage range to enable DR with OLTC. To comply with the limitations on the LV supply voltage level, the available voltage increase at the LV bus-bar shall be within $\Delta U_{up}^{LV_{bus-bar}}(t)$, as in equation 6.4.

$$\Delta U_{up}^{LV_{bus-bar}}(t) = U_n + U_{tap}(t) - U_{up,max}(t) \quad (6.4)$$

Similarly, the available voltage decrease at the LV bus-bar shall be

within $\Delta U_{down}^{LV_{bus-bar}}(t)$, as in equation 6.5.

$$\Delta U_{down}^{LV_{bus-bar}}(t) = U_n + U_{down,max}(t) - U_{tap}(t) \quad (6.5)$$

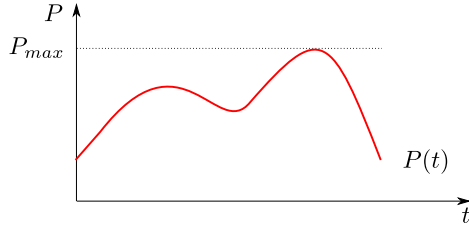
The available (allowed) voltage range can be defined as a function of time over the simulation period, where the voltage control adjustments within the range $\Delta U_{up}^{LV_{bus-bar}}(t)$ and $\Delta U_{down}^{LV_{bus-bar}}(t)$ can be applied for the proposed DR application. The available voltage control over a one week period in the summer time is depicted in figure 6.5 and for the winter period in figure 6.6. The voltage range limitations, to avoid voltage levels in the LV network $U_{min}^{POC} < U_n - 10\%$, can be noticed in figure 6.6 for the afternoon peak periods. In the investigated LV network, these periods coincide with high loads and consequently with expected high voltage drops, as depicted in figure 6.4.

6.2.3 The availability of induced DR

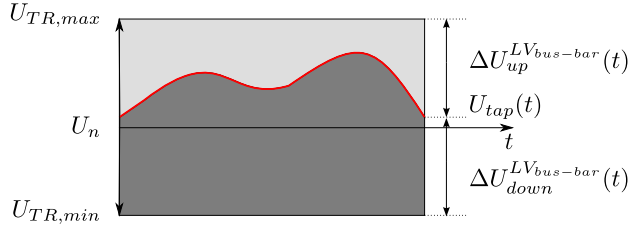
The principle of the proposed DR application induced via OLTC voltage control is presented in figure 6.7. As the loading at the MV/LV substation varies throughout a day, depicted in figure 6.7a, the OLTC tap position voltage $U_{tap}(t)$ is adjusted according to the OLTC control objective to maintain the LV bus-bar voltage at U_n . The OLTC operates within its operating limits $\langle U_{TR,min}; U_{TR,max} \rangle$. As the LV load increases during the day, adjustments with higher $U_{tap}(t)$ are set. The available voltage range, which can be used for DR purposes $\Delta U_{up}^{LV_{bus-bar}}(t)$, $\Delta U_{down}^{LV_{bus-bar}}(t)$, can be estimated with respect to limitations due to the LV voltage level conditions of network users, as discussed in 6.2.2. The available voltage range throughout a day is schematically depicted in figure 6.7b.

Due to the positive correlation between supplied power and voltage at IDS, a change of supply voltage will induce a changes in demanded power at the MV/LV substation according to the PU_{ratio} , as assessed in 6.2.1. Ergo, the on-line OLTC operation can be utilized to enable on-line power adjustments at the MV/LV substation. The voltage adjustments at the LV bus-bar can deliver a load increase $\Delta P_{up}^{LV_{bus-bar}}(t)$ or a load decrease of the actual load observed at the LV bus-bar, as depicted in figure 6.7c. The available $\Delta P_{up}^{LV_{bus-bar}}(t)$ and $\Delta P_{down}^{LV_{bus-bar}}(t)$ can be then determined in absolute terms (e.g., to be comparable with ancillary service deployment), as depicted in figure 6.7d. The availability of the proposed DR application depends on the actual load controlled via voltage adjustments, therefore maxima of $\Delta P_{up,max}^{LV_{bus-bar}}$ and $\Delta P_{down,max}^{LV_{bus-bar}}$ coincide with maxima of supplied load, as depicted in figure 6.7a and in figure 6.7d.

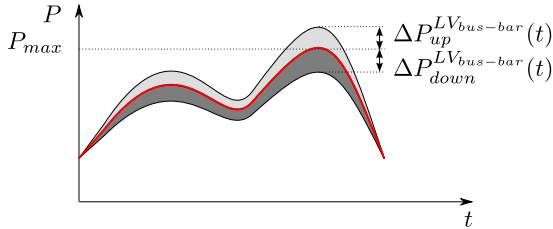
The available voltage range at the LV bus-bar for DR purposes (including presented limitations) $\Delta U_{up}^{LV_{bus-bar}}(t)$ and $\Delta U_{down}^{LV_{bus-bar}}(t)$ is estimated, as discussed in 6.2.2. The available DR at IDS can be then determined assuming the PU_{ratio} as measured at IDS and discussed in 6.2.1. The available DR per IDS as $\Delta P_{up}^{LV_{bus-bar}}(t)$ and $\Delta P_{down}^{LV_{bus-bar}}(t)$ can be consequently determined for each time period. The results of the available DR at IDS are estimated and presented for one week in the summer period, in figure 6.8, and for one week in the winter period in figure 6.9.



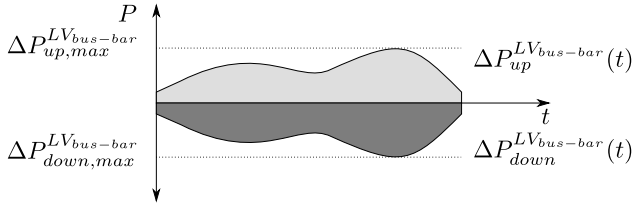
(a) Daily loading profile at a MV/LV substation.



(b) OLTC tap position $U_{tap}(t)$ adjustment following the load.



(c) Relative controllable load supplied by a MV/LV substation.



(d) Absolute controllable load supplied by a MV/LV substation.

Figure 6.7: The principle of the proposed voltage control at a MV/LV substation to enable on-line DR with OLTC. The loading at the MV/LV substation (a). Available voltage range to induce DR (b). The load at a MV/LV substation responds to the voltage changes according to the PU_{ratio} (c). The absolute value of controllable load (d).

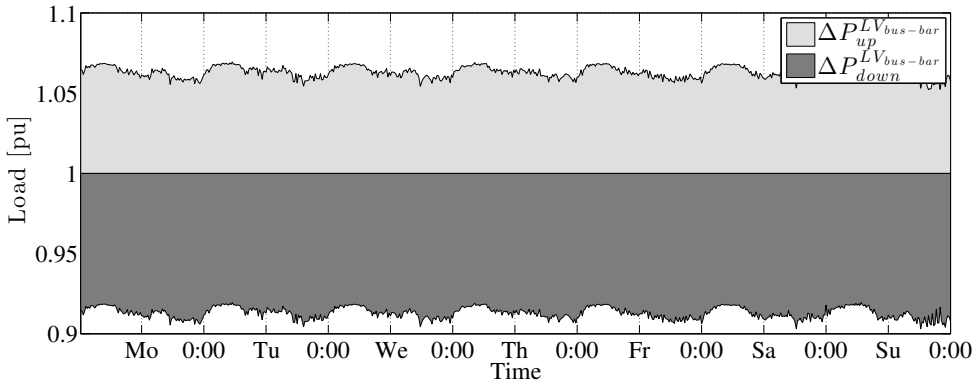


Figure 6.8: The available load (related to the actual load at IDS) for DR in the investigated LV network over one week period in the summer time with $PU_{ratio} = 1.5$.

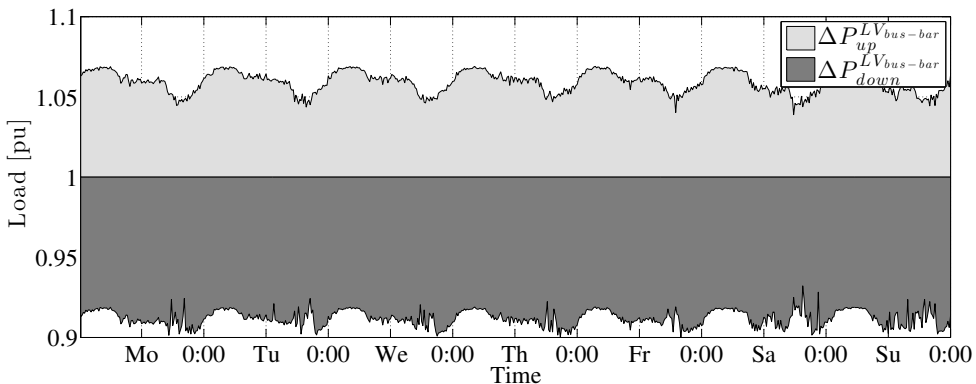


Figure 6.9: The available load (related to the actual load at IDS) for DR in the investigated LV network over one week period in the winter time with $PU_{ratio} = 1.5$.

6.2.4 Supporting system balancing with OLTC

In an electrical power system, the electricity generation has to match the electricity consumption to maintain the stable system frequency. The electricity consumption is predicted (forecasted) and the electricity generation is scheduled to match the consumption and as the electricity trade can't handle the very short-time deviations of the electricity consumption and generation, the system imbalances can occur in power systems. With the increasing share of the intermittent generation in the electricity generation mix, the needs for maintaining system stability and the needs for system balancing will increase [137]. Ergo, the proposed DR application with IDS can be

complementary to other approaches for system balancing with high penetration of intermittent generation to rationalize the power system operation [138].

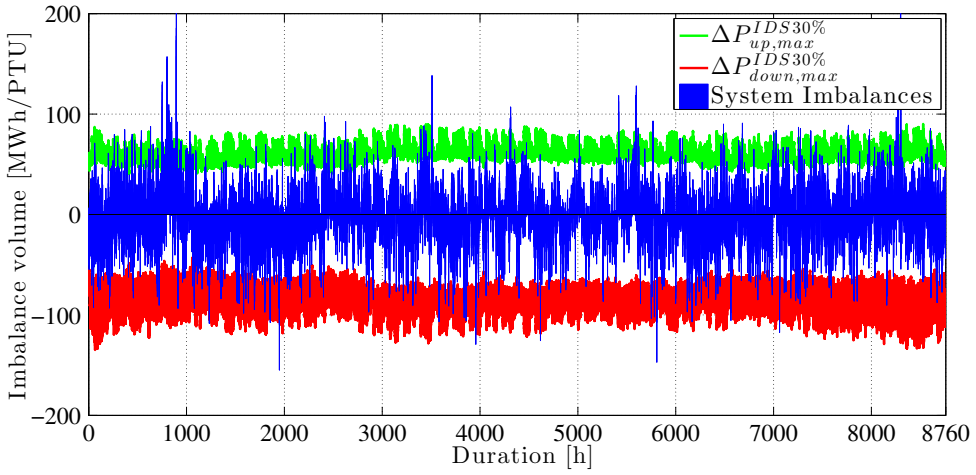
The system operator has the responsibility to maintain the system balance. This task is assigned in Europe to multiple transmission system operators (TSO). Each system operator controls in real-time the system balance (e.g., in the Netherlands every 4 s.) in its control area and calls bids for system area balancing (in market based load frequency control) to restore system balance in specified time frames. The system imbalances are also partially covered by passive contribution of generation units [137].

A set of case studies is presented to demonstrate the implications of the proposed DR application on provision of system services. The proposed DR application with IDSs focuses on participation on system area balancing (system area control) and implications of its deployment on secondary regulation are investigated. The generation scheduling in the power system in the Netherlands is based on hourly intervals, whereas the operational planning (settlement periods) are in 15 min. intervals called program time unit (PTU). The system balances are monitored real-time and recorded per PTU by the Dutch TSO (TenneT TSO).

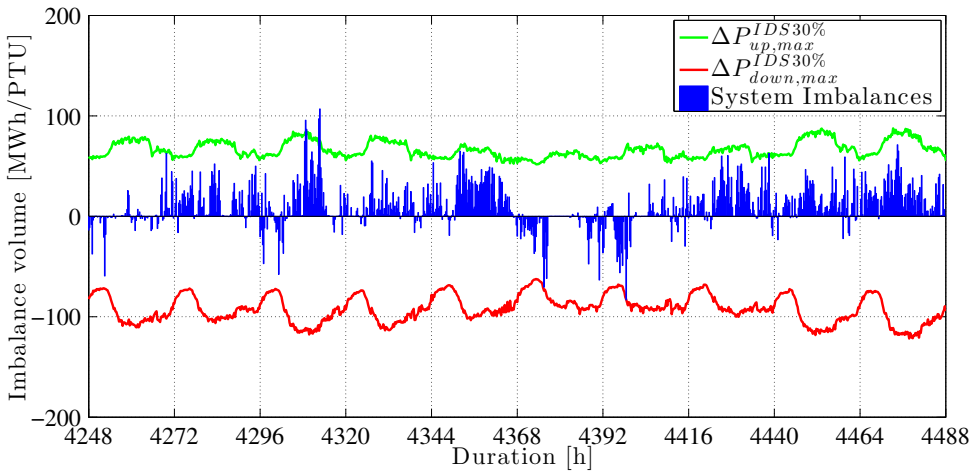
The proposed DR with IDS at the distribution level is evaluated as a new (ancillary) service participating in system area balancing. The proposed DR scheme can deliver DR actions, which are proportional to the load supplied by the MV/LV substation, as discussed in 6.2.3. In the Netherlands, about 30 % of the system load is supplied to residential customers via distribution network, where the voltage control with OLTC is applicable to induce proposed DR service in certain range, as discussed 6.2.2. Therefore, five penetration levels of IDS with OLTC in the distribution network are assessed. The evaluation of penetration levels of IDS in the system is estimated for 1 %, 5 %, 10 %, 20 % and 30 % of load supplied by $\approx 120\,000$ MV/LV substations in the Netherlands. The penetration levels are used as superscripts of mentioned variables (e.g., $IDS^{30\%}$). The evaluation of different penetration levels of IDSs in the system is estimated based on extrapolation.

The availability of the proposed DR depends on the load supplied, which is evaluated in 15 min. intervals. This resolution is suitable for a comparison with PTU lengths applied in the Netherlands for the imbalance market. The results are derived for each penetration level of IDS in the system contributing to mitigate system imbalances. The participation of IDS and the maxima of available DR provisioned by IDSs are evaluated for each penetration level of IDSs in the system. The imbalance data per PTU for the Netherlands in year 2012 are considered as input data for simulations (source: TenneT TSO).

Assume a case study, where IDSs with 30 % penetration level participated on the DR provision in the Netherlands in year 2012. The available DR provision over a year can be estimated within the available DR maxima for the specific penetration level $\langle \Delta P_{down,max}^{IDS^{30\%}}; \Delta P_{up,max}^{IDS^{30\%}} \rangle$ and contrasted with the occurrence of imbalance volumes in the Netherlands for the same year. The results per PTU are depicted in figure 6.10, where the overview of the year 2012 is presented in figure 6.10a and a detail presenting the time availability of DR $\langle \Delta P_{down,max}^{IDS^{30\%}}; \Delta P_{up,max}^{IDS^{30\%}} \rangle$ with imbalances recorded over the



(a) System imbalances and estimated available DR for year 2012.



(b) Detail of figure 6.10a for 10 days in mid 2012.

Figure 6.10: The estimated availability of the proposed DR application with IDS over one year period (a) and with a detail for a period of 10 days in mid 2012 (b). The availability of proposed DR is contrasted with the system imbalance data in the Dutch power system in year 2012. The DR availability as $\langle \Delta P_{down,max}^{IDS30\%}, \Delta P_{up,max}^{IDS30\%} \rangle$ is estimated for 30 % share of the total load supplied by IDS participating in system balancing.

period of 10 days in mid 2012 is depicted in figure 6.10b.

As shown in figure 6.10, with a detail in figure 6.10b, the time dependency of the available DR varies over time and presents an important factor, which has to be considered to correctly address the mitigation capabilities of the proposed DR scheme and its implications on system imbalances. It can be observed in figure 6.10, that in most of time instances throughout a year, the called system imbalances can be fully met by the means of the proposed DR provision by IDSs with 30 % penetration level.

Based on the actual imbalance data for the Netherlands in year 2012, the remaining imbalance volumes per PTU, after deployment of the proposed DR, can be estimated for each IDS penetration level with respect to the time availability of called imbalances and with respect to the time availability of proposed DR application. The duration curve of original imbalance data can be estimated, based on the imbalance data. The imbalance duration curves of remaining imbalance volumes per PTU for certain penetration level of IDS in the system can be contrasted with the original imbalance data for the Netherlands in year 2012. The results are presented in figure 6.11. Note that the available provision of proposed DR is proportional to the load supplied by IDS. Although a significant DR capacity on the system level can be provided by a high penetration of IDSs in the system, there can be still remaining imbalances in the system, which have to be mitigated in a conventional way. This can be observed in figure 6.11, where certain imbalances in the system can remain even for 30 % penetration level of IDSs in the system assumed, if the calls for imbalances are higher than the available $\Delta P_{down,max}^{IDS30\%}$, $\Delta P_{up,max}^{IDS30\%}$, as depicted in figure 6.10.

The simulation results point out, that the total amount and the magnitude of called imbalances volumes in the system can be significantly reduced if the proposed application is deployed. For instance, if 30 % penetration level of IDSs in the Dutch power system in the year 2012 participated in system balancing, the magnitude of peak imbalances volumes would have been reduced by $\approx 31\%$ for positive and by $\approx 42\%$ for the negative imbalances occurring in the system. The total amount of called imbalance volumes would be reduced and the remaining imbalance volumes (not covered by IDS) can be estimated based on the original called positive imbalance volumes in the year 2012 $\Delta P_{up}^{IMB2012}$ and for the negative called volumes in the same year $\Delta P_{down}^{IMB2012}$. The number of PTUs reflect the operation time of a power system considered, usually 8 760 h over a year would result in 8 760 · 4 PTUs in the Dutch power system. The reduction factor of called imbalance volumes, due to the 30 % of IDS participating on system balancing, for year 2012 $\Delta P_{up,red}^{IDS30\%,IM2012}$ can be estimated as in equation 6.6.

$$\Delta P_{up,red}^{IDS30\%,IM2012} = 1 - \sum_{t=1}^{PTUs} \left(\Delta P_{up}^{IM2012}(t) - \Delta P_{up,red}^{IDS30\%,IM2012}(t) \right) \quad (6.6)$$

Similarly, the reduction factor of called negative imbalance volumes for

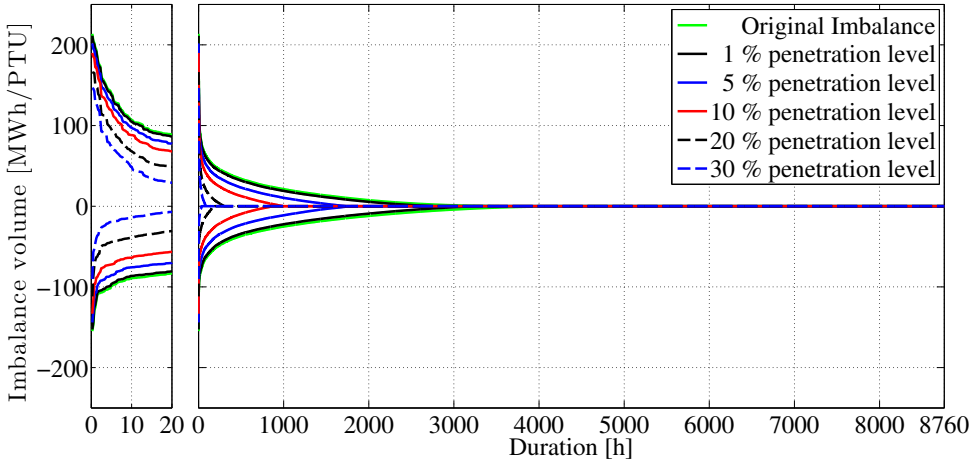


Figure 6.11: Original imbalance volumes duration curve based on the data for the Netherlands in year 2012 contrasted with the remaining imbalance volumes duration curves after deployment of available DR for system support. The results are depicted for all IDS penetration levels considered in the system.

30 % penetration level of IDSs in the system can be estimated as in equation 6.7.

$$\Delta P_{down,red}^{IDS30\%,IM2012} = 1 - \sum_{t=1}^{PTUs} \left(\Delta P_{down}^{IM2012}(t) - \Delta P_{down,red}^{IDS30\%,IM2012}(t) \right) \quad (6.7)$$

The reduction in the amount of called imbalance volumes in the power system would be significant, if IDSs provided DR for participation on system balancing. For instance in year 2012, the reduction of the amount of called imbalance volumes of $\Delta P_{up,red}^{IDS30\%,IM2012} = 97\%$ and $\Delta P_{down,red}^{IDS30\%,IM2012} = 99\%$ would be theoretically possible in the investigated power system.

The impact of the proposed DR provision to participate in system balancing can be assessed based on the utilization factors of the available DR capacity for each penetration level of IDSs in the system. The total amount of available DR capacity depends on IDS penetration level in the system and it is time dependent. Therefore, the utilization of available DR to support power system balancing depends also on IDS penetration level and on the coincidence of called imbalances with the available capacity in the system. The utilization factor of the available DR for mitigation of system imbalances $\Delta P_{down,util}^{IDS30\%,IM2012}$ and $\Delta P_{up,util}^{IDS30\%,IM2012}$, depends on the penetration level of IDSs in the investigated system and on the called imbalance volumes in the system over the investigated period. Those variables define the deployment

of available DR $\Delta P_{down,depl}$ and $\Delta P_{up,depl}$ in the system. The utilization factors are $\Delta P_{down,util} \vee \Delta P_{up,util} \leq 1$, and if $\Delta P_{down,util} = 1$, then all the available DR capacity is fully utilized and will be fully deployed for every called imbalance in the system. For instance, the utilization factor $\Delta P_{up,util}^{IDS30\%,IM2012}$ for the positive imbalance volumes in year 2012 and for IDS 30 % penetration level can be estimated, as in equation 6.8.

$$\Delta P_{up,util}^{IDS30\%,IM2012} = \sum_{t=1}^{PTUs} \left(\frac{\Delta P_{up,depl}^{IDS30\%,IM2012}(t)}{\Delta P_{up,max}^{IDS30\%,IM2012}(t)} \right) \quad (6.8)$$

Similarly, the utilization factor related to the provision of DR, for 30 % penetration level of IDSs in the system, to support system balancing of negative imbalances $\Delta P_{down,util}^{IDS30\%,IM2012}$, can be estimated as in equation 6.9.

$$\Delta P_{down,util}^{IDS30\%,IM2012} = \sum_{t=1}^{PTUs} \left(\frac{\Delta P_{down,depl}^{IDS30\%,IM2012}(t)}{\Delta P_{down,max}^{IDS30\%,IM2012}(t)} \right) \quad (6.9)$$

The utilization factors for each penetration level of IDS supporting system balancing were estimated based on the imbalance data for the Netherlands for the year 2012. The utilization factors related to participation on reduction of positive $\Delta P_{up,util}^{IM2012}$ and negative imbalances $\Delta P_{down,util}^{IM2012}$ are depicted in figure 6.12.

The results presented in figure 6.12 highlight the fact, that for 1 % penetration level of IDSs in the system, the available capacity of available DR is relatively small. Therefore, all the available DR capacity $\Delta P_{down,depl}^{IDS1\%,IM2012}$ and $\Delta P_{up,depl}^{IDS1\%,IM2012}$ would have fully participated on support of system balancing. This results in estimated unity utilization factors $\Delta P_{up,util}^{IDS1\%,IM2012}$ and $\Delta P_{down,util}^{IDS1\%,IM2012}$. The utilization factors rapidly decrease for higher penetration levels of IDSs supporting system balancing. In figure 6.11 can be observed, that more calls for negative imbalance volumes (down-regulation) would be possibly mitigated in year 2012 with the proposed DR application. This can explain the utilization factors $\Delta P_{down,util}^{IM2012} < \Delta P_{up,util}^{IM2012}$ for IDS penetration > 1 %, as depicted in figure 6.12.

Note that for higher IDS penetration levels, the utilization factors of available DR rapidly decrease. The proposed application of DR with OLTC is based on voltage adjustments (deviations) from nominal voltage at the MV/LV substation, as discussed in 6.2.1. Therefore, smaller voltage deviations will be required for higher penetration levels of IDSs to provide requested volumes of DR calls. For instance, an average deviation from the nominal voltage at the MV/LV substation $U_n \pm 0.3$ % can be expected for 30 % penetration level of IDSs in the system. Nevertheless, such small induced voltage deviations are lower than the currently occurring voltage deviation in the distribution network due to load variations. The deviations in order $U_n \pm 0.3$ % will

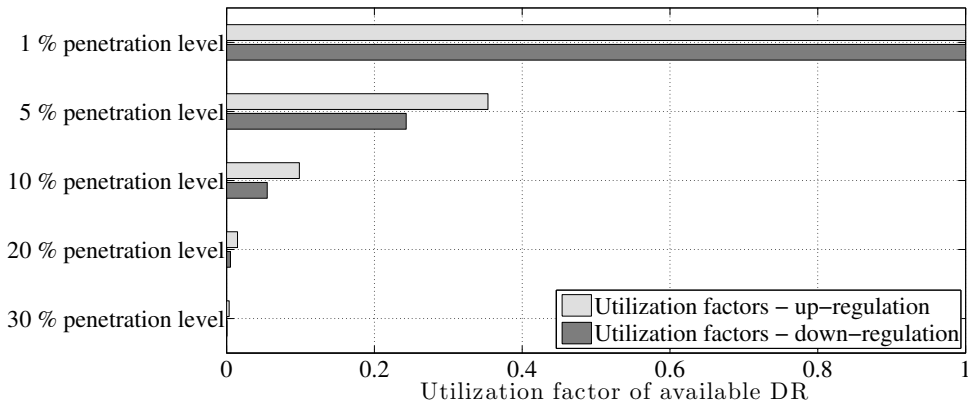


Figure 6.12: The utilization factors of available DR provided by IDs in the system and participating of system balancing. The values are estimated for the imbalance volumes in the Netherlands in year 2012 separately for $\Delta P_{down,util}^{IM2012}$ and $\Delta P_{up,util}^{IM2012}$ for all assessed penetration levels of IDS in the system.

Table 6.2: The overview of reduction capabilities of the proposed DR for supporting system balancing. The imbalance volumes reduction and the magnitude reduction of called imbalance volumes in the system for assessed IDS penetration levels. The results are based on imbalance volume data for the Netherlands in the year 2012.

IDS penetration level	Magnitude reduction		Imbalance volumes reduction	
	Up-regulation	Down-regulation	Up-regulation	Down-regulation
1 %	1.11 %	1.39 %	11.49 %	15.10 %
5 %	5.54 %	6.95 %	43.88 %	54.28 %
10 %	11.08 %	13.90 %	68.75 %	79.27 %
20 %	22.16 %	27.81 %	90.58 %	96.03 %
30 %	31.41 %	41.71 %	96.68 %	99.42 %

be most probably unnoticed by network users, but they can significantly support system balancing and reduce the amount of called imbalance volumes in the system and their magnitude.

The results related to the reduction of remaining imbalance volumes, after the deployment of proposed OLTC application, in the Netherlands in the year 2012 for assessed IDS penetration levels are presented together with the magnitude reduction of called imbalance volumes in table 6.2.

6.2.5 Impact on distribution network losses

The proposed DR application, provided by IDS, will influence loading in the distribution network and if participating on supporting system balancing, it will affect also distribution network losses. Therefore, in this section, the changes of the distribution network losses related to the IDS participation on system balancing support are assessed. To keep the consistency with previous results, the evaluation is made for the MV/LV distribution network, which is equipped by IDS and provide DR by means of voltage control with OLTC, as discussed in 6.2.3. The distribution network losses were estimated for a normal operation of IDS, where IDS does not participate in system support, and for a situation, where IDS participate in supporting system balancing. The distribution network losses are compared for both situations and the relative change of the distribution losses (including transformer losses and all cables and feeders losses in the LV network) due IDS provisioning system support is indicated. In reality the impact on energy loss can be more complex. In principle, as the voltage at the MV/LV substation increases or decreases, the power drawn by connected loads changes accordingly, based on their PU_{ratio} , as discussed in 6.2.1. Consequently, voltage changes will result in alternation of current flows in the network. The distribution network losses will change accordingly to the current flows in the observed LV network. However, the distribution network losses are not linearly correlated with the induced voltage changes. It is observed, that as the voltage increases (e.g., OLTC adjusted to induce up-regulation), connected loads in the LV network draw more power and the overall distribution network losses increase. Vice versa, for the provision of a down-regulation, the OLTC reduces the supplied voltage and the power demanded by connected loads decreases and simultaneously the distribution network losses can be reduced. The resulting change in total distribution network losses depends also on called imbalance volumes in the investigated system.

The participation of the proposed DR application on system balancing will require different voltage adjustments for different DR calls throughout the investigated period. The changes in distribution network losses are estimated with respect to the participation in system balancing, for up-regulation and down-regulation over the investigated period of one year, as described in 6.2.4. The relative distribution network losses are estimated based on the distribution losses during normal operation ($\approx 3\%$) for the evaluated distribution network, as in 4.2. The changes of distribution network losses are evaluated as relative distribution losses change for IDS providing only voltage adjustments for a load increase (up-regulation), IDS providing only adjustments for a load decrease (down-regulation) and for IDS participating on provision of symmetrical service (both up-regulation and down-regulation). The results for all considered IDS penetration levels are depicted in figure 6.13.

Based on the imbalance data for the year 2012 in the Netherlands, IDSs in higher penetration levels in the system would be able to reduce more the remaining imbalance volumes for down-regulation than for up-regulation. This can be observed in figure 6.11, where remaining imbalance volumes for down-regulation are smaller

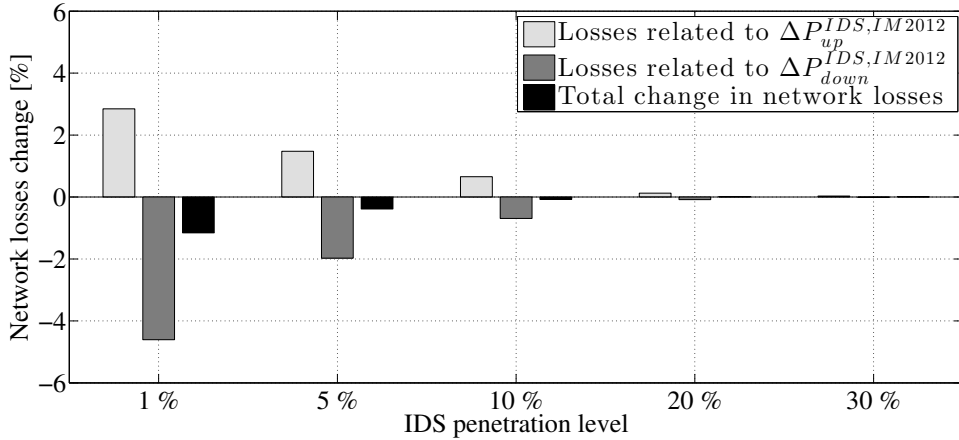


Figure 6.13: The estimated relative changes of distribution network losses for different penetration levels of IDSs in the system provisioning DR for support of system balancing. Based on called and reduced imbalance volumes in the Netherlands in year 2012, as depicted in figure 6.11.

than for up-regulation. As a consequence, the distribution network losses related to down-regulation outweigh the distribution network losses related to up-regulation. The overall distribution network losses associated with IDS participation on up-regulation as well as on down-regulation have only a marginal impact on the total distribution network losses (e.g., < 2 % relative change of current distribution network losses). The utilization of the available DR provided by IDSs decrease for higher penetration levels of IDSs in the system, as depicted in figure 6.12, consequently the required average voltage adjustments are also smaller. In addition, for higher IDS penetration levels, the change of distribution network losses compared to the normal operation decreases to negligible levels (e.g., 0.01 % change for 30 % IDS penetration level).

The summary of distribution network losses, estimated for different penetration levels of IDS participation in system balancing is presented in table 6.3. The results are based on data for the Netherlands in the year 2012.

6.2.6 Enabling technologies

The key enabling technologies for the presented DR application in the distribution network are:

- OLTC located in the MV/LV substation, such as in the experimental IDS. The OLTC in IDS operates within $\langle U_{TR,min}; U_{TR,max} \rangle$, given by the OLTC design as $\langle U_n - 5\%; U_n + 5\% \rangle$ [95]. Nevertheless, a larger accessible voltage range can

Table 6.3: The overview of relative changes of distribution network losses related to the IDS operation and system balancing support. The results are based on imbalance volume data for the Netherlands in year 2012.

IDS penetration level	Relative change of distribution network losses		
	Up-regulation	Down-regulation	Total
1 %	2.85 %	-4.61 %	-1.76 %
5 %	1.48 %	-1.97 %	-0.50 %
10 %	0.66 %	-0.69 %	-0.04 %
20 %	0.12 %	-0.08 %	0.04 %
30 %	0.03 %	-0.01 %	0.02 %

enlarge the available DR at a substation, reduce limitations in DR time dependent availability and can enable a higher reduction of called imbalance volumes in the system

- To assess the operational limits for a OLTC, on-line measurements of supplied power and voltage level at the LV bus-bar are required to estimate location specific $\langle \Delta U_{down,max}^{LV_{bus-bar}}(t); \Delta U_{up,max}^{LV_{bus-bar}}(t) \rangle$. Consequently the values of $\langle \Delta P_{down,max}^{LV_{bus-bar}}(t); \Delta P_{up,max}^{LV_{bus-bar}}(t) \rangle$ can be assessed on-line for a specific network configuration
- Additional measurements from network users POCs in the supplied network (voltage and supplied power) will enable accurate assessment of $U_{min}^{POC}(t)$ and $U_{max}^{POC}(t)$. The locally specific limiting factors can be used for estimation of the DR availability, such as in equation 6.3 and in equation 6.4. Additionally, location specific PU_{ratio} could be estimated as a function of time for the assessed LV network
- The available DR at a MV/LV substation level can be assessed locally based on local measurements, but communication means will be required to send the DR availability (e.g., $\langle \Delta P_{down,max}^{LV_{bus-bar}}(t); \Delta P_{up,max}^{LV_{bus-bar}}(t) \rangle$) to the DSO and to receive the calls for DR actions

The above mentioned enabling technologies will improve the utility of proposed DR application, nevertheless OLTC is the key enabler for this functionality and it can be reasonably operated also without additional measurements under assumptions presented in 6.2.2.

6.3 Theft detection

The total electricity loss in the system is due to technical and non-technical reasons. On the one hand, the technical loss is naturally present in the system due to energy dissipation in network components and is given by the physical properties of the network. On the other hand, non-technical loss (NTL) can coexist in the distribution system due to other reasons. The loss due to NTL presents a economic loss for DSOs and consequently also for network users.

The DSOs had limited means to fight NTL in the past, as only limited measurements from the distribution network were available to assess NTL. The detection of NTL used to be traced on random basis or after an external impulse to a DSO. As the automation of distribution network progress, more measurement data can be used by a DSO to tackle NTL. Therefore, the application exploiting measurement data from distribution network is proposed in this section, to systematically approach theft in LV distribution.

In this section, the value of NTL in the Netherlands is presented in 6.3.1, followed by an overview of detection methods currently applied to reveal illegal abstraction of electricity in 6.3.2. The proposed application for localization of illegal electricity abstraction is presented in 6.3.3.

6.3.1 Value of non-technical loss in the Netherlands

The estimation of NTL and even of the technical loss is complicated in the distribution network, because extensive data to estimate it are not available, the losses cannot be precisely computed. The average annual loss can be estimated and a certain fraction of it can be assumed to be associated with NTL and with illegal abstraction of electricity.

The illegal abstraction of electricity can be more common in some low-income and middle-income countries, where a substantial part of the electricity generated is attributed to total transmission and distribution loss. Significant NTL were encountered for instance in India, where 55 % of generated electricity was billed and only part of the bills was paid to supplier (year 2003) [139]. The electricity loss in India is extreme and could run electricity companies close to bankruptcy [140]. The total electricity loss in Lebanon is estimated to be about 50 % (year 2003) [141]. In Albania, Haiti or Bangladesh total loss higher than 30 % was estimated (year 2004) [22]. In Brazil, the total loss of about 15 to 17 % can be expected (year 2012) [142], [143]. But NTL can also significantly change over time as the efficiency of DSOs improves, such as in Latin America where a significant reduction of NTL was observed after the privatization of the power sector (e.g., Colombia) [143]. The study of socio-economical indicators, governance, institution democracy and corruption identified a correlation between the total loss (indicating illegal abstraction of electricity) and the socio-economic indicators of a country. It was found that in a well-governed countries, a lower total electricity loss can be expected [22].

The transmission and distribution of electricity in the Netherlands is very efficient and the average total electricity loss (from the year 2000 till 2010) was

only 4.32 % [23].

Nevertheless, illegal abstraction of electricity takes place also in high-income countries. The exact values of NTL associated with illegal abstraction of electricity are nowadays impossible to obtain. But in [22] is indicated that in a very efficient power system, the transmission and distribution loss shall be less than 6 % and the value of NTL (including electricity theft) in range from 1 to 2 % can be expected.

The estimated NTL due to illegal abstraction of electricity in the Netherlands is expected to be about 1 200 GWh per year, which represent about 1 % of the annual electricity consumption. This value corresponds to the lower boundary value in the indicated range of expected NTL in highly efficient power systems in [22]. In the Netherlands an electricity fraud or theft attempt is expected to take place on every second MV/LV substation on average [85].

The total electricity loss in distribution network can be divided into:

- Technical loss is due to physical properties of the distribution network, length of circuits and design practices (e.g., the use of underground cables in the Netherlands influenced by a relatively high population density)
- Administration loss is given by unknown connections or missing meters, which are not measured, but not intentionally tampered by network users for illegal abstraction of electricity
- Illegal abstraction of electricity (electricity fraud and theft), which is the non-metered electricity usage by intentional tampering of electricity meter or illegal connections

The share of the individual components of the total loss in the distribution network in the Netherlands is depicted in figure 6.14, where it can be seen that the estimated illegal abstraction of electricity accounts for 23 % of the total loss for DSOs in the Netherlands.

After ownership unbundling of distribution, transmission and production companies in the Dutch electricity sector, a DSO estimates the total loss as a fraction of energy distributed to network users. The network loss is estimated in the settlement process between the electricity traders and a DSO. The electricity to cover the total loss has to be purchased for a market price from independent production companies by a DSO. Therefore, illegally abstracted electricity represents additional cost for a DSO.

The cost of NTL is not only in terms of abstracted energy and a higher total loss in the system, but also in terms of sales reduction and reduction of retail margins of DSOs. The total cost related to the illegal abstraction of electricity in the Netherlands for DSOs is estimated to be about M€114 annually [85]. The illegally abstracted electricity also represents monetary losses for the government in terms of uncollected tax. The annual loss in the tax collection is estimated to be about M€120 [85]. The estimated total cost of illegal abstraction of electricity in the Netherlands is about M€234 annually. Currently, there are no means to estimate exactly the total loss and related cost of

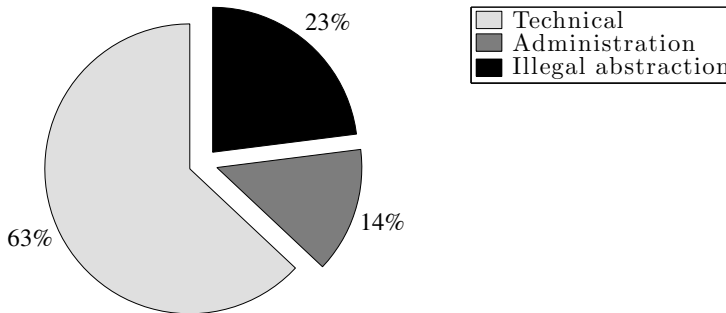


Figure 6.14: The estimated sources of electricity loss in the distribution network in the Netherlands [85].

electricity theft in the system, therefore the presented values are anticipated for the range of expected loss.

The literature related to electricity theft is limited. However, it is predicted, that utilities worldwide lose about M\$25 000 annually due to illegal abstraction of electricity [144]. For instance in United Kingdom, The Office of Gas and Electricity Markets (Ofgem) published an estimate of annual cost related to electricity theft, which indicate the cost to be in order of M£100 [145]. Similarly to the Netherlands, the loss due to electricity theft is recovered from all (paying) network users in form of higher bills.

In the USA, the cost of illegal abstraction of electricity is expected to be in range of 0.5 to 3.5 % of annual gross revenues in USA utilities [22]. And a recent surge in illegal abstraction of electricity is reported in relation to the downturn in economic cycle [146]. The utilities in the USA are expected to have loss due to the illegal abstraction of electricity in range of M\$1 000 till M\$6 000 annually [147]. For instance alone in the Huston area, the annual cost of M\$14 associated with illegal abstraction of electricity is passed on network users [148].

In Italy, one of the drives for the roll out of automated meter reading (AMR) infrastructure was the effort to reduce NTL in the network of ENEL. The main drivers of NTL reduction and effective control of contracted power helped to justify large investment into AMR [149].

In British Colombia (about M4.4 inhabitants in 2011), Canada, the loss due to illegal abstraction of electricity is estimated to be about M\$100 annually only for the British Columbia Hydro, where most of the illegally abstracted electricity is used for drugs cultivation. British Colombia Hydro reported that the perpetrators are becoming more sophisticated and loss due to illegal abstraction of electricity surged in last years [150].

6.3.2 Detection methods used to reveal illegal electricity abstraction

The illegal abstraction of electricity takes many different forms. Unauthorized connections to the overhead lines at the supply voltage level or disconnecting neutral wire from the meter are common techniques in many low-income and middle-income countries [144]. The distribution network in the Netherlands consist of underground cables, which does not allow an easy access for illegal connections outside network user premises. The illegal abstraction of electricity takes more subtle forms, usually such as tampering of the electricity meter alone, connection cables and meter terminals can be found together with a cut-off circuit.

Generally, two types of illegal abstraction of electricity from the distribution network can be recognized:

- Electricity theft corresponding to illegal network connections and to bypassing of the electricity meter
- Electricity fraud or efforts to deceive electricity usage, related to tampering of electricity meter, metered data, accuracy of the meter or inter-changing of meter terminals

In 95 % of the detected cases with illegal abstraction of electricity in the Netherlands, electricity theft was used for illegal drugs cultivation. The motivation for the perpetrators are the huge annual sales from this activity, which are estimated alone for the Netherlands to be in order of M\$3 000 [85].

The DSOs in the Netherlands are aware of the losses caused by illegal abstraction of electricity and carry out techniques for suppressing and detecting the tampering attempts. The current methodologies generally focus more on indirect theft detection, based on irregularities observed in distribution network. In most cases, the illegal abstraction of electricity is used for cultivation of drugs, which require periodical changes of periods with and without illumination. An example of measured currents related to suspected illegal abstraction of electricity for cultivation use in a LV network of a DSO in the Netherlands is depicted in figure 6.15.

Several techniques exist to fight the illegal abstraction of electricity. On the one hand, additional metering points in the distribution network are suggested to oversee the aggregated consumption of groups of network users [151]. But suspected network users can notice the installation and suspend the illegal abstraction [142].

On the other hand, some fraud detection methods rely on investigation of irregularities of network user consumption data [152]. The measured data can be collected and investigated with data mining techniques to reveal abnormalities or suspicious changes in the network user consumption behavior. The principle of outliers detection in a data set of network users consumption data is commonly used form of detection. The consumption data can be also used for more advanced data mining techniques to find irregularities indicating NTL [153]. The classification techniques of network user consumption data can be used to filter network users with suspicion on

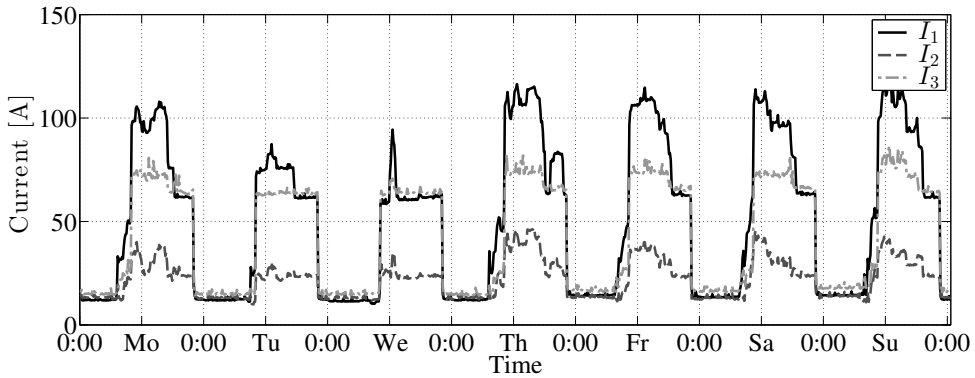


Figure 6.15: Measured currents at a feeder section in the LV network of one Dutch DSO with suspected illegal abstraction of electricity.

NTL presence [154]. Advanced classification for NTL detection on a large consumption datasets is proposed in [147] and the soft computing methods with machine learning considering an imperfect knowledge are proposed for fraud detection in [155].

Other detection methods rely for instance on estimation of propagation of higher frequencies (e.g., power-line communication) in the network, which is expected to be attenuated by some illegally connected loads [140]. However, the techniques assume that abnormal consumption behavior is correlated with NTL. Nevertheless, the alternation in network user consumption data does not always imply involvement in illegal abstraction of electricity and can lead to embarrassment of honest network users if no irregularity is found by (costly) inspection teams [142].

An automated methodology to fight NTL in the network is proposed in [144]. If higher NTL are detected in the network, genuine network users are temporarily disconnected, a harmonic generator is switched on to destroy illegal loads and after that, genuine network users are reconnected [144]. Although with a strong psychological impact on network users, the drawback of this method lies in an easy application of a cut-off circuit, which will protect illegal loads of dishonest network users.

The presented methods to reveal electricity theft reflect local specifics and available measurements in the network. But the detection can be more complicated if network users employ techniques to illegally abstract electricity on a temporary basis or to bypass the meter to connect only some heavy loads [144], e.g., similarly to the profile in figure 6.15.

In the Netherlands, mostly (irregular) electricity theft takes place in the network by bypassing the electricity meter. Therefore, the electricity theft does not necessarily affect network user load profile. In addition, to efficiently fight NTL in the system, the

perpetrator localization is needed. Therefore, the presented detection methods can not yield required results to efficiently fight NTL in the Netherlands.

6.3.3 Proposed application to reveal NTL

The proposed application of measurement data from LV network shall overcome the issues related to commonly used detection method of illegal abstraction of electricity. It should not be biased by changes in network user load behavior and it should be able to indicate the location of illegal abstraction in the network.

The LV networks in the Netherlands are commonly designed for a designated neighborhoods, constructed by a property developer, which allows keeping a good overview of network assets and network users connections to the network. A good knowledge of network assets in the Netherlands is fundamental for the proposed application for detection of illegal abstraction of electricity.

The proposed method is based on load flow analysis. Assume the typical LV network in the Netherlands, as presented in 4.2. A feeder in the LV network supplies distributed loads at network users POCs. The voltage level at each POC in the LV network is a function of the voltage at the LV bus-bar in the MV/LV substation U^{SS-LV} , network impedances Z_{net} and power injections (positive or negative) in the network at each POC S^{POC} . The load flow calculations are governed by the principle presented in equation 6.10.

$$[U^{POC}] = [Z_{net}] \cdot [I^{POC}] \quad (6.10)$$

Where in equation 6.10, $[I^{POC}]$ is the vector of current injections at each POC estimated from S^{POC} , $[U^{POC}]$ is the vector of voltages at each POC and $[Z_{net}]$ is the network impedance matrix. For the radial distribution network with possible power injections from connected DGs, the unbalanced load flow analysis based on iteration process with forward and backward sweep is used. The load flow can be formulated as a set of non-linear equations for all network users and the solution can be found, as presented in [156], [157], [158]. The resulting $[U^{POC}]$ yields the vector of voltages at each POC for assumed LV network configuration. The estimation can be done for each time instance t of available data from the smart metering infrastructure.

The load flow analysis enables to estimate the total technical loss in the distribution network for each time instance t as the sum of technical loss in the connection cable $P_{loss,cc}^{POC(i)}$ and in the main feeder $P_{loss,f}^{POC(i)}$. The loss in a cable section connecting POC(i) with $R_{cc}^{POC(i)}$ can be computed as in equation 6.11 [159].

$$P_{loss,cc}^{POC(i)} = R_{cc}^{POC(i)} \cdot \frac{(P^{POC(i)})^2 + (Q^{POC(i)})^2}{|U^{POC(i)}|^2} \quad (6.11)$$

Similarly to equation 6.11, the loss in a feeder section can be computed based on the power flow in a feeder section between two POCs or MV/LV substation (considered

as $P^{POC(0)-POC(1)}$ in the network, as in equation 6.12.

$$P_{loss,f}^{POC(i-1)-POC(i)} = R_f^{POC(i-1)-POC(i)} \cdot \frac{(P^{POC(i-1)-POC(i)})^2 + (Q^{POC(i-1)-POC(i)})^2}{|U^{POC(i-1)-POC(i)}|^2} \quad (6.12)$$

The total technical loss in the LV network or in a feeder can be computed as in equation 6.13.

$$P_{loss}(t) = \sum_{i=1}^{n.POC} P_{loss,cc}^{POC(i)}(t) + \sum_{i=1}^{n.POC} P_{loss,f}^{POC(i-1)-POC(i)}(t) \quad (6.13)$$

The power injection in a feeder in the LV network for each time instance t can be estimated as in equation 6.14.

$$S^{SS-LV}(t) = \sum_{i=1}^{n.POC} S^{POC(i)}(t) + P_{loss}(t) \quad (6.14)$$

The smart metering infrastructure enables access to the measurements of active $P^{POC}(t)$ and reactive power $Q^{POC}(t)$ and voltage magnitude $U^{POC}(t)$ at each POC as a series of measurements at time intervals t . This measurements can be exploited to reconstruct conditions in the LV network. The theft detection can be applied on per feeder basis in the LV network. Based on the measured data from smart meters, the expected power injection in a feeder can be estimated $S_{est}^{SS-LV}(t)$, as in equation 6.14.

In the first phase of the theft detection method, the measured $S^{SS-LV}(t)$ at the MV/LV substation and the estimated $S_{est}^{SS-LV}(t)$ are compared. If $S^{SS-LV}(t) \neq S_{est}^{SS-LV}(t)$ within a specified bandwidth for mismatch errors, it can be assumed, that a illegal abstraction of electricity takes place in the investigated feeder. In practice, the loss can be assumed as a function of supplied load.

If the theft in a feeder is detected, the localization procedure can be initiated. The proposed application exploits the measurement data from smart meters in the network and it is based on comparison of estimated voltages at a POC $U_{est}^{POC}(t)$ and measured voltage at the same POC $U^{POC}(t)$. The network user is billed based on energy consumed and current capacity at the POC, ergo based on this power measurements, the expected voltage level at the POC can be estimated. The electricity theft does not influence the recorded power at a POC, but any illegal abstraction of electricity (e.g., load connected before the electricity meter) will influence the voltage conditions in the investigated LV network and at the POC with the illegal abstraction of electricity. The localization of illegal abstraction of electricity in the network is reduced to maxima search of $|U_{est}^{POC}(t) - U^{POC}(t)|$ over the investigated period. The detection algorithm is presented as a pseudo-code in algorithm 6.1, for n measurements available for $t \in \langle t_1; t_n \rangle$ and for m POCs in the network.

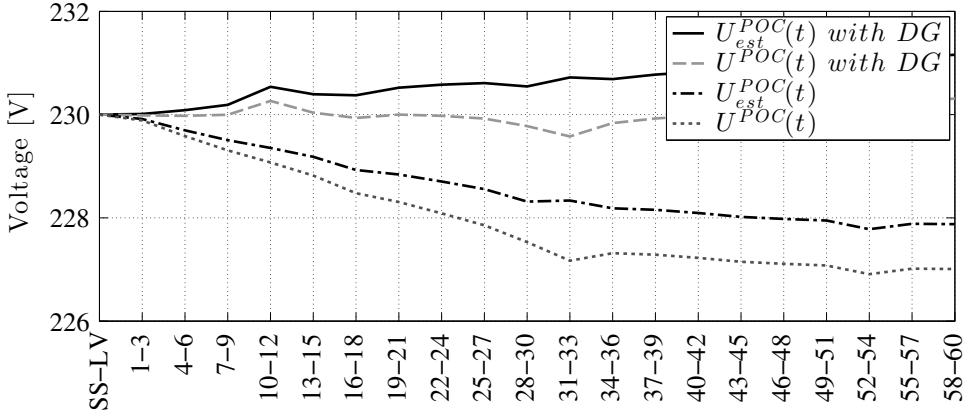


Figure 6.16: Example of one phase voltage profile for POCs along a feeder, where a illegal abstraction of electricity takes place close to $POC(31)$. In presence of electricity theft, the measured voltages $U^{POC}(t)$ will be different in comparison with estimated voltages $U_{est}^{POC}(t)$.

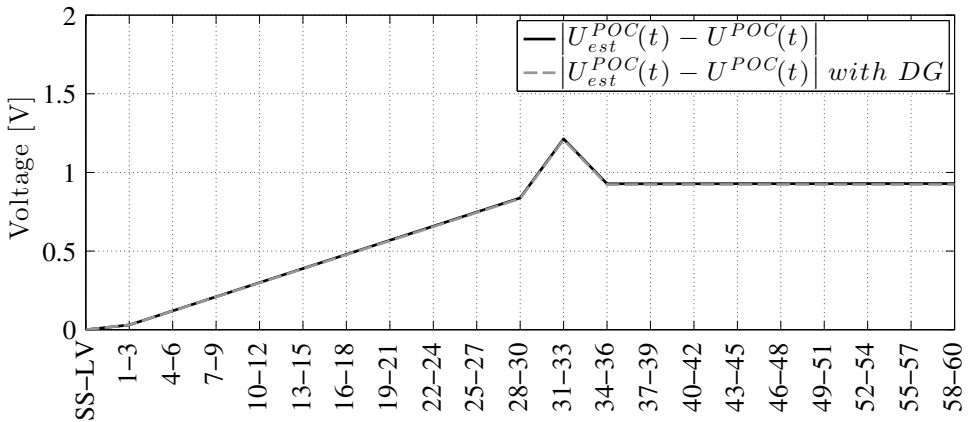


Figure 6.17: The estimated absolute difference between measured $U^{POC}(t)$ with smart meters and estimated $U_{est}^{POC}(t)$ over one week period (single-phase). The illegal abstraction of electricity takes place at $POC(31)$.

The detection method can be demonstrated on two example case studies of one feeder from the typical LV network, as presented in 4.2, with connected network users, as presented in 4.3 and with OLTC control (A), as discussed in 4.5. The first case study does not include any DGs and the second case study considers five three-phase DGs connected at $POC(10)$, $POC(20)$, $POC(30)$, $POC(50)$ and $POC(60)$,

Algorithm 6.1 Pseudo-code for detection and localization

```

▷ Detect the presence of illegal abstraction in the LV network
for  $t \in \langle t_1; t_n \rangle$  do
  if  $S_{est}^{SS-LV}(t) \neq S^{SS-LV}(t)$  then
    ▷ Illegal abstraction detected
    Read  $U^{POC(m)}(t) \forall m \in All\ POCs$ 
    Read  $P^{POC(m)}(t) \forall m \in All\ POCs$ 
    Estimate  $U_{est(m)}^{POC}(t) \forall m \in All\ POCs$ 
    for  $\forall m \in All\ POCs$  do
       $avg. \left| U_{est}^{POC(m)}(t_1 \rightarrow t) - U^{POC(m)}(t_1 \rightarrow t) \right|$ 
      ▷ Test is a sufficient  $n$  of measurements is processed
      if  $avg. \left| U_{est}^{POC(m)}(t_1 \rightarrow t) - U^{POC(m)}(t_1 \rightarrow t) \right| \leq f(U_{ia,min}, P_{ia,min}, u_\epsilon)$  then
        ▷ Localization of illegal abstraction
        find  $m$  with  $\left( \max \left| U_{est}^{POC(m)}(t_1 \rightarrow t) - U^{POC(m)}(t_1 \rightarrow t) \right| \right)$ 
        ▷ Illegal abstraction located at  $POC(m)$ 
      end if
    end for
  else
    ▷ No illegal abstraction detected
  end if
end for

```

resulting in $DG_{ratio} = 10\%$ in the investigated LV network. The measured PV profile is considered for DG output as presented in 4.5. Assume, that a three-phase illegal abstraction of electricity with $P_{theft}(t) = 3 \cdot 3.68\text{ kW}$ takes place close to the $POC(31)$ in the network, e.g., the illegal load is connected by a bypass connection before the smart meter at $POC(31)$. The difference between the measured $U^{POC}(t)$ and estimated $U_{est}^{POC}(t)$ can be observed in both case studies with and without DG. The results for one phase are shown in figure 6.16 for one time instance ($t \approx 12:00$). The loads connected at a POC influence the voltage profile in the feeder. However, if metered, the voltage drop measured at a POC would correspond to the estimated voltage drop expected at the POC. Therefore, the maximal deviation between $U^{POC}(t)$ and $U_{est}^{POC}(t)$ indicates the presence of not metered loads connected, ergo the location of the illegal abstraction in the network. For the results presented in figure 6.16, $\max \left| U_{est}^{POC}(t) - U^{POC}(t) \right|$ is found for $POC(31)$, which corresponds to the theft location in the network. The estimated absolute average difference of measured $U^{POC}(t)$ and estimated $U_{est}^{POC}(t)$ for the investigated feeder over one week period for both case studies is depicted in figure 6.17. In figure 6.17, the value of $\max \left| U_{est}^{POC}(t) - U^{POC}(t) \right|$ indicates the POC, where the illegal abstraction of electricity takes place.

6.3.4 Influence of topology and measurement uncertainty

In real applications, uncertainties are present in all measurements used for the proposed detection method of illegal abstraction of electricity. Therefore, the influence of uncertainties in considered network topology and measurement data from smart metering infrastructure is investigated. The aim of the presented consideration is to define the minimum detectable current $I_{ia,min}$ and the minimum detectable power $P_{ia,min}$ of the illegal abstraction of electricity in the network.

The localization of the illegal abstraction of electricity requires a good knowledge of the network topology to reconstruct the load flow from measured data. Even in a well-documented LV network topology, lengths and impedances of individual network components are uncertain. To simulate the impact of those uncertainties, every component in the investigated network was assumed to have a random deviation $\leq \pm 10\%$ from the expected impedance value.

The measurements from smart metering infrastructure are also coupled with uncertainties. The methodology related to uncertainties estimation in measurements data presented in [160] was reversely reproduced to investigate the influence of measurement uncertainties from smart metering infrastructure and from measurement provided at the MV/LV substation.

As suggested in [160], the uncertainties in repeated measurements can be characterized by normal distribution, where the population standard deviation can be defined to provide an estimate of the uncertainty due to repeatability of measurements. Ergo, the uncertainty of a measurements u_ε can be defined and their impact on the estimation of the illegal abstraction of electricity can be simulated. The proposed method exploits the power (or current) and the voltage measurements from smart metering infrastructure and from the MV/LV substation, which were burdened by measurement uncertainty u_ε .

The resulting uncertainties of measured data and network model were estimated based on the Monte Carlo simulation and the uncertainty distribution in the LV network over the period of 50 weeks was investigated. The variance of statistically independent population of measurement can be estimated as σ^2 . It is than possible to bound the measured value in a specific level of confidence. The confidence limits of measurements for the theft detection estimation can be expressed by t-statistics as multiples of sample standard deviation. The confidence limits of $\pm 3 \cdot \sigma$, where $\approx 99.7\%$ of measurements lies within the confidence interval, are assumed in the evaluation. Ergo, by repeating measurements, the values of the minimum detectable current $I_{ia,min}$ and the value of the minimum detectable power $P_{ia,min}$ due to the illegal abstraction of electricity can be defined as a function of n repeated measurements by $\frac{\pm 3 \cdot \sigma}{\sqrt{n}}$.

Four cases of assumed uncertainties of measurements provided by the smart metering infrastructure and of measurements in the MV/LV substation are presented. The impact of different measurement uncertainties $u_\varepsilon \in 1.0\%, 0.5\%, 0.2\%, 0.1\%$ on the minimum detectable $I_{ia,min}$ and $P_{ia,min}$ is investigated.

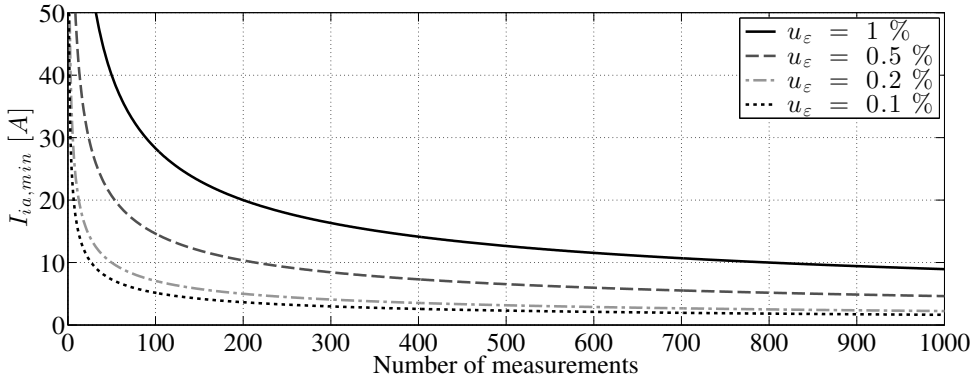


Figure 6.18: The minimum detectable current $I_{ia,min}$ due to illegal abstraction of electricity in the LV network, as a function of measurement repetitions for different measurement uncertainties u_ε involved.

The estimated results for the minimum detectable current $I_{ia,min}$, as a function of number of repeated measurements and as a function of considered measurement uncertainty, are depicted in figure 6.18.

Similarly, the minimum detectable power $P_{ia,min}$ due to illegal abstraction of electricity in the LV network can be defined as a function of repeated measurements and different uncertainties involved in those measurements. The results for the minimum detectable power $P_{ia,min}$ are depicted in figure 6.19.

The requirements for the smart metering infrastructure in the Netherlands, defined in NTA 8130 [62], indicates that 15 min. measurements shall be provided from smart meters, and 960 readings shall be stored within the metering installation. Considering the proposed application for theft detection, this can be sufficient to detect most cases of illegal abstraction of electricity in the Netherlands. The time needed to locate certain illegal abstraction of electricity in the LV network can be expressed in the required measurement time from smart meters, as presented in table 6.4.

It can be noted in table 6.4, that even with assumption of high measurement uncertainties $u_\varepsilon = 1.0\%$, the example of the illegal abstraction of electricity in LV network in the Netherlands presented in figure 6.15 would be detected within a day with the proposed application.

In some distribution networks the connection of network users to phases, feeders or to the MV/LV substations is unknown or uncertain. The methodology to improve the connection data as proposed in [161] can be used to improve the connection data of network users. Afterwards, parameters of distribution network can be identified, based on the methodology proposed in [158]. The resulting improvements in the network user connectivity and estimated network parameters enable utilization of the

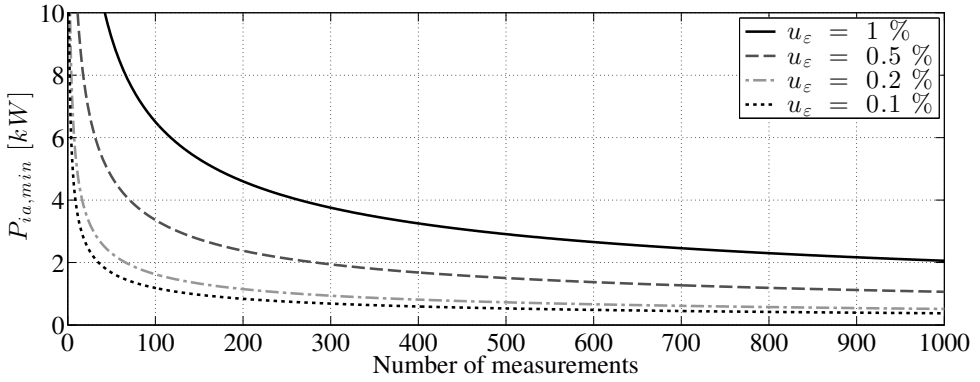


Figure 6.19: The minimum detectable power $P_{ia,min}$ due to illegal abstraction of electricity in the LV network, as a function of measurement repetitions for different measurement uncertainties u_ϵ involved.

Table 6.4: The expected time required to detect $P_{ia,min}$ due to illegal abstraction of electricity in the LV network with the current smart metering infrastructure [62] for different measurement uncertainties.

Measurement uncertainties	Detectable $P_{ia,min}$ with smart meters within		
	One day	Two days	One week
$u_\epsilon = 1.0\%$	6.6 kW	4.7 kW	2.5 kW
$u_\epsilon = 0.5\%$	3.4 kW	2.4 kW	1.3 kW
$u_\epsilon = 0.2\%$	1.7 kW	1.2 kW	0.6 kW
$u_\epsilon = 0.1\%$	1.2 kW	0.9 kW	0.5 kW

proposed application to detect the location of the illegal abstraction of electricity also to distribution networks with limited topology knowledge.

6.4 Evaluating heavy loading conditions in LV network

The distribution networks were in the past designed to accommodate network users by the "fit-and-forget" scheme and without considering DGs. Nevertheless, high penetrations of DGs and new form of loads (e.g., EVs) are envisioned to increase the uncertainty in the power system in the future, as discussed in 2.3. Therefore, the possible implications of those developments on the LV distribution network, in terms of heavy loading conditions, were investigated and the results are presented in this section.

DG generation in the LV network generally does not guarantee that the network will be simultaneously able to integrate new forms of additional loads, such as EVs, and congestion or voltage drop problems can occur, as presented in [162]. The concentration of DGs and additional loads in the LV network can cause conditions, where the currently used protection scheme can be insufficient to adequately react on potential hidden overloads in the LV network, which can be theoretically expected. Heavy load conditions (leading to high current conditions or congestions) in the network can contribute to degradation of distribution network assets due to overload of network components.

The exploitation of measurement data from smart metering infrastructure is proposed to evaluate the current conditions in the LV network and to reveal a possible high current conditions, which could lead to possible overloads. This new functionality can be enabled by a smart metering infrastructure, although not initially designated for this particular application. An advanced assessment of current conditions in the LV network can on the one hand improve utilization of distribution network assets without jeopardizing their reliability and operational constraints, and on the other hand it can improve the service provision to connected network users.

The current protection scheme is introduced in section 6.4.1. A set of case studies is presented to underpin the proposed application with simulation results in 6.4.2. The requirements on measurements enabling the proposed functionality are presented in 6.4.3.

6.4.1 Predisposition of LV networks to heavy loading conditions

The LV network protection in the Netherlands is usually realized by fuses located in the MV/LV substation and by fuses or circuit breakers at each network user POC in the LV network. The typical values for protection devices are based on the time-current characteristic with indication of the maximal current I_{max} . The LV feeder is typically protected only at its LV bus-bar connection in the MV/LV substation. The typical maximal current for LV feeders is set as $I_{max}^{SS-LV} = 200 A$ by the protection fuses in the MV/LV substation. Each network user has maximal current limit set by the main circuit breaker (or fuse) at the POC, which is typically $I_{max}^{POC} = 40 A$ for single-phase network users. The LV distribution network design takes the load diversity represented by the load factor of connected network users into account. The load factor is defined as the ratio of the average load to the maximal load over a certain period. The LV distribution networks in the Netherlands have been designed for relative low load factor of $\approx 10 \%$. Based on observation, the average power at each POC, denoted as S_{avg}^{POC} , is only about 5 % of the maximal power accessible at a POC, denoted as S_{max}^{POC} . The value of 10 % approximately corresponds to the average peak load of residential network users, which is used for distribution network planning, as presented in table 4.1. However, it is envisioned that the load factor can increase in the future as the share of new types of loads (or additional loads) connected to the LV network increase (e.g., due to connection of EVs, air-conditioners, etc.).

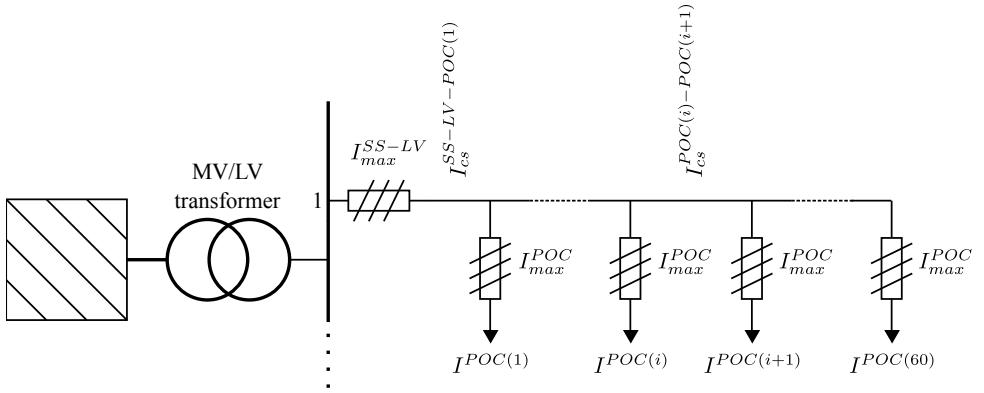


Figure 6.20: A detail of the typical LV distribution network topology in the Netherlands, as depicted in figure 4.1.

If an overload is noticed at protected sections in the LV network (at I_{max}^{POC} and I_{max}^{SS-LV}), it will be cleared by protection devices in the network. Nevertheless, in a situation with a high penetration of DGs and/or simultaneously operating additional LV loads, bi-directional power flows in the network can result in an overload or congestion of a LV feeder, which can occur unnoticed somewhere along the feeder without violating I_{max}^{POC} or I_{max}^{SS-LV} values. As a consequence, conditions presented in equation 6.15 will occur and an overload of a feeder section can develop.

$$I_{max}^{SS-LV} < \sum_{i=1}^{n.POCs} I^{POC(i)} \quad (6.15)$$

Assume a plausible (future) case, where DGs and additional loads are connected with a high penetration level to the LV network and they operate simultaneously (e.g., to utilize locally generated electricity with locally connected loads). As the electricity generated in the LV network is at the same time consumed within the network, the simultaneous operation of DGs and additional loads can lead to overload of network components without violating the maximal current limits, which will trigger the LV feeder protection.

Let's label each feeder section based on the closest POCs in the LV network structure as in figure 4.6. The current in the first feeder section, between the MV/LV substation and $POC(1)$, is denoted as $I_{cs}^{SS-LV-POC(1)}$ and etc, as depicted in figure 6.20.

To cause an overload in the LV network, which is not cleared by the current protection devices, high current values have to be reached somewhere in the LV

feeder $I_{cs}^{POC(i)-POC(i+1)}$. In this situation, the value of $I_{cs}^{POC(i)-POC(i+1)}$ can be higher than I_{max}^{SS-LV} and $I_{cs}^{SS-LV-POC(1)}$, as stated in equation 6.16.

$$I_{cs}^{SS-LV-POC(1)} \leq I_{max}^{SS-LV} \leq I_{cs}^{POC(i)-POC(i+1)} \quad (6.16)$$

If the conditions in equation 6.16 are met, the overload of a feeder section occur in the LV network without tripping of protection devices. If a sufficient power is supplied to the LV network from locally connected DGs, the conditions presented in equation 6.16 can be actual.

6.4.2 Case studies

The possibility of distribution network components being overloaded in the Netherlands is identified as a problem that can occur with high penetration levels of EVs and DGs in the distribution network [39]. Similarly [162], it is also shown that voltage drop problems can be expected in the distribution network due to charging of EVs, but with a lower probability than the overload of network components [39].

Nevertheless, the residential customer load profiles commonly utilized in studies about EVs charging assume passive network users characterized only by their load (with a certain increase over coming decades), but without participation on electricity supply with DGs connected at network users premises. Therefore, the presented case studies aim to examine the simultaneous operation of DGs and additional loads (AL) with stochastic characteristics, to analyze the implications related to the operation of LV networks. One case study with a fixed location of ALs in the network is presented in detail and the remaining case studies are derived from the presented one with a random allocation of ALs and for a different penetration levels of AL in the investigated network.

A typical Dutch LV network, as presented in 4.2, is adopted in the case studies. The distribution of DGs and their output per feeder is according to table 4.3, for $DG_{ratio} = 100\%$. The allocation of DGs among the feeder is retained for feeders 1, 3 and 4, where feeder 4 is without DGs. Only DGs connected at feeder 2 are relocated from the last four POCs to the first four POCs at the same feeder to assess different DG-load allocations.

An additional load can represent for instance charging of EVs or operation of air-conditioners randomly dispersed in the LV network. The elaboration of possible charging strategies of EVs is not considered. An inquisitive reader can find more information, for instance about the complexity of deriving EVs charging profiles in [162], [163] or with specific input data for the Netherlands in [40], [44], [42]. A generic new type of additional loads (denoted as AL) are considered for all case studies.

Similarly to the DG_{ratio} , the ratio of additional loads AL_{ratio} quantifies the share of combined maximal demand of number of additional loads in the LV network ($n.AL$)

relatively to the rating of 400 kVA MV/LV transformer, as in equation 6.17.

$$AL_{ratio} \approx \frac{\sum_{i=1}^{n,AL} (P_{max}^{AL,POC(i)})}{S^{tr}} \quad (6.17)$$

All additional loads are assumed to be a single phase loads with $P_{max}^{AL} = 3.68 \text{ kW}$ (corresponding to $I_{max}^{AL} \approx 16 \text{ A}$) and ALs are active in periods when DGs generate electricity.

A set of case studies aims to evaluate the impact of a random allocation of ALs (based on Monte Carlo simulation) in the LV network to assess possible situations in real LV network. However, to clearly demonstrate high current conditions in LV network on an example, one additional case study with fixed locations of ALs is assessed in detail. In this case study, 12 ALs are connected to each of feeders 2 and 3 in the investigated LV network. All ALs are equally distributed over the three phases and are connected at POCs close to the middle of feeders 2 and 3. The measured PV output profile in the Netherlands, as in figure 4.5, is adopted as the output of considered DGs in the network to be consistent with the evaluation in 4.5.1. The simultaneous operation of DGs and additional loads in the investigated network over one week period is depicted in figure 6.21, where ALs and DGs are active over 61.6 % of the time. For this particular case study, the locations of ALs are fixed and to distinguished this case study from other case studies presented later, the $AL_{ratio} = 22.1 \%$ is used. The resulting AL_{ratio} is estimated based on 12 ALs with P_{max}^{AL} , which are connected to each of feeders 2 and 3 in this particular case study.

The typical network user load profiles, as discussed in 4.3, are used and the loads associated with ALs are superimposed on individual load profiles of network users. Based on presented assumptions, the assessment of current conditions for each feeder section in the investigated LV network can be performed. To keep consistency with simulations presented in 4.5.1, the results are presented per feeder section either for all feeders, or only for selected feeders in the LV network over the investigated one week period. As ALs are connected to feeders 2 and 3, the detailed results with the current conditions per feeder section of feeders 2 and 3 are depicted in figure 6.22. Where in each box in figure 6.22, the central mark is the median value, the edges of the box represent 25th and 75th percentiles and the data outliers are plotted individually outside the whiskers.

The combination of ALs and DGs in the LV network can result in higher currents in a feeder section $I_{cs}^{POC(i)-POC(i+1)} > I_{max}^{SS-LV}$ at exposed feeders without violating the maximal current I_{max}^{SS-LV} at the beginning of the feeder. Feeder section currents $I_f > I_{max}^{SS-LV} = 200 \text{ A}$ can be observed between $POC(28)$ and $POC(48)$. Ergo, on this example it can be demonstrated that the occurrence of high currents in the LV network is possible and can occur without tripping of the protection devices in the network. The presented case study shows that the assumptions from equation 6.16 are actual even for a relative low AL_{ratio} .

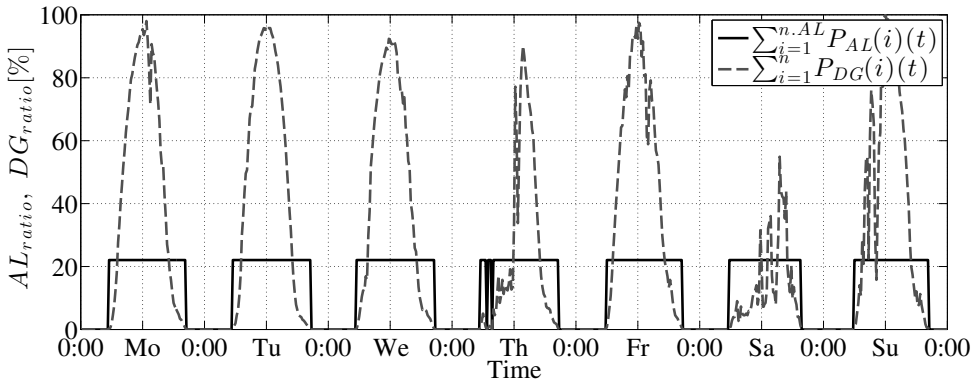


Figure 6.21: The total DG generation (with $DG_{ratio} = 100\%$) and the total additional load (with $AL_{ratio} = 22.1\%$) in the investigated LV network as a share of the MV/LV transformer rating over a week period.

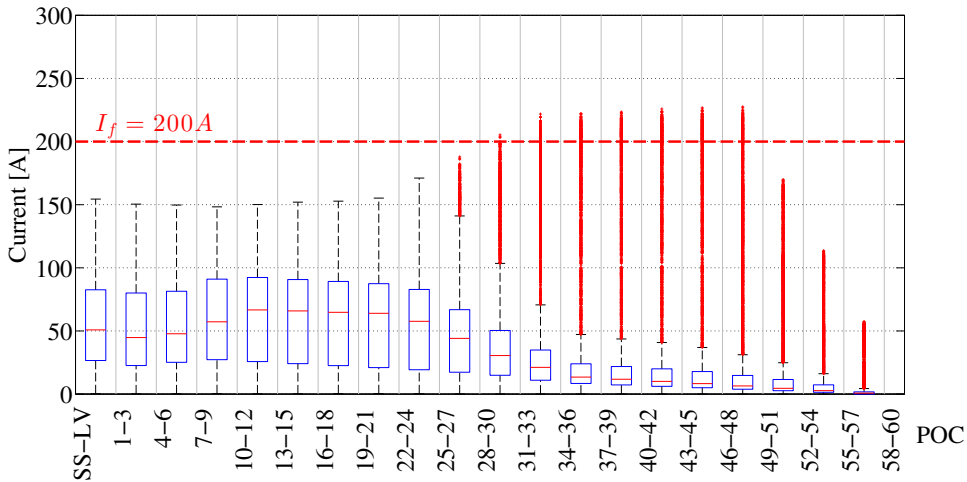


Figure 6.22: The current conditions per feeder section in the investigated LV network for feeders 2 and 3, where ALs are connected. The results are for an example with $AL_{ratio} = 22.1\%$ and $DG_{ratio} = 100\%$.

Additionally, the occurrence of higher currents can be evaluated for the whole LV network as a function of time over the investigated period. The occurrence is defined as the relative share of feeder sections with currents higher than defined limit over

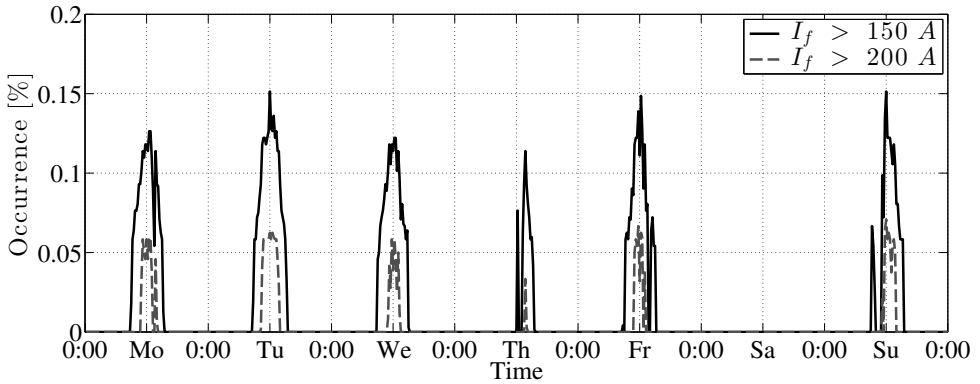


Figure 6.23: The occurrence of higher currents ($I > 150 A$ and $I > 200 A$) in the investigated LV network as a function of time over a one week period. The results are for $AL_{ratio} = 22.1 \%$ and $DG_{ratio} = 100 \%$.

the total number of feeder sections in the investigated LV network. The occurrence of higher currents, higher than defined limits, for instance $I_f > 150 A$ and $I_f > 200 A$ can be assessed in the investigated LV network, as depicted in figure 6.23. It can be observed, that the higher currents coincide with the simultaneous operation of DGs and ALs in the LV network as in figure 6.21. Therefore, the consideration related to the operation of ALs in the distribution network shall be accompanied with the evaluation of DG operation to provide more realistic results.

It can be reasonably expected that a high penetration of ALs or DGs will consequently lead to deterioration of voltage level conditions of LV network users before unwanted high current conditions are observed in the LV network, as discussed for DGs in 4.5.2. For that reason, the voltage level conditions in the LV network are evaluated next to the current conditions. If no OLTC is present at the MV/LV substation, the most suitable fixed tap position of the MV/LV transformer would be for instance $U_n + 0 \%$ or $U_n - 2.5 \%$. In both cases, the voltage level conditions for all POCs in the investigated LV network would be within $\langle U_n - 10 \%, U_n + 10 \% \rangle$, as depicted in the example for fixed tap position set to $U_n + 0 \%$ in figure 6.24. Assume also that the investigated LV network is supplied by a MV/LV transformer with OLTC operating with a control strategy A to accommodate DGs, as discussed in 4.5.1. The voltage level conditions for all POCs in the investigated LV network can be evaluated and the results are presented in figure 6.25. The maximal difference between the voltage level maxima and minima in the investigate LV network will be within $15.6 \% U_n$ for the case with no OLTC and $11.6 \% U_n$ for OLTC applied at the MV/LV substation with the control strategy A.

It can be observed in figure 6.25 that the voltage level conditions in the investigated LV network are within the limits for supplied voltage level, as discussed in 4.4.

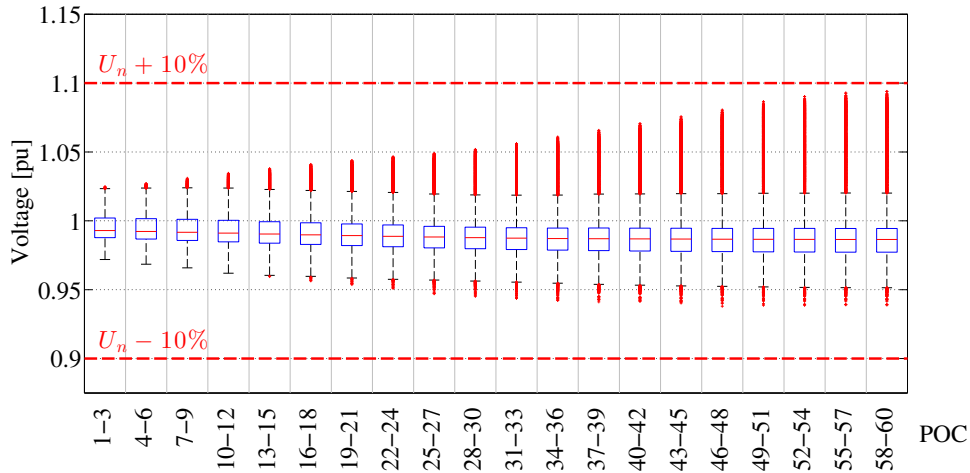


Figure 6.24: The voltage deviations in the investigated LV network for all POCs over a one week period. The LV network is supplied via MV/LV transformer without OLTC with fixed tap position set to $U_n + 0\%$. The results are for $DG_{ratio} = 100\%$ and $AL_{ratio} = 22.1\%$.

Nevertheless, higher currents can simultaneously occur in the LV network as presented in figure 6.22. Although, I_{max}^{SS-LV} for all feeders, I_{max}^{POC} and the voltage level for all network users in the LV network are not violated, currents $I_f > I_{max}^{SS-LV}$ can be observed in the LV network already for $AL_{ratio} = 22.1\%$. Ergo, implications of higher penetration levels of ALs on the distribution network should be also investigated.

A set of case studies was evaluated for different penetration levels of ALs in the investigated LV network configuration. The allocation of ALs in real distribution network can be random, therefore the Monte Carlo method is employed to numerically evaluate the impact of randomly allocated ALs on the current conditions in the investigated LV network. The number of additional loads in the network is estimated based on the evaluated AL_{ratio} . The maximal power demanded by all additional loads in the investigated network $\sum_{i=1}^{n_{AL}} (P_{max}^{AL}(i))$ is presented together with the number of ALs considered n_{AL} , for each AL_{ratio} in table 6.5. The corresponding number of ALs (according to the AL_{ratio}) is randomly assigned to different locations in the LV network and the current conditions are evaluated for each of 1 000 Monte Carlo repetitions in duration of one week. Based on the simulation results, the impact on the LV current conditions and the probability of a high current occurrences can be assessed.

The relative occurrences of currents higher than defined limit is estimated for each AL_{ratio} , based on the ratio of all feeder sections in the network with currents higher than defined threshold over the number of all feeder sections during the investigated period. The results are presented for all repetitive simulations evaluated with the Monte Carlo method. The numerical results are shown in table 6.5 for thresholds set

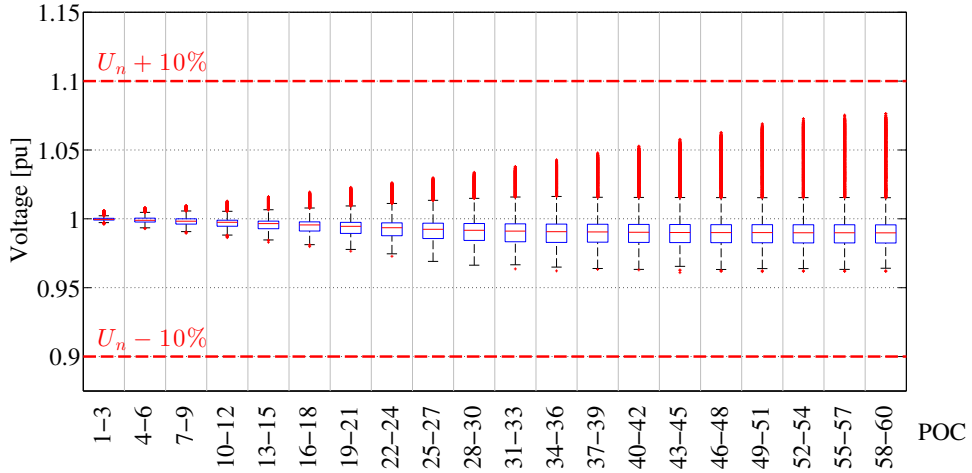


Figure 6.25: The voltage deviations in the investigated LV network for all POCs over a one week period. The control strategy A is applied to adjust the OLTC in the MV/LV substation as discussed in 4.5.1. The results are for $DG_{ratio} = 100\%$ and $AL_{ratio} = 22.1\%$.

to $I_f > 150\text{ A}$, $I_f > 200\text{ A}$ and $I_f > 250\text{ A}$.

It can be noted that due to DGs connected in the LV network without ALs (for $AL_{ratio} = 0\%$), the electricity generated from locally connected DGs is not primarily consumed within the network, but transported from a LV feeder towards the MV/LV substation. Therefore, a higher share of currents per a feeder section $I_f > 150\text{ A}$ can be observed already for low values of AL_{ratio} and even for $AL_{ratio} = 0\%$. Nevertheless, this case study demonstrates that the LV network can accommodate a high penetration of DGs without occurrence of higher currents in the network and without violation of voltage level conditions, as discussed before in 4.5. With increasing amount of ALs in the LV network, this effect diminishes as the locally generated electricity is increasingly also consumed locally by ALs. Therefore, among the investigated case studies the minimum share of observations with $I_f > 150\text{ A}$ can be found for $AL_{ratio} = 30\%$. With higher values of AL_{ratio} , the share of electricity consumed in the investigated LV network increases. As a consequence, the share of observations with $I_f > 150\text{ A}$ increases as the locally connected DGs supply more ALs in the LV network. The amount of observations with currents higher than given threshold increases in the LV network, as more observations are associated with feeder sections between DGs and ALs, similarly such as depicted in figure 6.22.

The impact of ALs on the LV network is investigated as a function of AL_{ratio} , which results in varying number of ALs in the LV network, as detailed in table 6.5. The current distribution and their occurrence in the investigated network can be depicted for moderate penetration levels of ALs, as in figure 6.26. It can be observed, that the

Table 6.5: The overview of evaluated case studies with different levels of AL_{ratio} , the number of ALs considered for each case study and the evaluation of current conditions in the investigated network for all investigated case studies based on their AL_{ratio} .

Case study with AL_{ratio}	Number of ALs (n_{AL})	Occurrence of $I_f > 150 A$	Occurrence of $I_f > 200 A$	Occurrence of $I_f > 250 A$	Total rating of all ALs $\sum_{i=1}^{n_{AL}} (P_{max}^{AL}(i))$
100 %	109	17.95 %	4.18 %	0.42 %	401 kW
90 %	98	13.46%	2.44 %	0.21 %	361 kW
80 %	87	9.57 %	1.23 %	0.060 %	320 kW
70 %	76	6.55 %	0.60 %	0.018 %	280 kW
60 %	65	4.24 %	0.29 %	0.0025 %	239 kW
50 %	54	2.85 %	0.16 %	0 %	199 kW
40 %	43	2.35 %	0.19 %	0 %	158 kW
30 %	33	2.32 %	0.23 %	0 %	121 kW
20 %	22	2.78 %	0.31 %	0 %	81 kW
10 %	11	3.11 %	0.45 %	0 %	40 kW
0 %	0	3.62 %	0.62 %	0 %	0 kW

currents in the investigated LV network can reach higher values $I_f > 200 A$, but with a very low occurrence probability. The occurrence of higher currents $I_f > 200 A$ increase with higher penetration levels of ALs in the investigated network, as depicted in figure 6.27. The current $I_f > 250 A$ can be observed for $AL_{ratio} \geq 60 \%$ in figure 6.27, similar conditions in the LV network could lead to overload of distribution network components. The current conditions $I_f > 300 A$ can be observed in figure 6.27 for $AL_{ratio} \geq 80 \%$, but with a negligible occurrence probability. Simultaneously, the voltage level conditions for all AL_{ratio} in the investigated network are comfortable with the standard for supplied voltage quality, as discussed in 4.4.

6.4.3 Practical implications

A serious impact of overloading in the network, due to higher currents in the LV feeder, can be a thermal damage of network components. Nevertheless, thermal constants for LV cables with a cross section area $A \geq 70 mm^2$ are longer than 15 min. [164]. The proposed application focuses on feeders, which have $A \geq 70 mm^2$ and are commonly used in the LV distribution networks in the Netherlands. Therefore, the assessment based on 15 min. measurements will be sufficient.

There are usually no direct measurements along LV feeders, which can be used to assess the current conditions per feeder section. As the occurrence is not location specific in the LV network, the utilization of measurements from smart metering infrastructure is suggested for the proposed application to evaluate the current conditions per feeder section. The assessment of current conditions, as presented in

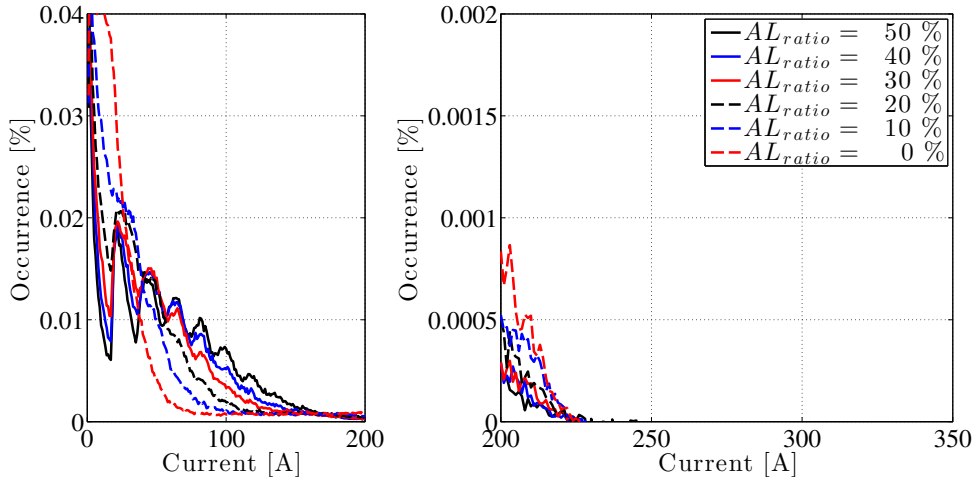


Figure 6.26: The occurrence of higher current for AL_{ratio} from 0 % till 50 %. The results are for $DG_{ratio} = 100$ %.

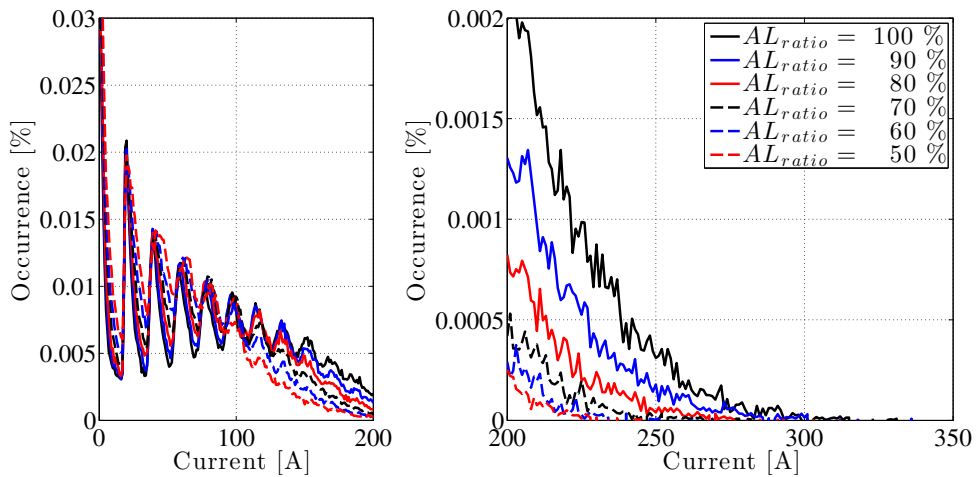


Figure 6.27: The occurrence of higher current for AL_{ratio} from 50 % till 100 %. The results are for $DG_{ratio} = 100$ %.

this section, can be enabled by collecting and processing average current or power measurements from metering points at network users POCs. The measurements

as 15 min. average current values should be accessible with the smart metering infrastructure as proposed in the NTA 8130 standard [62] and, with a priori knowledge of the LV network topology, can be utilized to enable the assessment of the current conditions in LV feeders.

The measurements from smart metering infrastructure can be combined with current measurements at each LV feeder and with LV bus-bar voltage measurements. The data concentrators for smart metering infrastructure can be located in the MV/LV substation, depending on the technology used, ergo the data processing could be done locally to prevent unnecessary data transfers during normal operation. Only status messages could be transmitted to DSO on regular basis. A threshold could be set (e.g., if $I_f > 200 A$) to notice the DSO operating the network about possibility of overloads occurrence. The preventive actions can be undertaken, before operational limits of exposed network components would be reached.

The proposed approach is applicable in a similar manner to MV distribution, where the measurements from LV level can be used to estimate the current conditions in the MV part of the network.

6.5 Conclusions

The developments in distribution automation are considered to unlock new network functions at the distribution level. Therefore, applications of data, measurements and advanced distribution assets are presented in three sections of this chapter.

In 6.2 is discussed the application of OLTC in IDS to induce DR. The advancements in distribution network automation in the future, such as the development of IDS, will unlock opportunities for new applications, which can be utilized by distribution network assets. For instance, as the on-line voltage control can take a commonplace in distribution networks, new applications can widespread. Therefore, in this section, the use of on-line voltage control, which is made available with IDS, is proposed to enable DR application at distribution level. The proposed DR can be used for instance to support system balancing, as presented also in this section.

The proposed DR application can function in the network without jeopardizing of its initial goal to improve supplied voltage quality. Nevertheless, it is estimated that the DR potential can be significant for a high IDS penetration in power system and it can have significant impact on called imbalance volumes.

The proposed DR will be available as a share of the total load supplied by IDSs in the system. The higher the IDS penetration level (the higher the share of total load in the system supplied by IDSs), the lower the utilization factor of induced DR actions at an individual IDS will be required. As the proposed technique is based on voltage level changes at IDS, the higher the IDS penetration level, the smaller the voltage adjustments required to meet the calls for imbalance volumes. The average voltage fluctuations, due to IDSs participating on system balancing, will be much smaller than the currently

observed voltage fluctuations in the distribution networks. The voltage fluctuations, due to load variations in the network, will be mitigated by IDS. Ergo, network users will experience improved voltage quality despite IDS provision of DR to support system balancing. It is shown, that with higher IDS penetration levels, the required average voltage adjustments will have only an imperceptible effect on connected network users.

The implications of the proposed DR application on distribution network losses are only negligible and relative changes $< 2\%$ of current distribution network losses can be expected.

The proposed system respects the presumption that at any moment, during a normal operation, all connected network users are supplied with voltage level in accordance to the standard for supplied voltage quality. Nevertheless, this assumption could be overridden during emergency events, when higher voltage deviations would be justified. In this case, the proposed DR application would be able to provide response to even larger imbalance calls.

The proposed application has some unique characteristics, especially it will be available round-the-clock and with a dispatch speed limited practically only by the means of applied communication and power electronics. The service provision is also symmetrical (for both up-regulation and down-regulation) and can be changed instantly or kept active throughout many subsequent PTUs. The service availability is predictable as it follows daily load patterns and the availability can be more precisely assessed based on local network users load data. The proposed application can have a very high reliability, because it depends on many IDSs coordinating simultaneously their voltage adjustments in incremental steps. In case of a failure of some IDSs, the required DR could be fulfilled by additional adjustment of remaining IDSs in the system. The high reliability of the proposed DR approach is essential for a successful integration into power system operation.

As more challenges can be expected in the future in the area of power system balancing, the proposed concept could contribute to better integration of intermittent power generation in the power system. Since developments in substation automation will make the provision of the proposed service possible, this resource shall be considered, because it can profoundly increase the amount of readily available operating reserves in power systems. The proposed DR application could help in rationalization of power system operation and in reduction of called imbalance volumes in the system.

Note, that the application of CVR techniques is sometimes accompanied with some controversy about its feasibility and magnitude of achievable load response. Although the results presented in 6.2.1 are comparable with recent work, as presented in table 6.1, additional simulations were done to present more comprehensive results to support the proposed DR application. To address the concerns related to the applicability of the CVR technique, results presented in 6.2 are evaluated also under the assumption, that the load response ratio is only 50 % of the measured one, as presented in 6.2.1. Additional results are presented in Appendix B.

In 6.3 is proposed application for electricity theft detection in distribution networks. The problem of illegal abstraction of electricity is not unique for the Netherlands, but is common in many countries worldwide. Nevertheless, it is a complex phenomenon with many aspects and with a certain social and law enforcement dimension.

The application for detection of illegal abstraction of electricity presented in this section exploits the data available from the smart metering infrastructure. The presented application not only indicates the presence of illegal abstraction of electricity in the network, but it distinguishes itself from other proposed methods by the possibility to identify the location, where the illegal abstraction takes place. Based on evaluation of measurement uncertainties and their impact on the detectable illegal abstraction of electricity, it is pointed out, that with the current smart metering infrastructure in the Netherlands, the most common source of illegal abstraction of electricity could be detected within a day. The proposed application was also experimentally verified in a field test in the distribution network of one of the Dutch DSOs.

Although, the potential to reduce the non-technical loss in the network is large, a prudent approach in estimation of the real benefits shall be undertaken. For instance, the potential reduction of losses related to the illegal abstraction of electricity with advanced detection techniques in range of only 25 % is expected in United Kingdom [145]. Therefore, a low level of non-technical loss in a very efficient power system can be acceptable in a case, where the cost related to the fight of the perpetrators in the network are higher than the achievable benefits for genuine network users.

In 6.4 is presented the application of heavy load assessment in distribution networks, which is based on exploitation of measurement data from smart metering infrastructure in LV network.

The presented case studies demonstrated that a combination of new forms of additional loads (ALs) and DGs can result in high current conditions (congestions) in LV network. In a severe case, the high current conditions could lead to overload of distribution network components for high penetrations of ALs. It is noted that high current conditions are nowadays not very probable in LV network in the Netherlands, as the penetration levels of DGs and ALs is still relatively low. Nevertheless, with a high penetration of ALs in the network, congestions in the LV network can occur.

Therefore, an application exploiting measurement data from smart metering infrastructure is proposed to assess the current conditions of exposed components in the network (feeder sections), which are not directly measured. The proposed application can provide better insight into the operation of LV networks, which can be then reliably operated close to their operation limits and can allow assessment of connection availability to new form of loads connected by network users.

Conclusions, contributions and recommendations

This chapter gives conclusions on the work presented in this dissertation. Also a review of main achievements and contributions within this work is given. Advancing the knowledge is a never-ending task, therefore some recommendations for future work are discussed.

7.1 Conclusions

The demands on our aging power system infrastructure are changing. The sustainability agenda implies unprecedented changes in our power system at different levels and especially with implications on the electricity distribution. The distribution network is going to be challenged by the need of accommodating many new developments as many network users are going to change their roles from only consumers to producers of electricity. Especially decentralized generation together with the shift towards electro-mobility are among the key drivers for distribution system operators (DSO) to search for new technical alternatives applicable alongside their current distribution network assets.

The distribution networks of the future have to be therefore as flexible as possible in implementing a variety of new (and even unforeseen) developments connected to them. The network shall be also monitored to recognize possible operation states, which can jeopardize its reliability and quality of service provision.

The work presented in this dissertation provides new perspectives in flexible distribution network operation. The possible application of data and advanced network technologies were analyzed to enhance distribution network performance. The expected requirements and functionality of the network are assessed. As a consequence of it, it is recognized that more insight into the network operation and provided quality of service is needed. The network users connected to the network require certain

quality of supplied voltage which needs to be monitored by a DSO. The evaluation of required measurements and their locations in the distribution network is assessed to support reasonable investment in the monitoring system. Substation automation as a technological alternative applicable within the regulatory framework of Dutch DSOs is analyzed to increase the hosting capacity of the distribution network and to actively improve service quality.

In this work it is demonstrated that the performance of the current network can be improved with proposed applications, which include on-line voltage control in the distribution network and utilization of measurement data from the sensing infrastructure. Many applications intended for the distribution network are mostly single-purpose technologies. Many new opportunities for their utilization can be found if applied in the currently passive networks. Some of them are demonstrated in this dissertation. It is shown that enhanced network functionality can be achieved with new assets in the network. New synergies, e.g., in system support, stemming from the distribution network are found and their impact on the power system is quantified. The distribution network is an inevitable part of the future power system vision which has to also advance to materialize it.

7.2 Dissertation contributions

The main contributions of this work can be summarized as follows:

- By using the AHP technique, the requirements at the functionality level of the current and the future distribution network are characterized with the focus on MV/LV distribution substations. The fulfillment of the expected functionality by the available technological alternatives is evaluated and the applicability of them in the context of Dutch regulatory framework is assessed.
- The application of on-line control at MV/LV substations is proposed for voltage level conditioning in presence of a high penetration level of distributed generators in the network. The evaluation of different control strategies is presented and the implications for the LV as well as for the MV network are quantified to derive the most applicable control strategy.
- It is shown that the currently used methodology for prediction and characterization of residential network user load has its limitation and it can be improved. An improved methodology for characterization of load profiles based on field measurements is proposed and evaluated to improve the accuracy of simulations on distribution networks.
- The propagation of power quality phenomena (harmonic distortion and flicker) in the Dutch distribution network is assessed. The most suitable locations for measurement placement are proposed to provide a DSO with an sufficient overview about the distortion levels in the network.

- A new application of the on-line voltage level control at the MV/LV substation to manage demand is proposed. It is pointed out that the accessible capacity with this application can reduce system imbalances in a power system without severe impact on distribution network losses and on the provided quality of service to network users. In addition, the proposed application has some particular characteristics, which would enable its reliable integration into the power system.
- A new application exploiting the data from the smart metering infrastructure for detection of illegal abstraction of electricity is proposed and tested. Distinct for this application is the use of measurements already available with the currently installed smart meters in the Netherlands without additional hardware requirements. Unique for this application is the localization capability of the connection with illegal abstraction of electricity in the network.
- An advanced application exploiting measurement data from smart metering infrastructure is proposed to assess the current condition in the distribution network. The probability of a high loading occurrence in the presence of emerging technologies in the LV distribution network is presented. The proposed data application uses available data from the smart metering infrastructure to deliver information about assets not directly measured, but prone to experience a heavy loading conditions. This application increases DSO's insight into the assets utilization during the operation of its distribution network.

7.3 Recommendations for future work

This work answers the main research questions, but other important questions are raised. The operation of the distribution network can be managed from the perspective of the Distribution System Operator (DSO) as addressed in this dissertation. However, a DSO operates its distribution network in regulated environment and interacts with other entities to comply with the demands of connected network users. Therefore, the considerations on the interaction between a DSO, other entities and network users in the network can be further investigated in several perspectives:

- The area of incentives design to encourage sufficient network user involvement to ease operation of distribution network should be examined. There can be conflicting objectives of different entities in the system, which can have impact on reliable operation of the network. In addition, challenges and limitations in terms of enabling technology, e.g., requirements on communication, should be addressed. The collaborative voltage level coordination including local resources in combination with the proposed approach in chapter 4 is an example where new effective synergies could be found.

- Special attention shall be given to the implications related to the proliferation of electro-mobility, which is dynamically developing [165] and is able to present new opportunities for the system operation. Many issues could arise if the shift towards electro-mobility is not managed with a comprehensive vision, nevertheless many issues could be solved when the potential offered by this emerging technology is embraced in depth, such as the vehicle-to-grid application.
- The proposed application of use of distribution network assets with the aim to support system balancing in 6.2.4 can be examined together with the other means for balancing and demand management. The combination with other means of system support provisioning can be assessed at the technical as well as at the economical level.
- The measurements related to power quality can provide DSOs with insight about the distortion levels in the network. However, additional measurements can be considered to improve DSOs awareness of the network operation, to provide input for distribution network state estimation and to enable distribution network state prediction.
- The connection of single-phase DERs, and DGs in particular, in the three-phase LV network can alter the voltage profile in the distribution network and not only in the connected phase. Due to the spacial allocation of the single-phase installations, the aspects of distribution network operation to attenuate voltage unbalances and to coordinate DER connections could be investigated further.
- Incentives for DSOs, new business models and the economic impact of proposed applications in chapter 6 should be analyzed. As their technological maturity progresses, the benefits of proposed applications can be reasonably assessed and weighted against the deployment cost to reduce the uncertainty for investment. A thorough economic analysis of proposed applications could be done in the future as an extension of this work.

Transfer coefficients

A.1 Flicker propagation

The network parameters and examples for the flicker propagation estimation presented in 4.6.2 is detailed.

The values for the flicker propagation as in equation 4.11, the network parameters as in table A.1 are used. The transfer coefficient for the flicker propagation upstream to the LV bus-bar form $POC(30)$, located in the middle of the LV feeder is denoted as $T_{P_{st}}^{POC(30) \rightarrow LV_{bus-bar}}$ and detailed in equation A.1. The typical LV feeder has length $l = 500 \text{ m}$, therefore the $l^{POC(30)} = 250 \text{ m}$ is assumed.

$$\begin{aligned}
 T_{P_{st}}^{POC(30) \rightarrow LV_{bus-bar}} &= \left| \frac{Z_{MV} + Z_{tr}}{Z_{MV} + Z_{tr} + Z_{ca} \cdot l^{POC(30)}} \right| \\
 &= \left| \frac{0.00492 + 0.01848ij}{0.00492 + 0.01848ij + (0.214 + 0.079j) \cdot 0.250} \right| \quad (\text{A.1}) \\
 &= 0.274
 \end{aligned}$$

The P_{st} value for a flicker source in the network, can be estimated as in equation 4.8. The numerical example for $P_{st}^{POC(60)}$ is provided in equation A.2. The reference values from table A.1 are used. The voltage drop is estimated based on equation 4.2, where a motor start-up with inrush current $I_{ir} = 3 \cdot 16 \text{ A}$ and start-up power factor $PF = 0.4$ is assumed.

$$\begin{aligned}
 P_{st}^{POC(60)} &= 0.337 \cdot F \cdot r^{\frac{1}{3.2}} \cdot \left(\frac{\Delta U^{POC(60)}}{U^{POC(60)}} \right) \cdot 100 \\
 &= 0.337 \cdot 1 \cdot 1^{\frac{1}{3.2}} \cdot 1.219 \\
 &= 0.654
 \end{aligned} \quad (\text{A.2})$$

Table A.1: The variables used for estimation of the flicker propagation in 4.6.2.

Notation	Value	Description and comments
Z_{MV}	$0.00032 + 0.00318j \Omega$	MV network impedance, based on $S_{k,MV} = 50 \text{ MVA}$
Z_{tr}	$0.0046 + 0.0153j \Omega$	Impedance of the 400 kVA MV/LV transformer
Z_{ca}	$0.214 + 0.079j \Omega \cdot km^{-1}$	LV feeder impedance, based on $A = 150 \text{ mm}^2 \text{ (Al)}$, four-core (PEN)
F	1	The waveform shape factor [27]
r	$1 \text{ n.repetitions} \cdot \text{min.}^{-1}$	The repetition rate of distorting source, e.g., number of repeated motor start-ups

A.2 Harmonic propagation

The propagation of harmonic distortion in LV networks is influenced by the frequency dependent characteristics of network components. The transfer coefficients for $T_{u_1}^{POC \rightarrow LV_{bus-bar}}$ are based on distribution network parameters, as presented in A.1. For higher frequencies, the evaluation is more complex as all network components are frequency dependent. Therefore, the model of LV distribution network with same parameters as in A.1 was build in commercial software DigSILENT PowerFactory, where a current source with $I = 48 \text{ A} = I_5$ was used to simulate the distortion source to

estimate $\frac{\Delta u_5^{LV_{bus-bar}}}{u_5^{LV_{bus-bar}}}$ and $\frac{\Delta u_5^{POC}}{u_5^{POC}}$ values for different locations in the LV network. The

parameters were recorded and the transfer coefficients $T_{u_5}^{POC \rightarrow LV_{bus-bar}}$ were estimated for different POCs in the network. The results are presented in table B.2.

Table A.2: The estimated values of $\frac{\Delta u_5^{LV_{bus-bar}}}{u_5^{LV_{bus-bar}}}$, $\frac{\Delta u_5^{POC}}{u_5^{POC}}$ and resulting $T_{u_5}^{POC \rightarrow LV_{bus-bar}}$ used in figure 4.15.

POC	$\frac{\Delta u_5^{LV_{bus-bar}}}{u_5^{LV_{bus-bar}}}$	$\frac{\Delta u_5^{POC}}{u_5^{POC}}$	$T_{u_5}^{POC \rightarrow LV_{bus-bar}}$
SS-LV	1.97 %	1.97 %	1.00
POC(1)	1.97 %	2.18 %	0.90
POC(2)	1.97 %	2.40 %	0.82
POC(3)	1.97 %	2.63 %	0.75
POC(4)	1.97 %	2.85 %	0.69
POC(5)	1.96 %	3.08 %	0.64
POC(6)	1.96 %	3.30 %	0.59
POC(7)	1.96 %	3.53 %	0.56
POC(8)	1.96 %	3.76 %	0.52
POC(9)	1.96 %	3.99 %	0.49
POC(10)	1.96 %	4.22 %	0.46
POC(11)	1.96 %	4.45 %	0.44
POC(12)	1.96 %	4.68 %	0.42
POC(13)	1.96 %	4.91 %	0.40
POC(14)	1.97 %	5.19 %	0.38
POC(15)	1.97 %	5.43 %	0.36
POC(16)	1.97 %	5.67 %	0.35
POC(17)	1.97 %	5.91 %	0.33
POC(18)	1.97 %	6.14 %	0.32
POC(19)	1.97 %	6.38 %	0.31
POC(20)	1.97 %	6.62 %	0.30

Demand Response with IDS

As pointed out in 6.5, the results from 6.2 are also evaluated under the assumption that the load response ratio is only 50 % of the measured one, as presented in 6.2.1.

Under this assumption, the imbalance duration curves of remaining imbalance volumes per PTU for certain penetration level of IDS in the system can be contrasted too with the original imbalance data for the Netherlands in the year 2012. The results are presented in figure B.1. Note that the available provision of proposed DR is proportional to the load supplied by IDS (to the penetration level of IDSs in the system) and to the load response ratio of the supplied loads, therefore differences can be observed in comparison to results presented in figure 6.11.

Also the total amount of the available DR capacity depends on IDS penetration level in the system and on PU_{ratio} . The DR availability is time dependent. Therefore, also the utilization of available DR to support power system balancing depends on considered PU_{ratio} and on the coincidence of called imbalances in the system. Based on the called imbalance volumes in the Netherlands in the year 2012, the utilization factors for different DR penetration levels in the system can be estimated for 50 % of the measured PU_{ratio} , as discussed in 6.2.1. The results are presented in figure B.2. The available DR capacity is smaller with reduced PU_{ratio} , ergo results in a higher utilization of the available capacity for DR, as in figure B.2 compared with utilization factors presented in figure 6.12.

The results related to the capacity factor reduction of called imbalance volumes in the Netherlands in the year 2012 for assessed IDS penetration levels are presented together with the magnitude reductions of called imbalance volumes in table B.2. The results are estimated for assumption, that loads respond to applied voltage change only with 50 % of the measured PU_{ratio} , as discussed in 6.2.1.

The resulting distribution network losses related to the examined DR provision and participation on system balancing are presented in figure B.3 and the numerical values are given in table B.1. The results in figure B.3 can be compared with results in figure 6.13. The available capacity to provide DR will be utilized more for system

Table B.1: The overview of relative changes of distribution network losses related to the IDS operation and supporting system balancing. The results are based on imbalance volume data for the Netherlands in the year 2012. The results are depicted for all IDS penetration levels considered in the system with assumption, that loads respond to applied voltage change only with 50 % of the measured PU_{ratio} , as discussed in 6.2.1.

IDS penetration level	Relative change of distribution network losses		
	Up-regulation	Down-regulation	Total
1 %	3.17 %	-5.20 %	-2.04 %
5 %	2.13 %	-3.19 %	-1.07 %
10 %	1.39 %	-1.83 %	-0.44 %
20 %	0.58 %	-0.59 %	-0.01 %
30 %	0.23 %	-0.19 %	0.04 %

Table B.2: The overview of reduction capabilities of the proposed DR for supporting system balancing. The results are based on imbalance volume data for the Netherlands in the year 2012 and with assumption that loads respond to applied voltage change only with 50 % of the measured PU_{ratio} , as discussed in 6.2.1.

IDS penetration level	Magnitude reduction		Capacity factor reduction	
	Up-regulation	Down-regulation	Up-regulation	Down-regulation
1 %	0.59 %	0.75 %	6.51 %	8.62 %
5 %	2.97 %	3.73 %	26.96 %	34.55 %
10 %	5.95 %	7.46 %	46.21 %	56.82 %
20 %	11.89 %	14.92 %	71.35 %	81.59 %
30 %	17.84 %	22.38 %	85.07 %	92.31 %

balancing when reduced $0.5 \cdot PU_{ratio}$ is considered. As a consequence, higher changes in distribution network losses related to individual calls for DR provision could be observed even for higher penetration levels of IDS in the system.

The results presented in this section demonstrate, that despite the reduced PU_{ratio} assumed in the evaluation, the proposed DR can have notable implications on power system balancing as it can help to reduce significantly the called imbalance volumes and magnitude of the called imbalance volumes in the system.

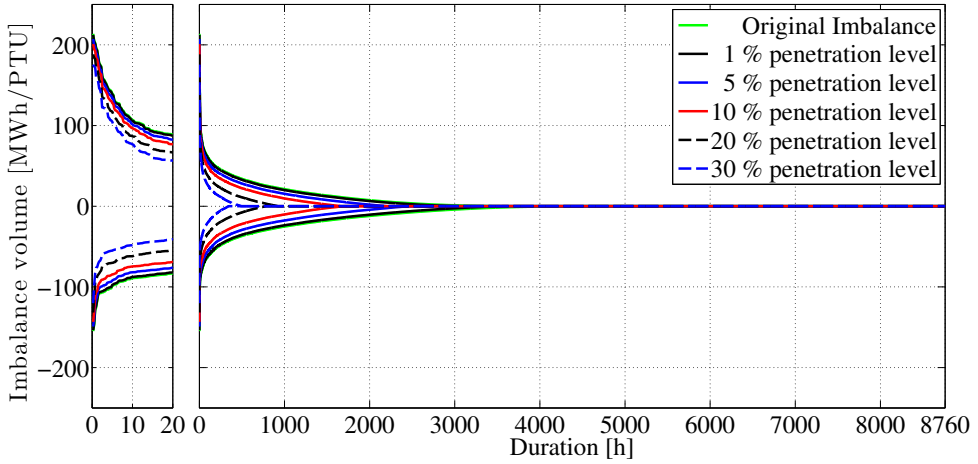


Figure B.1: Original imbalance volumes duration curve based on the data for the Netherlands in the year 2012 contrasted with the remaining imbalance volumes duration curves after deployment of available DR to support system balancing. The results are depicted for all IDS penetration levels considered in the system with assumption, that loads respond to applied voltage change only with 50 % of the measured PU_{ratio} , as discussed in 6.2.1.

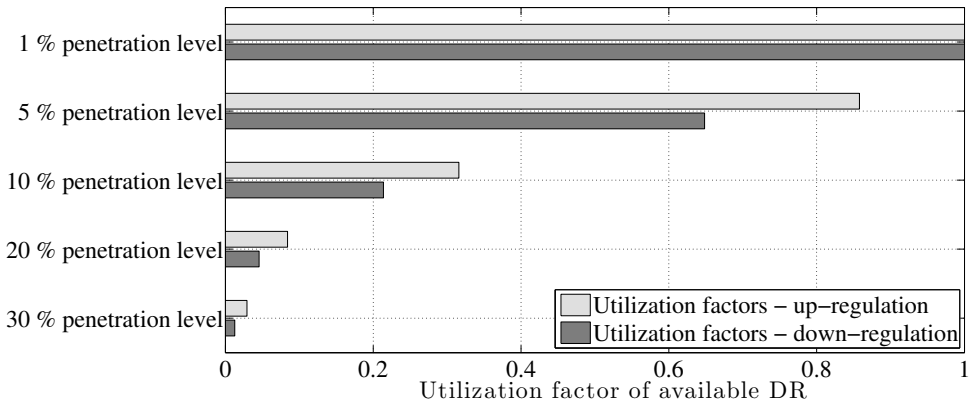


Figure B.2: The utilization factors of available DR provided by IDSs in the system and participating of system balancing. The values are estimated for the imbalance volumes in the Netherlands in the year 2012 separately for $\Delta P_{down,util}^{IM2012}$ and $\Delta P_{up,util}^{IM2012}$ for all assessed penetration levels of IDS in the system, assuming 50 % of the measured PU_{ratio} , as discussed in 6.2.1.

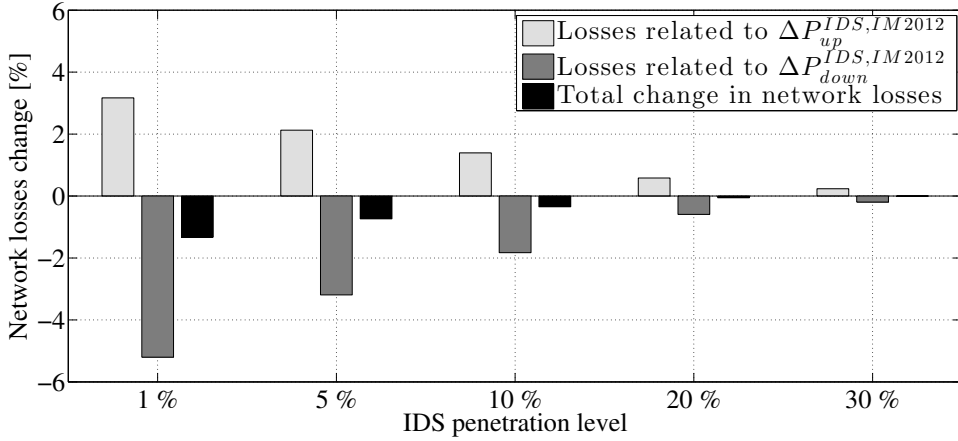


Figure B.3: The estimated relative changes of distribution network losses for different penetration levels of IDSs in the system providing DR for system balancing. Based on called imbalance volumes data in the Netherlands in the year 2012, as depicted in figure 6.11. The results are given for all IDS penetration levels considered in the system with the assumption, that loads respond to applied voltage change only with 50 % of the measured PU_{ratio} , as discussed in 6.2.1.

Bibliography

- [1] Ingmar Schumacher and Eric Strobl. Economic development and losses due to natural disasters: The role of hazard exposure. *Ecological Economics*, 72:97–105, December 2011.
- [2] Sung-Kwan Joo, Jang-Chul Kim, and Chen-Ching Liu. Empirical Analysis of the Impact of 2003 Blackout on Security Values of U.S. Utilities and Electrical Equipment Manufacturing Firms. *IEEE Transactions on Power Systems*, 22(3):1012–1018, August 2007.
- [3] C. Clastres and C. Locatelli. European Union energy security: The challenges of liberalisation in a risk-prone international environment. *2012 9th International Conference on the European Energy Market*, pages 1–9, May 2012.
- [4] European Commission Directorate-General for Energy in collaboration with Climate Action DG and Mobility and Transport DG. EU energy trends to 2030 - update 2009, 2010.
- [5] European Commission. Report from the Commission to the European Parliament, the Council, the European Economic and Social Committee and the Committee of the Regions - Renewable energy progress report (COM(2013) 175 final). Technical report, 2013.
- [6] Directive 2009/28/EC Of The European Parliament And Of The Council Of 23 April 2009 on the promotion of the use of energy from renewable sources and amending and subsequently repealing directives 2001/77/EC and 2003/30/EC, 2009.
- [7] International Energy Agency. World Energy Outlook 2012, 2012.
- [8] ENTSO-E. Scenario Outlook & Adequacy Forecast 2012-2030. Technical report, 2012.

- [9] U.S. Energy Information Administration. Petroleum & Other Liquids - Europe Brent Spot Price FOB, 2013. Available online at: <http://www.eia.gov/dnav/pet/hist/LeafHandler.ashx?n=PET&s=RB RTE&f=A> Accessed on: April 5, 2013.
- [10] E.F. Fuchs. *Power conversion of renewable energy systems*. 2011.
- [11] Xinghuo Yu, Carlo Cecati, Tharam Dillon, and M. Simões. The New Frontier of Smart Grids. *IEEE Industrial Electronics Magazine*, 5(3):49–63, September 2011.
- [12] IEEE Standards Association. IEEE Std 2030-2011 IEEE Guide for Smart Grid Interoperability of Energy Technology and Information Technology Operation with the Electric Power System (EPS), End-Use Applications, and Loads, 2011.
- [13] H. Farhangi. The path of the smart grid. *IEEE Power and Energy Magazine*, 8(1):18–28, January 2010.
- [14] Agentschap NL - Ministerie van Economische Zaken. IOP Elektromagnetische Vermogenstechniek (IOP EMVT), 2013. Available online at: <http://www.agentschapnl.nl/programmas-regelingen/iop-elektromagnetische-vermogenstechniek-iop-emvt> Accessed on: April 8, 2013.
- [15] Michiel de Nooij and Barbara Baarsma. Divorce comes at a price: An ex ante welfare analysis of ownership unbundling of the distribution and commercial companies in the Dutch energy sector. *Energy Policy*, 37(12):5449–5458, December 2009.
- [16] J.G. Slootweg, E. Veldman, and J. Morren. Sensing and control challenges for Smart Grids. In *Networking, Sensing and Control (ICNSC), 2011 IEEE International Conference on*, pages 1–7, April 2011.
- [17] TenneT. Annual Report TenneT 2011. Technical report, 2012.
- [18] Directive 2009/72/EC of the European Parliament and of the Council of 13 July 2009. Technical report, 2009.
- [19] Netbeheer Nederland. Energie Trends 2012. Technical report, 2012.
- [20] S. Bhattacharyya, Z. Wang, J.F.G. Cobben, J.M.A. Myrzik, and W.L. Kling. Analysis of Power Quality Performance of The Dutch Medium And Low Voltage Grids. *ICHQP 2008 13th International Conference on Harmonics and Quality of Power*, pages 1–6, 2008.
- [21] Edward Coster. *Distribution Grid Operation Including Distributed Generation*. Ph.D. dissertation, Eindhoven University of Technology, 2010.
- [22] T.B. Smith. Electricity theft: a comparative analysis. *Energy Policy*, 32(18):2067–2076, December 2004.

- [23] The World Bank. World Development Indicators - Electric power transmission and distribution losses, 2013. Available online at: <http://data.worldbank.org/indicator/EG.ELC.LOSS.ZS> Accessed on: March 6, 2013.
- [24] Petr van Oirsouw. *Netten voor distribution van elektriciteit*. Phase to Phase B.V, Arnhem, the Netherlands, 2011.
- [25] Frans Provoost. *Intelligent Distribution Network Design*. Ph.D. dissertation, Eindhoven University of Technology, 2009.
- [26] Phuong Hong Nguyen. *Multi-Agent System based Active Distribution Networks*. Ph.D. dissertation, Eindhoven University of Technology, 2010.
- [27] J.F.G. Cobben. *Power Quality Implications at the Point of Connection*. Ph.D. dissertation, Eindhoven University of Technology, 2007.
- [28] Sharmistha Bhattacharyya. *Power Quality Requirements and Responsibilities at the Point of Connection*. Ph.D. dissertation, Eindhoven University of Technology, 2011.
- [29] R.J.M. Heskes. *Minimizing the impact of resonances in low voltage grids by power electronics based distributed generators*. Ph.D. dissertation, Eindhoven University of Technology, 2011.
- [30] E. Veldman, M. Gibescu, J.G. Slootweg, and W.L. Kling. Scenario-based modelling of future residential electricity demands and assessing their impact on distribution grids. *Energy Policy*, 56:233–247, February 2013.
- [31] Centraal Bureau voor de Statistiek. *Hernieuwbare energie in Nederland 2011, 2012*.
- [32] Martin Braun, Thomas Stetz, Roland Bründlinger, Christoph Mayr, Kazuhiko Ogimoto, Hiroyuki Hatta, Hiromu Kobayashi, Ben Kroposki, Barry Mather, Michael Coddington, Kevin Lynn, Giorgio Graditi, Achim Woyte, and Iain MacGill. Is the distribution grid ready to accept large-scale photovoltaic deployment? State of the art, progress, and future prospects. *Progress in Photovoltaics: Research and Applications*, 20(6):681–697, September 2012.
- [33] Jan Appen, Martin Braun, Thomas Stetz, Konrad Diwold, and Dominik Geibel. Time in the Sun: The Challenge of High PV Penetration in the German Electric Grid. *IEEE Power and Energy Magazine*, 11(2):55–64, March 2013.
- [34] CBS Statistics Netherlands. Substantial increase in use of solar panels, 2012.
- [35] National renewable energy action plan (Directive 2009/28/EC). 2009.
- [36] RE-thinking 2050 A 100% Renewable Energy Vision for the European Union. Technical report, European Renewable Energy Council, 2010.

- [37] M. C. Benhabib, J.M.A. Myrzik, and J.L. Duarte. Harmonic effects caused by large scale PV installations in LV network. In *2007 9th International Conference on Electrical Power Quality and Utilisation*, pages 1–6. IEEE, October 2007.
- [38] TenneT TSO. Vision2030. Technical report, 2008.
- [39] R.A. Verzijlbergh, Z. Lukszo, J.G. Slootweg, and M.D. Ilic. The impact of controlled electric vehicle charging on residential low voltage networks. In *2011 International Conference on Networking, Sensing and Control*, pages 14–19. IEEE, April 2011.
- [40] R.A. Verzijlbergh, Z. Lukszo, E. Veldman, J.G. Slootweg, and M.D. Ilic. Deriving electric vehicle charge profiles from driving statistics. In *2011 IEEE Power and Energy Society General Meeting*, pages 1–6. IEEE, July 2011.
- [41] N. Leemput, J. Van Roy, F. Geth, P. Tant, B. Claessens, and J. Driesen. Comparative analysis of coordination strategies for electric vehicles. In *2011 2nd IEEE PES International Conference and Exhibition on Innovative Smart Grid Technologies*, pages 1–8. IEEE, December 2011.
- [42] R.A. Verzijlbergh, M.O.W. Grond, Z. Lukszo, J.G. Slootweg, and M.D. Ilic. Network Impacts and Cost Savings of Controlled EV Charging. *IEEE Transactions on Smart Grid*, 3(3):1203–1212, September 2012.
- [43] Informatie Rijksoverheid. Elektrisch rijden, 2012.
- [44] Alicja Lojowska, Dorota Kurowicka, Georgios Papaefthymiou, and Lou van der Sluis. Stochastic Modeling of Power Demand Due to EVs Using Copula. *IEEE Transactions on Power Systems*, 27(4):1960–1968, November 2012.
- [45] S.K. Ronnberg and M.H.J. Bollen. Interaction Between Narrowband Power-Line Communication and End-User Equipment. *Power Delivery, IEEE*, 26(3):2034–2039, 2011.
- [46] Nederlands Normalisatie-insituut. European Standard EN 50160 - Voltage characteristics of electricity supplied by public distribution networks. Technical report, NEN, Delft, 2010.
- [47] Energiekamer. Netcode Elektriciteit. Technical report, 2012.
- [48] Netbeheer Nederland. Spanningskwaliteit in Nederland, resultaten 2011. Technical report, Netbeheer Nederland and Movares Nederland B.V., Utrecht, 2012.
- [49] CEER. 5th CEER Benchmarking Report on the Quality of Electricity Supply 2011. Technical report, Council of European Energy Regulators, 2012.

- [50] Position Paper on Smart Grids An ERGEG Public Consultation Paper. Technical report, European Regulators' Group for Electricity and Gas - E09-EQS-30-04, Bruxelles, 2009.
- [51] M. Godoy Simoes, R. Roche, E. Kyriakides, A. Miraoui, B. Blunier, K. McBee, S. Suryanarayanan, P.H. Nguyen, and P.F. Ribeiro. Smart-grid technologies and progress in Europe and the USA. In *2011 IEEE Energy Conversion Congress and Exposition*, pages 383–390. IEEE, September 2011.
- [52] European SmartGrids Technology Platform, Vision and Strategy for Europe's Electricity Network of the Future. Technical report, European Commission, 2006.
- [53] European Technology Platform SmartGrids. SmartGrids SRA 2035 Strategic Research Agenda Update of the SmartGrids SRA 2007 for the needs by the year 2035. Technical report, 2012.
- [54] European Technology Platform SmartGrids, Strategic Research Agenda For Europe's Electricity Networks Of The Future. Technical report, European Commission, 2007.
- [55] Final Guidelines of Good Practice on Regulatory Aspects of Smart Metering for Electricity and Gas. Technical report, European Regulators' Group for Electricity and Gas, Bruxelles, 2011.
- [56] Directive 2006/32/EC Of The European Parliament And Of The Council of 5 April 2006 on energy end-use efficiency and energy services and repealing Council Directive 93/76/EEC. Technical report, 2006.
- [57] C. Cuijpers and B.J. Koops. Smart Metering and Privacy in Europe: Lessons from the Dutch Case. *European Data Protection: Coming of Age*, 2012.
- [58] W. Heck (at nrc.nl). Smart energy meter will not be compulsory, 2009. Available online at: http://vorige.nrc.nl/international/article2207260.ece/Smart_energy_meter_will_not_be_compulsory Accessed on: April 17, 2013.
- [59] KEMA Nederland B.V. Smart meters in the Netherlands; Revised financial analysis and policy advice. Technical report, 2010.
- [60] SmartRegions - Promoting best practices of innovative smart metering services to European regions. European Smart Metering Landscape Report 2012.
- [61] European Commission. A joint contribution of DG ENER and DG INFSO towards the Digital Agenda, Action 73: Set of common functional requirements of the SMART METER. Technical report, 2011.
- [62] Netherlands Normalisation-Instituut. Netherlands Technical Agreement NTA 8130, Minimum set of functions for metering of electricity, gas and thermal energy for domestic customers. Technical report, 2007.

- [63] Nederlands Normalisatie-instituut. NTA 8150-1 - System Interface AMI Systems. Technical report, 2010.
- [64] Nederlands Normalisatie-instituut. NTA 8150-2 - System API. Technical report, 2010.
- [65] J. Kester, P. Heskes, S. Kaandorp, J.F.G. Cobben, G. Scchoonenberg, D. Malyna, E. De Jong, B. Wargers, and T. Dalmeijer. A smart MV/LV-station that improves power quality. Reliability and substation load profile. In *Cired 2009*, Prague, 2009.
- [66] Smart MV/LV-substation features. Available online at: <http://www.smartsubstation.eu/features/> Accessed on: September 7, 2012.
- [67] I. Melnik, F. Provoost, and W. Bos. Intelligent Distribution Substation Improves Power Quality. In *21st International Conference and Exhibition on Electricity Distribution, CIRED 2011*, pages 1–4, 2011.
- [68] PF Ribeiro, H. Polinder, and M. Verkerk. Planning and Designing Smart Grids: Philosophical Considerations. *IEEE Technology and Society Magazine*, 31(3):34–43, January 2012.
- [69] R.K. Rietz and S. Suryanarayanan. A review of the application of analytic hierarchy process to the planning and operation of electric power microgrids. In *2008 40th North American Power Symposium*, volume 80401, pages 1–6. IEEE, September 2008.
- [70] Thomas L. Saaty. *Fundamentals of Decision Making and Priority Theory*. RWS Publications, Pittsburgh, 2006.
- [71] Omkarprasad S. Vaidya and Sushil Kumar. Analytic hierarchy process: An overview of applications. *European Journal of Operational Research*, 169(1):1–29, February 2006.
- [72] S.D. Pohekar and M. Ramachandran. Application of multi-criteria decision making to sustainable energy planning-A review. *Renewable and Sustainable Energy Reviews*, 8(4):365–381, August 2004.
- [73] J. Mitra and S. Suryanarayanan. System analytics for smart microgrids. In *IEEE PES General Meeting*, pages 1–4. IEEE, July 2010.
- [74] K.A. Nigim, S. Suryanarayanan, R. Gorur, and R.G. Farmer. The application of analytical hierarchy process to analyze the impact of hidden failures in special protection schemes. *Electric Power Systems Research*, 67(3):191–196, December 2003.

- [75] D.P. Bernardon, M. Sperandio, V.J. Garcia, L.L. Pfitscher, W. Reck, E.F.B. Daza, M. Ramos, and L. Comassetto. Automatic reestablishment of power supply in distribution systems using AHP method. *2011 International Conference on Power Engineering, Energy and Electrical Drives*, (May):1–6, May 2011.
- [76] Daniel Pinheiro Bernardon, Mauricio Sperandio, Vinícius Jacques Garcia, Luciane Neves Canha, Alzenira Da Rosa Abaide, and Eric Fernando Boeck Daza. AHP Decision-Making Algorithm to Allocate Remotely Controlled Switches in Distribution Networks. *IEEE Transactions on Power Delivery*, 26(3):1884–1892, July 2011.
- [77] Mehdi Arian, Mohammad Ameli, Vahid Soleimani, Asadollah Gharighi, Alireza Fereidunian, Amir Kazembakhshi, and Jalal Mohammad. IT infrastructure selection for smart grid using AHP. *2011 IEEE Power Engineering and Automation Conference*, pages 45–50, September 2011.
- [78] Alexandre Barin, Luciane Neves Canha, Alzenira da Rosa Abaide, and Karine Faverzani Magnago. Selection of storage energy technologies in a power quality scenario - the AHP and the fuzzy logic. *2009 35th Annual Conference of IEEE Industrial Electronics*, pages 3615–3620, November 2009.
- [79] Mostafa Hosseini and Homa Famil Bahmani. Evaluation and routing of power transmission lines by using AHP method and genetic algorithm. *2011 IEEE Symposium on Computers & Informatics*, pages 68–73, March 2011.
- [80] Mohammad Zare Ernani and Asghar Akbari Azirani. A method based on Analytical Hierarchy Process for generator fault diagnosis. *2010 10th IEEE International Conference on Solid Dielectrics*, pages 1–4, July 2010.
- [81] H.H. Goh, B.C. Kok, S.W. Lee, and A.A.M. Zin. Load Shedding Scheme in Large Pulp Mill by Using Analytic Hierarchy Process. *AIP Conference Proceedings*, (December):2–4, 2011.
- [82] Chongming Liu, Dan Chen, and Yan Feng. Post-Evaluating of Wind Power Project Based On AHP Model. *2010 Asia-Pacific Power and Energy Engineering Conference*, pages 1–4, 2010.
- [83] D. Cooke. Empowering customer choice in electricity markets. Technical report, International Energy Agency, 2011.
- [84] M.P.F. Hommelberg, B.J. van der Velde, C.J. Warmer, I.G. Kamphuis, and J.K. Kok. A novel architecture for real-time operation of multi-agent based coordination of demand and supply. In *2008 IEEE Power and Energy Society General Meeting - Conversion and Delivery of Electrical Energy in the 21st Century*, pages 1–5. IEEE, July 2008.

- [85] P. Kadurek, J. Blom, J.F.G. Cobben, and W.L. Kling. Theft detection and smart metering practices and expectations in the Netherlands. In *Innovative Smart Grid Technologies Conference Europe (ISGT Europe), 2010 IEEE PES*, pages 1–6. IEEE, October 2010.
- [86] J. Benítez, X. Delgado-Galván, J.A. Gutiérrez, and J. Izquierdo. Balancing consistency and expert judgment in AHP. *Mathematical and Computer Modelling*, 54(7-8):1785–1790, October 2011.
- [87] Vincent S. Lai, Bo K. Wong, and Waiman Cheung. Group decision making in a multiple criteria environment: A case using the AHP in software selection. *European Journal of Operational Research*, 137(1):134–144, February 2002.
- [88] Koen Kok, Bart Roossien, Pamela MacDougall, Olaf van Pruissen, Gerben Venekamp, Rene Kamphuis, Joost Laarakkers, and Cor Warmer. Dynamic pricing by scalable energy management systems - Field experiences and simulation results using PowerMatcher. In *2012 IEEE Power and Energy Society General Meeting*, pages 1–8. IEEE, July 2012.
- [89] A. Capasso, W. Grattieri, R. Lamedica, and A. Prudenzi. A bottom-up approach to residential load modeling. *IEEE Transactions on Power Systems*, 9(2):957–964, May 1994.
- [90] A. Cagni, E. Carpaneto, G. Chicco, and R. Napoli. Characterisation of the aggregated load patterns for extraurban residential customer groups. *Proceedings of the 12th IEEE Mediterranean Electrotechnical Conference (IEEE Cat. No.04CH37521)*, pages 951–954 Vol.3, 2004.
- [91] Runming Yao and Koen Steemers. A method of formulating energy load profile for domestic buildings in the UK. *Energy and Buildings*, 37(6):663–671, June 2005.
- [92] F. Provoost and M. van Lumig. The use of smart meters to improve customer load models. In *Electricity Distribution, 2011. CIRED 2011. 21st International Conference and Exhibition on*, pages 1–4, 2011.
- [93] Thomas Stetz, Frank Marten, and Martin Braun. Improved Low Voltage Grid-Integration of Photovoltaic Systems in Germany. *IEEE Transactions on Sustainable Energy*, (1):1–9, 2012.
- [94] CEER. Energy regulators’ pledge to ensuring good quality of electricity supply. *FS-0901*, 2009.
- [95] P. Bauer and S.W.H. de Haan. Electronic tap changer for 500 kVA/10 kV distribution transformers: design, experimental results and impact in distribution networks. In *Industry Applications Conference, 1998. Thirty-Third IAS Annual Meeting. The 1998 IEEE*, volume 2, pages 1530–1537 vol.2, 1998.

- [96] H. Abdulrahman, P. Bauer, and J.H.R. Enslin. Smarttrafo and Flicker. In *2006 IEEE PES Power Systems Conference and Exposition*, pages 803–809. IEEE, 2006.
- [97] P. Kadurek, J.F.G. Cobben, and W.L. Kling. Future LV distribution network design and current practices in the Netherlands. In *2011 2nd IEEE PES International Conference and Exhibition on Innovative Smart Grid Technologies*, pages 1–6. IEEE, December 2011.
- [98] P. Kadurek, J.F.G. Cobben, and W.L. Kling. Smart MV/LV transformer for future grids. In *International Symposium on Power Electronics Electrical Drives Automation and Motion (SPEEDAM)*, pages 1700–1705, June 2010.
- [99] P. Kadurek, J.F.G. Cobben, and W.L. Kling. Smart transformer for mitigation of voltage fluctuations in MV networks. In *10th International Conference on Environment and Electrical Engineering*, pages 1–4. IEEE, May 2011.
- [100] Milos Maksic, Bostjan Blazic, and Igor Papic. Comparison of calculated and measured flicker values for two different network topologies. In *2009 IEEE Bucharest PowerTech*, pages 1–8. IEEE, June 2009.
- [101] Rong Cai. *Flicker Interaction Studies and Flickermeter Improvement*. Ph.D. dissertation, Eindhoven University of Technology, 2009.
- [102] L.W. White and Subhashish Bhattacharya. A Discrete Matlab-Simulink Flickermeter Model for Power Quality Studies. *IEEE Transactions on Instrumentation and Measurement*, 59(3):527–533, March 2010.
- [103] Randy Horton and Timothy A. Haskew. Effect of Transfer Coefficients on MV and LV Flicker Levels. *IEEE Transactions on Power Delivery*, 26(2):632–639, April 2011.
- [104] S. Perera, D. Robinson, S. Elphick, D. Geddey, N. Browne, V. Smith, and V. Gosbell. Synchronized Flicker Measurement for Flicker Transfer Evaluation in Power Systems. *IEEE Transactions on Power Delivery*, 21(3):1477–1482, July 2006.
- [105] M. Halpin, R. Cai, E. de Jaeger, I. Papic, S. Perera, and X. Yang. A review of flicker objectives related to complaints, measurements, and analysis techniques. In *CIGRE 2009*, pages 1–4, June 2009.
- [106] P.G.V. Axelberg, M.H.J. Bollen, and I.Y.-H. Gu. Trace of Flicker Sources by Using the Quantity of Flicker Power. *IEEE Transactions on Power Delivery*, 23(1):465–471, January 2008.
- [107] P.G.V. Axelberg and M.H.J. Bollen. An Algorithm for Determining the Direction to a Flicker Source. *IEEE Transactions on Power Delivery*, 21(2):755–760, April 2006.

- [108] J.C. Das. *Power System Analysis: Short-Circuit Load Flow and Harmonics*. Marcel Dekker, Inc., New York, 1 edition, 2002.
- [109] Y. Baghzouz, R.F. Burch, A. Capasso, A. Cavallini, A.E. Emanuel, M. Halpin, R. Langella, G. Montanari, K.J. Olejniczak, P.F. Ribeiro, S. Rios-Marcuello, F. Ruggiero, R. Thallam, A. Testa, and P. Verde. Time-varying harmonics. II. Harmonic summation and propagation. *IEEE Transactions on Power Delivery*, 17(1):279–285, 2002.
- [110] A. Mansoor, W.M. Grady, P.T. Staats, R.S. Thallam, M.T. Doyle, and M.J. Samotyj. Predicting the net harmonic currents produced by large numbers of distributed single-phase computer loads. *IEEE Transactions on Power Delivery*, 10(4):2001–2006, 1995.
- [111] Task Force on Harmonics Modeling and Simulation. Modeling and simulation of the propagation of harmonics in electric power networks. II. Sample systems and examples. *IEEE Transactions on Power Delivery*, 11(1):466–474, 1996.
- [112] V. Cuk, J.F.G. Cobben, W.L. Kling, and P.F. Ribeiro. Considerations on harmonic impedance estimation in low voltage networks. In *2012 IEEE 15th International Conference on Harmonics and Quality of Power*, pages 358–363. IEEE, June 2012.
- [113] R. Burch, G. Chang, C. Hatziaioniu, M. Grady, Y. Liu, M. Marz, T. Ortmeyer, S. Ranade, P. Ribeiro, and W. Xu. Impact of aggregate linear load modeling on harmonic analysis: a comparison of common practice and analytical models. *IEEE Transactions on Power Delivery*, 18(2):625–630, April 2003.
- [114] J. Wasilewski, W. Wiechowski, and C.L. Bak. Harmonic domain modeling of a distribution system using the DIGSILENT PowerFactory software. In *2005 International Conference on Future Power Systems*, pages 7 pp.–7. IEEE, 2005.
- [115] Alliander. Annual report 2011. Technical report, 2012.
- [116] P.M.S. Carvalho, P.F. Correia, and L.A.F. Ferreira. Distributed Reactive Power Generation Control for Voltage Rise Mitigation in Distribution Networks. *IEEE Transactions on Power Systems*, 23(2):766–772, May 2008.
- [117] Randy Horton and T.A. Haskew. Determination of Flicker Transfer Coefficients Near Large Synchronous Generators. *IEEE Transactions on Power Delivery*, 25(1):260–269, January 2010.
- [118] International Electrotechnical Commission. IEC/TR 61000-3-7 - Electromagnetic compatibility (EMC) - Part 3-7: Limits - Assessment of emission limits for the connection of fluctuating installations to MV, HV and EHV power systems. Technical report, 2008.

- [119] DigSILENT Solutions PowerFactory Software. *IEEE Power and Energy Magazine*, 4(5):3–3, 2006.
- [120] Terminology Task Force. Part I of II Parts Glossary of Terms Related to Load Management. *IEEE Transactions on Power Apparatus and Systems*, PAS-104(9):2381–2386, 1985.
- [121] Le-Ren Chang-Chien, Luu Ngoc An, Ta-wei Lin, and Wei-jen Lee. Incorporating Demand Response With Spinning Reserve to Realize an Adaptive Frequency Restoration Plan for System Contingencies. *IEEE Transactions on Smart Grid*, 3(3):1145–1153, September 2012.
- [122] M. Albadi and E. Elsaadany. A summary of demand response in electricity markets. *Electric Power Systems Research*, 78(11):1989–1996, November 2008.
- [123] A.J. Conejo, J.M. Morales, and L. Baringo. Real-Time Demand Response Model. *IEEE Transactions on Smart Grid*, 1(3):236–242, December 2010.
- [124] P Faria and Z. Vale. Demand response in electrical energy supply: An optimal real time pricing approach. *Energy*, 36(8):5374–5384, August 2011.
- [125] US Department of Energy. Benefits of demand response in electricity markets and recommendations for achieving them. Technical report, 2006.
- [126] Brian R. Scalley and Donald G. Kasten. The Effects of Distribution Voltage Reduction on Power and Energy Consumption. *IEEE Transactions on Education*, 24(3):210–216, 1981.
- [127] B.W. Kennedy and R.H. Fletcher. Conservation voltage reduction (CVR) at Snohomish County PUD. *IEEE Transactions on Power Systems*, 6(3):986–998, 1991.
- [128] D.M. Lauria. Conservation Voltage Reduction (CVR) at Northeast Utilities. *IEEE Transactions on Power Delivery*, 2(4):1186–1191, 1987.
- [129] W.G. Sunderman. Conservation voltage reduction system modeling, measurement, and verification. In *Transmission and Distribution Conference and Exposition (T&D), 2012 IEEE PES*, pages 1–4, May 2012.
- [130] Thomas L Wilson. Measurement and verification of distribution voltage optimization results for the IEEE power & energy society. In *IEEE PES General Meeting*, pages 1–9. IEEE, July 2010.
- [131] R.M. Delgado. Demand-side management alternatives. *Proceedings of the IEEE*, 73(10):1471–1488, 1985.

- [132] S. van Koten and A. Ortmann. The unbundling regime for electricity utilities in the EU: A case of legislative and regulatory capture? *Energy Economics*, 30(6):3128–3140, November 2008.
- [133] P Kadurek, M.M. Sarab, J.F.G. Cobben, and W.L. Kling. Assessment of demand response possibilities by means of voltage control with intelligent MV/LV distribution substation. In *IEEE Power and Energy Society General Meeting*, pages 1–6, San Diego, July 2012. IEEE.
- [134] Pacific Northwest National Laboratory report for U.S. Department of Energy. Evaluation of Conservation Voltage Reduction (CVR) on a National Level. Technical report, Pacific Northwest National Laboratory, 2010.
- [135] Mohammad Khurmy and Bader Alshahrani. Measurement & verifications of voltage optimization for conserving energy. In *2011 10th International Conference on Environment and Electrical Engineering*, pages 1–5. IEEE, May 2011.
- [136] T.J. Krupa and H. Asgeirsson. The Effects of Reduced Voltage on Distribution Circuit Loads. *IEEE Transactions on Power Systems*, 2(4):1013–1018, 1987.
- [137] Jasper Frunt. *Analysis of Balancing Requirements in Future Sustainable and Reliable Power Systems*. Ph.D. dissertation, Eindhoven University of Technology, 2011.
- [138] H. Lund and E. Münster. Management of surplus electricity-production from a fluctuating renewable-energy source. *Applied Energy*, 76(1-3):65–74, September 2003.
- [139] S. De, R. Anand, A. Naveen, and S. Moinuddin. e-Metering Solution for checking energy thefts and streamlining revenue collection in India. In *2003 IEEE PES Transmission and Distribution Conference and Exposition (IEEE Cat. No.03CH37495)*, volume 2, pages 654–658. IEEE, 2003.
- [140] V. Paruchuri and S. Dubey. An approach to determine non-technical energy losses in India. In *Advanced Communication Technology (ICACT), 2012 14th International Conference on*, pages 111–115.
- [141] Raymond F. Ghajar and Joseph Khalife. Cost/benefit analysis of an AMR system to reduce electricity theft and maximize revenues for Électricité du Liban. *Applied Energy*, 76(1-3):25–37, September 2003.
- [142] L.J. Hernandez, L.C. Duarte, F.O. Morais, E.C. Ferreira, and J.A. Siqueira-Dias. Optimizing the Inspection Routine for the Detection of Electrical Energy Theft in AES Eletropaulo in São Paulo, Brazil. *WSEAS Transaction on Power Systems*, 7(2):80–89, 2012.

- [143] Reducing Technical and Non-Technical Losses in the Power Sector. Technical report, World Bank, 2009.
- [144] Soma Shekara Sreenadh Reddy Depuru, Lingfeng Wang, and Vijay Devabhaktuni. Electricity theft: Overview, issues, prevention and a smart meter based approach to control theft. *Energy Policy*, 39(2):1007–1015, February 2011.
- [145] Domestic Metering Innovation. Technical report, The Office of Gas and Electricity Markets (Ofgem), London, 2006.
- [146] Paul Davidson, USA TODAY. Electricity thefts surge in bad times, 2009. Available online at: http://usatoday30.usatoday.com/money/industries/energy/2009-03-16-electricity-thefts_N.htm Accessed on: March 6, 2013.
- [147] Soma Shekara Sreenadh Reddy Depuru, Lingfeng Wang, Vijay Devabhaktuni, and Robert C. Green. High performance computing for detection of electricity theft. *International Journal of Electrical Power & Energy Systems*, 47:21–30, May 2013.
- [148] Jeff McShan, khou.com, Texas. Electricity theft: Dangerous trend that's costing honest Houstonians money, 2010. Available online at: <http://www.khou.com/news/Electricity-theft-a-dangerous-trend-thats-costing-honest-Houstonians-money-92450694.html> Accessed on: March 7, 2013.
- [149] Jorge Vasconcelos. Survey of Regulatory and Technological Developments Concerning Smart Metering in the European Union Electricity Market. *RSCAS Policy Papers*, (RSCAS PP 2008/01), 2008.
- [150] CBC News. Electricity theft by B.C. grow-ops costs \$100M a year, 2010. Available online at: <http://www.cbc.ca/news/canada/british-columbia/story/2010/10/08/bc-hydro-grow-op-theftw.html> Accessed on: March 7, 2013.
- [151] C.J. Bandim, J.E.R. Alves, A.V. Pinto, F.C. Souza, M.R.B. Loureiro, C.A. Magalhaes, and F. Galvez-Durand. Identification of energy theft and tampered meters using a central observer meter: a mathematical approach. In *2003 IEEE PES Transmission and Distribution Conference and Exposition (IEEE Cat. No.03CH37495)*, pages 163–168. IEEE.
- [152] Soma Shekara Sreenadh Reddy Depuru. *Modeling, Detection, and Prevention of Electricity Theft for Enhanced Performance and Security of Power Grid*. Ph.D. dissertation, University of Toledo, 2012.
- [153] A.H. Nizar, Z.Y. Dong, J.H. Zhao, and P. Zhang. A Data Mining Based NTL Analysis Method. In *2007 IEEE Power Engineering Society General Meeting*, number 3, pages 1–8. IEEE, June 2007.

- [154] A.H. Nizar, Z.Y. Dong, and Y. Wang. Power Utility Nontechnical Loss Analysis With Extreme Learning Machine Method. *IEEE Transactions on Power Systems*, 23(3):946–955, August 2008.
- [155] J.E. Cabral, E.M. Gontijo, J.O.P. Pinto, and J.R. Filho. Fraud detection in electrical energy consumers using rough sets. In *2004 IEEE International Conference on Systems, Man and Cybernetics (IEEE Cat. No.04CH37583)*, pages 3625–3629. IEEE, 2004.
- [156] C.S. Cheng and D. Shirmohammadi. A three-phase power flow method for real-time distribution system analysis. *IEEE Transactions on Power Systems*, 10(2):671–679, 1995.
- [157] T.L. Baldwin and S.A. Lewis. Distribution Load Flow Methods for Shipboard Power Systems. *IEEE Transactions on Industry Applications*, 40(5):1183–1190, September 2004.
- [158] S. Weckx, C. Gonzalez, J. Tant, T. de Rybel, and J. Driesen. Parameter identification of unknown radial grids for theft detection. In *3rd IEEE PES Innovative Smart Grid Technologies Europe (ISGT Europe)*, pages 1–6. IEEE, October 2012.
- [159] R. Srinivasa Rao, K. Ravindra, K. Satish, and S. V. L. Narasimham. Power Loss Minimization in Distribution System Using Network Reconfiguration in the Presence of Distributed Generation. *IEEE Transactions on Power Systems*, 28(1):317–325, February 2013.
- [160] Measurement Uncertainty Analysis Principles and Methods. *NASA Measurement Quality Assurance Handbook*, (NASA-HDBK-8739.19-3), 2010.
- [161] Tom Pycke, Dirk Costrop, and Luc Henderieckx. Improving the data quality of the LV-connectivity. In *Cired 2011*, 2011.
- [162] Kejun Qian, Chengke Zhou, Malcolm Allan, and Yue Yuan. Modeling of Load Demand Due to EV Battery Charging in Distribution Systems. *IEEE Transactions on Power Systems*, 26(2):802–810, May 2011.
- [163] Niamh O’Connell, Qiuwei Wu, Jacob Ostergaard, Arne Hejde Nielsen, Seung Tae Cha, and Yi Ding. Electric Vehicle (EV) charging management with dynamic distribution system tariff. In *2011 2nd IEEE PES International Conference and Exhibition on Innovative Smart Grid Technologies*, number 081216, pages 1–7. IEEE, December 2011.
- [164] Georg Kerber. *Aufnahmefähigkeit von Niederspannungsverteilstnetzen für die Einspeisung aus Photovoltaikkleinanlagen*. Ph.D. dissertation, Technische Universität München, 2011.

-
- [165] James H. Pikul, Hui Gang Zhang, Jiung Cho, Paul V. Braun, and William P. King. High-power lithium ion microbatteries from interdigitated three-dimensional bicontinuous nanoporous electrodes. *Nature Communications*, 4:1732, April 2013.

Nomenclature

List of acronyms

Acronym	Meaning
AC	Alternating Current
AHP	Analytic Hierarchy Process
Al	Aluminium
AL	Additional Load
Alt.	Alternative
AM	Asynchronous Motor
AMR	Automated Meter Reading
c	Criterion
Cu	Copper
CWI	"Centrum Wiskunde & Informatica"
DER	Distributed Energy Resource
DG	Distributed Generation
DL	Distorting Load
DR	Demand Response
Dyn	Winding connection: Δ primary, wye secondary with n-wire
ECDF	Empirical Cumulative Distribution Function
ENTSO-E	European Network of Transmission System Operators for Electricity
EU	European Union
HV	High Voltage
h	Hours (time)
IDeaNeD	Intelligent and Decentralized Management of Networks and Data

Acronym	Meaning
IDS	Intelligent Distribution Substation
IOP EMVT	"Innovatiegerichte Onderzoeksprogramma's Elektromagnetische Vermogenstechniek"
K-S	Kolmogorov-Smirnov (test)
LV	Low Voltage
M	Million
MCDA	Multi-Criteria Decision Analysis
min.	Minute
MV	Medium Voltage
NL	The Netherlands
NOP	Normally Open Point
NTL	Non-Technical Loss
OLTC	On-Load Tap Changer
PF	Power Factor
POC	Point Of Connection
PQ	Power Quality
PTU	Program Time Unit
pu	Per-Unit
PV	Photovoltaic
s	Second(s), a sixtieth of a minute of time
SAIDI	System Average Interruption Duration Index
SAIFI	System Average Interruption Frequency Index
THD	Total Harmonic Distortion
TSO	Transmission System Operator
USA	United States of America
V2G	Vehicle to Grid

List of symbols

Symbol	Meaning	Units
A	Answer matrix for AHP	–
A	Cross section area	mm^{-2}
AL_{ratio}	AL ratio in the network	%
CR	Consistency Ratio	–
$\cos\varphi$	Power factor	–
DG_{ratio}	DG ratio in the network	%
F	Shape factor of the voltage waveform	–
f	Grid frequency	Hz
G_{st}^{LV}	Maximal global contribution of LV loads to P_{st}^{LV}	–
I	Current	A
$I_{ia,min}$	Minimal detectable current due to illegal abstraction of electricity	A
I_{ir}	Inrush current	A
I_{max}^{POC}	Maximal current at a POC, set by a protection at POC	A
I_{max}^{SS-LV}	Maximal current of a feeder, set by a protection in the MV/LV substation	A
l	Length	m
n_{AL}	Number of Additional Loads	–
$n_{feeders}$	Number of LV feeders	–
n_{POCs}	Number of POCs in the LV network	–
n_{resp}	Number of responses	–
NC	Number of choices (objective functions)	–
P	Active power	W
$PTUs$	Number of PTUs	–
p^{DG}	Power output for a DG	W
$P_{ia,min}$	Minimal detectable power due to illegal abstraction of electricity	W
P_{inst}	Installed capacity	W
P_{lt}	Long-term flicker severity	–
P_m	Rated mechanical power	W
P_{st}	Short-term flicker severity	–
PU_{ratio}	Load response ratio	–
ΔP_{red}	Reduction factor of called imbalance volumes	pu
ΔP_{dep}	Deployed DR with IDS	pu
ΔP_{util}	Utilization factor of the available DR	pu
Q	Reactive power	var
R	Electrical resistance	Ω

Symbol	Meaning	Units
RI	Random index	–
S	Apparent Power	VA
S_{max}^{POC}	Maximal power demand accessible by a network user at POC	VA
S_q''	Short-circuit power	VA
S^{tr}	Transformer rating	VA
r	Repetition rate	min^{-1}
RI	Random Index	–
T	Transfer coefficient	–
t	Time instance	–
$T_{P_{st}^{MV(1) \rightarrow MV(2)}}$	Flicker transfer coefficient from a MV node 1 to a MV node 2	–
$T_{P_{st}^{POC \rightarrow LV_{bus-bar}}}$	Transfer coefficient of P_{st} from LV bus-bar to a POC	–
$T_{u_5^{MV(1) \rightarrow MV(2)}}$	Transfer coefficient from a MV node 1 to a MV node 2 for u_5	–
U	Voltage (rms, if not indicated otherwise)	V
u_ε	Uncertainty of a measurement	–
U_c	Declared supply voltage level	V
$U_{down}^{LV_{bus-bar}}$	Available voltage decrease with OLTC	pu
u_h	Harmonic voltage, where additional number can indicate specific harmonics	%
$U_{MV,max}$	Maximal MV voltage which can be mitigated by OLTC	pu
$U_{MV,min}$	Minimal MV voltage which can be mitigated by OLTC	pu
U_n	Nominal voltage level	V or pu
U_{tap}	Voltage level related to the OLTC tap position	pu
$U_{TR,max}$	Maximum OLTC voltage (from manufacturer)	pu
$U_{TR,min}$	Minimum OLTC voltage (from manufacturer)	pu
$U_{up}^{LV_{bus-bar}}$	Available voltage increase with OLTC	pu
w_i	Weight factor of i criterion	–
$w_{i,j}$	Weight factor between i, j criteria	–
X	Electrical reactance	Ω
Z	Impedance	Ω
σ	Standard deviation	–
\wedge	Logical conjunction	–
\vee	Logical disjunction	–

List of indices

Index	Meaning
<i>agg</i>	Aggregated
<i>AL</i>	Additional Load
<i>avg</i>	Average value
<i>c</i>	Declared
<i>cc</i>	Connection Cable
<i>cs</i>	Cable Section
<i>depl</i>	Deployed
<i>DG</i>	Distributed Generation
<i>down</i>	Down-regulation
<i>est</i>	Estimated
<i>f</i>	Feeder
<i>g</i>	Generator
<i>ia</i>	Related to Illegal Abstraction of electricity
<i>IDS%</i>	Penetration level of IDS
<i>IM</i>	Imbalance
<i>inst</i>	Installed
<i>loss</i>	Technical Loss
<i>lt</i>	Long-Term
<i>LV</i>	Low Voltage
<i>LV_{bus-bar}</i>	Substation LV bus-bar
<i>max</i>	Maximum value
<i>MV</i>	Medium Voltage
<i>MV(1)→MV(2)</i>	From node MV(1) to MV(2)
<i>n</i>	Nominal
<i>N</i>	Neutral (wire in four-wire system)
<i>net</i>	Network
<i>POC</i>	POC
<i>POC→LV_{bus-bar}</i>	Direction from POC to LV bus-bar
<i>POC←LV_{bus-bar}</i>	Direction from LV bus-bar to POC
<i>rms</i>	Root Mean Square
<i>st</i>	Short-Term
<i>SS-LV</i>	Substation (LV side)
<i>tap</i>	Related to Tap position of OLTC
<i>tr</i>	Transformer
<i>up</i>	Up-regulation
<i>util</i>	Utilization
\bar{U}	Arithmetic mean of e.g., <i>U</i>

List of publications

Journal publications

2013

- P. Kadurek, J.F.G. Cobben, W.L. Kling, and P.F. Ribeiro. Aiding Power System Support by Means of Voltage Control with Intelligent Distribution Substation. *Under review of IEEE Transactions on Smart Grid*, 2013.
- P. Kadurek, J.F.G. Cobben and W.L. Kling. Additional Overloading Assessment for Future Low Voltage Networks Based on Smart Metering. *Journal of Energy and Power Engineering*, Vol. 7, ISSN 1934-8983, 2013.

2009

- P. Kadurek. Sao Miguel Island as a case study on a possible usage of Electric vehicle to store energy. *World Electric Vehicle Journal*, Vol. 3, ISSN 2032-6653, 2009.

Conference publications

2013

- P. Kadurek, A. Zipperer, S. Suryanarayanan and J.F.G. Cobben. An Application of a Decision-Making Algorithm for an Intelligent Distribution Substation. *IEEE Power and Energy Society General Meeting 2013*, Vancouver, BC, Canada, 2013.
- P. Kadurek, J.F.G. Cobben, P.F. Ribeiro and W.L. Kling. Electricity Demand Characterization for Analyzing Residential LV Distribution Networks. *IEEE Powertech Grenoble 2013 Conference*, Grenoble, France, 2013.

- T. Gu, P. Kadurek, J.F.G. Cobben and A.W. Endhoven. Power Quality Data Evaluation in Distribution Networks Based on Data Mining Techniques. *12th International Conference on Environment and Electrical Engineering (EEEIC)*, Wroclaw, Poland, 2013, d.o.i. 10.1109/EEEIC.2013.6549589.

2012

- P. Kadurek, M.M. Sarab, J.F.G. Cobben and W.L. Kling. Assessment of demand response possibilities by means of voltage control with intelligent MV/LV distribution substation. *IEEE Power and Energy Society General Meeting 2012*, San Diego, CA, USA, 2012, d.o.i. 10.1109/PESGM.2012.6345553.
- J. van Tongeren, P. Kadurek, J.F.G. Cobben and W.L. Kling. Operational data measurements in intelligent medium voltage networks. *CIGRE 2012 workshop, Integration of Renewables into the Distribution Grid*, Lisbon, Portugal, 2012, d.o.i. 10.1049/cp.2012.0731.

2011

- P. Kadurek, J.F.G. Cobben and W.L. Kling. Future LV distribution network design and current practices in the Netherlands. *2011 2nd IEEE PES International Conference and Exhibition on Innovative Smart Grid Technologies (ISGT Europe)*, Manchester, UK, 2011, d.o.i. 10.1109/ISGTEurope.2011.6162831.
- P. Kadurek, J.F.G. Cobben and W.L. Kling. Overloading Protection of Future Low Voltage Distribution Networks. *2011 IEEE Trondheim PowerTech*, Trondheim, Norway, 2011, d.o.i. 10.1109/PTC.2011.6019166.
- F. van den Bergh, P. Kadurek, J.F.G. Cobben and W.L. Kling. Electricity Theft Localization Based On Smart Metering. *21st International Conference on Electricity Distribution (CIGRE 2011)*, Frankfurt, Germany, 2011.
- P. Kadurek, J.F.G. Cobben and W.L. Kling. Smart Transformer for mitigation of voltage fluctuations in MV networks. *2011 10th International Conference on Environment and Electrical Engineering (EEEIC)*, Rome, Italy, 2011, d.o.i. 10.1109/EEEIC.2011.5874838.

2010

- P. Kadurek, J. Blom, J.F.G. Cobben and W.L. Kling. Theft detection and smart metering practices and expectations in the Netherlands. *2010 IEEE PES International Conference and Exhibition on Innovative Smart Grid Technologies (ISGT Europe)*, Gothenburg, Sweden, 2010, d.o.i. 10.1109/ISGTEUROPE.2010.5638852.

- P. Kadurek, J.F.G. Cobben and W.L. Kling. Additional features of smart metering. *IEEE Fifth IEEE Young Researchers Symposium in Electrical Power Engineering (YRS 2010)*, Leuven, Belgium, 2010.
- P. Kadurek, J.F.G. Cobben and W.L. Kling. Smart MV/LV transformer for future grids. *2010 International Symposium on Power Electronics Electrical Drives Automation and Motion (SPEEDAM)*, Pisa, Italy, 2010, d.o.i. 10.1109/SPEEDAM.2010.5545067.

2009

- P. Kadurek, A. Pina, Ch. Ioakimidis and P. Ferrao. Sao Miguel Island as a case study on a possible usage of Electric vehicle to store energy. *The 24th International Battery, Hybrid and Fuel Cell Electric Vehicle Symposium & Exhibition (EVS 24)*, Stavanger, Norway, 2009.
- P. Kadurek, Ch. Ioakimidis and P. Ferrao. Electric Vehicles and their impact to the electric grid in isolated systems. *International Conference on Power Engineering, Energy and Electrical Drives (POWERENG '09)*, Lisbon, Portugal, 2009, d.o.i. 10.1109/POWERENG.2009.4915218.

Acknowledgements

Many people have supported me during the four years of my Ph.D. and I am very thankful for their support. I would especially like to give thanks to my supervisors Sjef Cobben and Wil Kling for their guidance and constructive criticism I received during my research and for their feedback during the compilation of this manuscript.

I would also like to express my gratitude to Sjef for being a great and objective "chef" with humanistic views. Taking a new path is never easy, and I am very grateful to both Sjef and Wil for their help in realizing my stay as a visiting researcher. I will always be appreciative of having the opportunity to join Siddharth Suryanarayanan and his colleagues at Colorado State University, so that I could spend a very productive time under his guidance. Thank you also for making my stay a pleasant experience.

My gratitude goes also to my committee members, namely J.G.(Han) Slootweg, Siddharth Suryanarayanan, J.A.(Han) La Poutré, J.(Johan) Driesen, J.M.A.(Johanna) Myrzik and A.C.P.M.(Ton) Backx, for being part of my Ph.D. examination committee. In addition, I gratefully acknowledge the support of Paulo Ribeiro during my research.

Appreciation goes out to go to all my colleagues, of the last four years, who I have really enjoyed working with at Electrical Energy System (EES) group at TU/e. Special thanks to Jasper Frunt and Phuong Nguyen for being very supportive and for being more than my scientific gurus. Ioannis Lampropoulos and Jasper, you have been great workmates, thanks. To all my dear students, thank you for letting me guide you so smoothly throughout your studies. There are too many friends to name all of them, but it was my great pleasure to be a part of our collective. I enjoyed our coffee time, our big discussions on matters of little importance and our activities outside the office very much.

Throughout my research, I was grateful to receive valuable feedback from industrial partners in my project so I would like to thank Alfen, Alliander, DNV KEMA, Eneco, Phase to Phase and Stedin, thank you for your support, the work presented in this dissertation can bridge scientific and industrial perspectives. I would like to emphasize the support of Alliander for allowing me to validate proposed applications in real

conditions.

Along with my studies, I had the honor to serve my colleagues for many years as the president of our Ph.D. group. On the one hand, I would like to thank my colleagues, Helder Lopes Ferreira, Jerom de Haan and Shima Mousavi Gargari, who were always ready to help with the organization of our activities. On the other hand, I would like to thank the numerous companies and institutions, which welcomed us, to name but a few: BritNed, DNV KEMA, Electrabel, E.ON, ENTSO-E, IBM, Imperial College London, K.U. Leuven, TenneT TSO, Smit Transformers and RWTH Aachen. Guus Pemen and Wil, I appreciate your support for our group activities and in particular, I would like to thank you for allowing us to make our team-building exercise, in London, become a reality. Thanks must also go out to Geert Wessel Boltje and Agentschap NL for their active support of our Ph.D. group.

Finally, to my parents and family, I thank you for giving me the opportunity to pursue my dreams. Last, but not least, to my dear Bibiana, thank you for being such a wonderful partner, for your relentless support during my studies and for encouraging me on my other adventures.

Curriculum Vitae

Petr Kaďurek was born in Přilepy, Czech Republic (former Czechoslovakia) on October 27th, 1982. He received a Master degree in Electrical Engineering and Informatics, with the main field of study in Electric Power Engineering, from the Technical University of Prague in 2008. During his Master studies, he joined the Gottfried Wilhelm Leibniz Universitat, Hannover, Germany, from 2006 until 2007, where he worked on his Master thesis at the Institute of Electric Power Systems, High Voltage Engineering Section (Schering-Institute) next to his M.Sc. pensusum. He was awarded several grants for excellence during his M.Sc. studies.

Along with his M.Sc. studies he worked part-time in the industry before he joined the company Eltodo full-time from 2007 until 2008. He worked as a designer and a project manager in the area of power systems.

He was selected to join the MIT Portugal Program in Lisbon, Portugal, where he received the Postgraduate diploma of Advanced Studies in Sustainable Energy Systems, in 2009. He received a grant for excellent students from the Foundation for Science and Technology (FCT).

In September 2009, he joined the Electrical Energy System group at the faculty of Electrical Engineering at Eindhoven University of Technology. His research was done within the IDEaNeD (Intelligent and Decentralized Management of Networks and Data) project, which dealt with the aspects of a future electricity distribution infrastructure. He focused on data applications for advanced distribution networks operation and the results of his work are presented in this dissertation. In 2012, within the IDEaNeD project he joined Colorado State University, in the Department of Electrical and Computer Engineering at Fort Collins, as a visiting researcher at the college of Engineering under the supervision of Siddharth Suryanarayanan.

He received the Master of Business Administration (MBA) degree from the Sheffield Business School at Sheffield Hallam University, UK. He concluded his studies with a distinction (the highest award for MBA students at Sheffield Business School) and received the student prize for the best student of the year. He was given the honour

of delivering the graduation speech during the final MBA ceremony in 2013.

Besides his research, he was involved in teaching tasks and in organization of different events such as SIP (System Integration Projects) and LPQF (Leonardo Energy Power Quality Forum) held in Eindhoven. He is the author of several articles for the Connecthor magazine.

From 2010 until 2013, he served as the president of the student society (Ph.D. group) at the Electrical Energy System group.

